Reg # 1022

NACA

RESEARCH MEMORANDUM

INVESTIGATION OF SYMMETRICAL BODY INDENTATIONS DESIGNED

TO REDUCE THE TRANSONIC ZERO-LIFT WAVE DRAG OF A

45° SWEPT WING WITH AN NACA 64A006 SECTION AND

WITH A THICKENED LEADING-EDGE SECTION

By George H. Holdaway and Elaine W. Hatfield

Ames Aeronautical Laboratory
Moffett Field, Calif.

Classification cancelled (... Unclassified...)

By Authority .. NASA Tech Pub Announcement #3
(....)

H Feb. 61

NK

GRADE OF OFFICER MAKING CHANGE.)

15 May 61

NATIONAL ADVISORY COMMITTEE
FOR AERONAUTICS
WASHINGTON
March 19, 1957

NATIONAL ADVISORY COMMITTEE FOR AERONAUTICS

RESEARCH MEMORANDUM

INVESTIGATION OF SYMMETRICAL BODY INDENTATIONS DESIGNED

TO REDUCE THE TRANSONIC ZERO-LIFT WAVE DRAG OF A

45° SWEPT WING WITH AN NACA 64A006 SECTION AND

WITH A THICKENED LEADING-EDGE SECTION

By George H. Holdaway and Elaine W. Hatfield

SUMMARY

This wind-tunnel investigation was conducted at Reynolds numbers of about 7,000,000 based on the mean aerodynamic chord of the wing and the tests covered a Mach number range from 0.6 to 1.2. Two airfoils of the same maximum thickness were tested to evaluate the effect of a large leading-edge radius with increased thickness over the forward 40 percent of the chord on the reliability of the predictions of the supersonic area rule. The basic wing had an aspect ratio of 3, a leading-edge sweep of 45°, a taper ratio of 0.4, and NACA 64A006 sections perpendicular to a line swept back 39.45°, the quarter-chord line of these sections. The modified wing was similar to the basic wing in plan form; however, the leading-edge radius of the modified airfoil was about five times as great as that of the basic airfoil. Both wings were tested with a fineness-ratio-12.5 Sears-Haack body and with this body indented for the respective wings for design Mach numbers of 1.05 and 1.20. The basic-wing model was also tested with the body indented for a design Mach number of 1.00.

The test results indicated that indentations designed for the modified wing were as effective in reducing the wave drag as those for the basic wing. For this investigation the leading edges of the wings were at all times subsonic or behind the Mach lines. With all the indentations tested, substantial reductions in zero-lift drag were obtained at all supersonic speeds. The M = 1.05 indentations were almost as effective as the M = 1.20 indentations at M = 1.20, and as the M = 1.00 indentation (basic wing) at M = 1.00. Thus for the configurations tested the M = 1.05 design probably approaches the best compromise design for the test Mach numbers. For similar or thinner wings and similar body sizes relative to the wings, the test data indicated that the wing volume exposed by indentation of the body may be neglected in designing indentations for supersonic Mach numbers; however, this additional wing volume

was included in all the wave-drag computations. The experimental drag-
rise coefficients were adequately predicted at all supersonic Mach num-
bers by theoretical computations for the models with either the basic or
modified wing section.

INTRODUCTION

The wing-tunnel investigation of a thin swept wing reported in
reference 1 illustrated how a section modification, consisting of a
greatly increased leading-edge radius and slight forward camber, was
effective in improving the stability, drag, and high-lift characteristics
of the wing at low speeds. For the supersonic range of test Mach numbers
$M = 1.2$ to 1.9 (ref. 1), the modification resulted in an increase of wave
drag which made the modified wing inferior to the basic wing except at
lift coefficients greater than 0.6. The increase in wave drag was
attributed primarily to the change in area distribution.

The primary purpose of the present investigation was to determine if
the wave-drag penalty associated with the change of area-distribution of
the modified wing might be eliminated by suitable body contouring; in
other words, to determine if the supersonic area-rule principles of refer-
ences 2 and 3 can be successfully applied to a wing with a blunt airfoil
section for speeds at which the wing leading edge is subsonic (component
of velocity normal to the leading edge less than the speed of sound).

Another object of the investigation was to compare the relative merits
of various indentations (each designed for a specific Mach number) in terms
of average drag reduction through the transonic Mach number range. For
indentations designed for $M = 1.20$ an additional question considered was
whether indentations should be designed to compensate for wing volume
exposed by the indentation.

For the wind-tunnel investigation reported herein, a wing was selected
with the same thickness distribution as the modified wing of reference 1,
but with the camber removed to isolate the effect of the change in area
distribution. The basic wing of this investigation was the same as the
basic wing of reference 1. The fuselage indentations were generally
designed by the procedure outlined in reference 2, and the wave-drag
coefficients for each configuration were predicted by the computing
procedure of reference 4.

The tests were conducted in the 14-foot transonic wind tunnel at the
Ames Aeronautical Laboratory over a Mach number range of 0.6 to 1.2 at
Reynolds numbers of about 7,000,000 based on the mean aerodynamic chord
of the wing.

The symbols used in this report are defined in Appendix A.

WIND TUNNEL

A sectional view of the high-speed region of the Ames 14-foot transonic wind tunnel is shown in figure 1. This tunnel is of the closed return type with perforated walls in the test section. The flexible walls ahead of the test section are used to produce the convergent-divergent form required to generate supersonic Mach numbers up to 1.2.

Models are mounted by means of a sting and the forces are measured as electrical outputs from a strain-gage balance located within the model. A photograph of the model support system is shown in figure 2, which shows a rear view of the test section of the wind tunnel.

This tunnel is similar to the smaller Ames 2- by 2-foot transonic wind tunnel which is described in detail in reference 5. One exception, however, is that the 14-foot tunnel is not of the variable density type, but operates at atmospheric pressure.

MODELS AND TESTS

The models used in this investigation consisted of wing and body combinations of essentially the same plan form as illustrated in the dimensional sketch of figure 3. The basic body was a Sears-Haack body (body with minimum transonic drag for given volume and length) and had a closed-body fineness ratio of 12.5.

The basic wing had an aspect ratio of 3, a leading-edge sweep of 45°, a taper ratio of 0.4, and NACA 64A006 sections perpendicular to a line swept back 39.45° which was the quarter-chord line of these sections. The coordinates of this airfoil section are listed in table I with the corresponding coordinates of the streamwise section. The sweep of the streamwise quarter-chord line was 40.60°. The wing plan-form area was 8.72 square feet including the region within the body.

The modified wing had a leading-edge sweep angle of 45.3° and, in comparison with the basic wing, an airfoil with a greatly increased leading-edge radius (about five times) and with increased thickness on the forward 40 percent of the chord. These airfoil coordinates are also listed in table I. The leading-edge sweep was altered from that of the basic wing due to the increase of the streamwise length of the chords of about 2 percent. This modified wing had a symmetrical section of the same thickness distribution as the slightly cambered wing of reference 1.

Five different bodies were tested with the basic wing and four bodies with the modified wing. The body radii are listed in table II and the cross-sectional area distributions normal to the longitudinal axis are presented in figure 4.

Basic-Wing Bodies	Modified-Wing Bodies
Sears-Haack body	Sears-Haack body
M = 1.00 re-indentation	
M = 1.05 indentation	M = 1.05 indentation
M = 1.20 indentation	M = 1.20 indentation
M = 1.20 re-indentation	M = 1.20 re-indentation

The indentations were of circular cross section and were designed as outlined in reference 2 by indenting for the wing volume outside the given Sears-Haack body. The M = 1.00 and M = 1.20 re-indentations were computed as a function of the wing volume exposed by the indentation and hence were deeper than the normal indentations. The equations used for this type computation are given in Appendix B which also outlines the procedure used to compute the wing cross-sectional areas. For very thin wings the volume exposed by the indentation may be trivial, but for the wings tested, this was not the case, as is illustrated in figures 4(e) and 4(f).

Photographs of two of the models are shown in figure 5. The modified wing with the Sears-Haack body is shown in figure 5(a) and the basic wing with the M = 1.20 re-indentation is shown in figure 5(b). This re-indentation was the deepest indentation tested with the basic wing. The location of the pressure orifices for the body and the wings is presented in figures 6(a) and 6(b), respectively.

The test data included force, moment, and pressure measurements taken at angles of attack from about -4° to $+6^\circ$ at Mach numbers from 0.60 to 1.20. At a Mach number of 0.60 additional data were taken at higher angles of attack up to about $+9^\circ$. The Reynolds number per foot for these tests was almost 4,000,000 and the Reynolds number based on the mean aerodynamic chord of the basic wing varied from about 6,000,000 to 7,000,000 as shown in figure 7.

All coefficients are based on the area and the mean aerodynamic chord of the basic wing, and the pitching moments were computed about the quarter-chord point of the mean aerodynamic chord of the basic wing. Tunnel blockage for all models was less than one-half of one percent, based on either frontal area or the maximum cross-sectional area of the wing-body combinations, and the data should be relatively free of wall interference, as indicated in reference 5. The angle-of-attack data were corrected for tunnel air-stream angularity which was less than 1° for all Mach numbers. The drag data were corrected by the removal of base drag. To obtain this correction the pressure at the hollow base of each model was corrected to correspond to free-stream static pressure. As a check on this procedure for removing the base drag and as an approximate check for possible sting interference effects, the Sears-Haack body was tested without wings so that the drag data could be compared with the theoretical wave-drag value corrected for the cut-off portion of the body.

RESULTS AND DISCUSSION

The presentation of the various aerodynamic coefficients and their discussion will be in three parts: comparison of the basic-wing models with the modified-wing models, comparison of experimental and predicted zero-lift wave-drag coefficients, and comparison of indentations. Presentation of the pressure data will be secondary with emphasis primarily on their use to assist in the understanding of the drag data. Data for the model with the M = 1.00 re-indentation for the basic wing was obtained as part of another investigation and will be used in this report primarily for comparison with the results for the M = 1.05 indentation for the basic wing. (The simple M = 1.00 indentation for this wing has not been tested.) The results for the M = 1.20 re-indentations for the basic and modified wings were essentially identical to the results for normal indentations, so the presentation of the data for the re-indentations was restricted to the zero-lift drag coefficients which were slightly different. Throughout the report the experimental zero-lift drag coefficients for the various configurations are generally compared directly without taking incremental values of drag-rise coefficients, because greater confidence in the data results when it is evident that there are not any large variations in subsonic drag coefficients between models.

Comparison of Basic- and Modified-Wing Models

Static aerodynamic characteristics of the basic- and modified-wing models with the Sears-Haack body, the M = 1.05 indentations, and the M = 1.20 indentations are presented in figures 8, 9, and 10, respectively. Although the zero-lift drag data are of primary importance in the report, it is of interest to note first that the lift-curve slopes, stability changes, etc., are not very different for the two wings when tested with comparable bodies. For instance, the maximum lift-drag ratios for the two wings with various bodies are similar, as shown in figure 11. With the Sears-Haack body the modified-wing lift-drag ratios were equally as good as or better than the basic-wing model except at the highest test Mach number of 1.20. With the indented bodies, the modified-wing models had inferior maximum lift-drag ratios at the high subsonic speeds and at all supersonic speeds in comparison with the basic-wing models.

The zero-lift drag coefficients for the two wings with various bodies are presented in figure 12. This figure clearly indicates that at transonic speeds the zero-lift drag coefficients for the two wings are quite similar either with the Sears-Haack body or with their respectively indented bodies. Thus the indentations designed for the modified wing were fully as effective in reducing the zero-lift wave drag as those for the basic wing. An unexpected result, shown in figures 12 and 8(c), for the tests with the Sears-Haack body, is that at Mach numbers near 1 the

modified wing had the lower drag coefficients of the two wings. At Mach numbers near 1.2, the basic-wing models had drag coefficients which were consistently lower than the comparable modified-wing models.

The zero-lift pressure-coefficient distributions are presented for the basic- and modified-wing models over one quadrant of the models (figs. 13 and 14). Figure 13 presents the scales and layout which should be used with figure 14 for orientation of the pressure curves. The vertical lines in figure 14 are at orifice locations as defined in figure 6. In the pressure distributions shown in figure 14 the stagnation pressures have not been shown. Tabulated values of pressure distribution corresponding to each curve of figure 14 are listed in table III. A few stagnation pressures are missing from table III due to either a leak or a restriction in the pressure lines; however, the stagnation pressures were similar for the two wings.

As should be expected, the pressure distribution over the forward portion of each wing was quite different, that is, the pressure distribution for the basic wing is typical of a low-drag section and the distribution for the modified wing is somewhat similar to older conventional sections. In spite of this difference between wings shown in figure 14, it is of interest to note in the same figure that the body pressure distributions for the $M = 1.05$ indentations are very similar for the two wings at all Mach numbers except for body locations near the wing leading-edge juncture with the body.

Although this presentation (fig. 14) of the pressure data illustrates primarily the difference between wings, the favorable effects of the indentations, which will be discussed later, are particularly evident on the bodies and evident to some extent over the entire wing span.

Another comparison of the differences in the sections of the two wings can be made by plotting the pressure data in a different manner, as shown by a few examples in figure 15. These curves compare the basic- and modified-wing pressure coefficients at one spanwise station ($0.51 \, b/2$). The shaded regions are effectively thrust or drag parameters as defined by the equation

$$\frac{c}{z_{max}} \, C_{D_O} = \oint C_p \, \frac{dz}{z_{max}}$$

The thrust is defined in this case merely as negative drag. The pressure drag coefficient for the section can be obtained by multiplying the net area by half the maximum wing thickness and dividing by the local chord. For the curves shown in figure 15, it is evident for the representative spanwise station selected that the basic wing does not have any thrust at supersonic speeds. The basic wing on the body indented for $M = 1.05$

had a marked reduction of the section-pressure drag (fig. 15(c)) in comparison with this wing on the basic body (fig. 15(a)). A similar comparison for the modified wing models shows a marked increase in the thrust area as a result of the indentation. These curves also show that a large portion of the thrust area of the modified wing is offset by the drag area.

The similarity of the present zero-lift drag data for the basic and modified wings with the Sears-Haack body is somewhat in disagreement with the supersonic data from reference 1, which indicated a larger penalty in wave drag due to the modification of reference 1. (The data of reference 1 for $M = 1.20$ are relatively inaccurate because of large effects of reflected shock waves.) The zero-lift drag-rise coefficients for the two tests are compared in figure 16. The drag-rise coefficients were obtained by subtracting the subsonic zero-lift data at $M = 0.8$ from the zero-lift data at all higher Mach numbers. The friction-drag coefficient variation with Mach number was not considered, because it would be similar for the two wings and small for Mach numbers less than 1.2. Theoretical wave-drag coefficients were computed for the transonic speeds by the method of reference 4, and the solutions were limited to 25 terms; that is, effectively 25 harmonics of a Fourier sine series were used to represent the derivative of the area curves. The modification investigated in reference 1 included a slight amount of forward camber in the wing design but the airfoils had the same leading-edge radius and thickness distribution as those of the present investigation. The effect of the camber on the wave-drag coefficient was estimated in reference 6 as roughly 0.0015 at $M = 1.5$ and 0.0011 at $M = 1.9$. The difference in the Reynolds numbers of the tests might account for some of the drag difference; however, the data of reference 7 indicated that fixing transition had only a secondary effect on the drag-rise coefficients although a primary effect on the drag coefficients. For the large, unpolished models of the present tests the results are more equivalent to the transition-fixed data. The theoretical wave-drag coefficients tend to substantiate the data of the present report and will be discussed in detail in the next section of the report. It is reasonable to expect that the drag-rise coefficients due to the modification will increase at Mach numbers greater than those tested (Mach numbers for which the wing leading edge is sonic or supersonic); however, the transonic data indicate that the penalty for this modification is less than the penalty incurred through the modification tested in reference 1.

Comparison of Experimental and Computed Drag Coefficients

Experimental and theoretical (ref. 4) zero-lift drag coefficients are presented in figures 17 through 19. The effects of the various body indentations with the basic wing are shown in figure 17(a), and those with the modified wing in figure 17(b). Comparable zero-lift drag

coefficients for the two wings with the M = 1.20 re-indented bodies are
presented in figure 18. The experimental data points (figs. 17 and 18)
are essentially forebody data (i.e., drag coefficients for the wing and
the body ahead of the model base) since the base drag has been removed.
An illustrative plot of this procedure for removing the base-drag coeffi-
cients is shown in figure 19 for the test of the Sears-Haack body without
a wing. The base-drag coefficients are based on the wing area and are
fairly representative of the data obtained with all the models. Any pos-
sible effects of sting interference are evidently small since they are
probably within the magnitude of the indicated differences between the
computed and experimental forebody results of figure 19.

The theoretical wave-drag coefficients (figs. 17, 18, and 19) were
computed by the method of reference 4 and were plotted as increments above
the subsonic level of the experimental data near a Mach number of 0.8. As
mentioned previously, the variation in friction-drag coefficients with Mach
number is slight for this Mach number range and was neglected for these
comparisons. The theory used in these computations requires that the area
curves have zero slope at both ends of the body. For this investigation,
the coefficients were computed from area-distribution curves for models
with Sears-Haack bodies to closure, as shown by the area curves of fig-
ure 4. The computed wave-drag coefficients were then corrected by sub-
tracting the estimated contribution of the cut-off portion. This small
correction (C_{D_O} = 0.0006) is comparable to that used in reference 6 but
was estimated by a different procedure. In this case a supersonic pressure
distribution for M = 1.20 was computed for the Sears-Haack body using the
method of reference 8, and this pressure curve was used to evaluate the
drag contribution of the cut-off portion of the body.

In general, the agreement of the computed values of zero-lift drag
coefficients with the experimental results is very good. Even in the two
cases where the agreement was the poorest (basic wing with the M = 1.00
re-indented body, fig. 17(a) and the modified wing with the M = 1.20
re-indented body, fig. 18), the trends in the experimental data were
approximated by the theoretical computations. There is some indication
that the experimental data points at M = 1.075 are consistently high,
and perhaps a little low at M = 1.05 (figs. 17 and 18). Detailed cali-
bration of the tunnel is not yet completed, but the schlieren pictures at
these two Mach numbers did indicate the presence of weak reflected shocks.
These reflected shocks are known to be weak due to the lack of a positive
identification in any of the pressure data as shown in figure 14.

A comparative evaluation of the wave-drag predictions for the two
wings with the Sears-Haack body and with the indented bodies, including
the effect of the airfoil modification, is shown in figure 20. A com-
parison is made in this bar graph of the experimental drag-rise coeffi-
cients with the predicted wave-drag coefficients at a Mach number of 1.00
and at the two design Mach numbers, 1.05 and 1.20. The shortest bar of

the four at each Mach number is the goal sought by body contouring, that is, wave-drag for a wing-body combination which is no greater than the drag of an optimized body-alone shape. For bodies with circular cross-sections, this goal is probably attainable only at M = 1.00. The longest bar of the four at each Mach number is the computed wave-drag coefficient for the wings with the uncontoured Sears-Haack body. The crosshatched increment is the computed additional drag coefficient due to the wing modification. The middle two bars at each Mach number are the expected results with indented bodies. Note that the indented models designed for a specific Mach number have the lowest predicted wave drag at that Mach number, and the predicted additional drag due to the wing modification is essentially zero. Generally, the experimental results confirmed the predicted bar graphs with two interesting exceptions at M = 1.00. Agreement at M = 1.00 was not expected because the linearized theory is invalidated at this Mach number. The first exception was that the modified-wing models with the Sears-Haack body had lower, not higher, drag-rise coefficients. This effect was partially substantiated by the pressure data. The second exception, as noted in prior investigations such as reference 6, was that the predictions are pessimistically high at M = 1.00. It is also of interest to note that at M = 1.20 the predicted differences in ΔC_{D_O} between the indentations for M = 1.05 and M = 1.20 were not realized due to underestimating the experimental results in one case and overestimating them in the other. However, a designer might select the M = 1.05 indentation for this Mach number range, even without the more favorable experimental results, if the airplane had severe acceleration requirements for transonic Mach numbers.

A further evaluation of the theoretical computations is given in figure 21. This figure shows the comparison between the given area-distribution curves (modified-wing model with M = 1.05 indented body) and the computed check solutions for 25 harmonics. The area curves for the five cutting angles, θ, used in the M = 1.20 computation of the wave drag for this one model are shown. The agreement of the check solutions with the original area curves is considered to be satisfactory, considering that the boundary-layer displacement thickness was neglected in forming the area curves used in the theory. In addition, reference 4 has indicated that the use of a larger number of harmonics may not be realistic and may give poorer agreement with experimental results. In order to compare the variation of the area curves used in the theoretical computations, most of the area curves are shown at a reduced scale in figure 22. The curves for the M = 1.20 computations for $\theta = 70^O$ are deleted for clarity between curves.

Comparison of Indentations

The re-indentations for M = 1.20 in comparison with the indentations for M = 1.20 resulted in similar or higher zero-lift drag coefficients at

all Mach numbers for both the basic- and modified-wing models, as shown in figure 23. Part of the increased drag of the re-indented models is apparently due to a slight increase in friction drag. With the modified wing the re-indentations resulted in drag coefficients which were slightly higher even at the design Mach number of 1.20. As described in detail in Appendix B and mentioned previously, these re-indentations are designed as a function of the entire exposed wing volume including that wing volume exposed by the indentation. The comparison of these experimental results with theory was given previously in figures 17 and 18 and good agreement is shown for the models with the basic wing. The computed wave-drag coefficients for the re-indentations were only slightly lower than those for the normal indentations at the design Mach number of 1.20 (C_{D_O} = 0.0001 and 0.0003 less than the normal indentations, basic- and modified-wing models, respectively) and were higher at all other Mach numbers. Thus the, experimental and the computed data indicate that the added wing volume due to the indentation (for similar or thinner wings and similar relative body sizes) can be neglected in designing indentations, since at the design Mach number it makes little difference whether the first or second approximation to the indentation is made. However, in all cases the added wing area at each station was included in the total area curves when the wave-drag computations were made.

The effects of the various indentations on the experimental zero-lift drag coefficients are compared in figure 24 for the basic- and modified-wing models. For all the indentations tested, substantial reductions in zero-lift drag were obtained at all the supersonic speeds. The M = 1.20 indentations for the two wings resulted in substantial reductions in drag coefficients of 0.0045 to 0.0070 at all supersonic speeds tested and, as predicted by the theory, the lowest drag at M = 1.20. The M = 1.00 re-indentation for the basic-wing model was successful in reducing the drag coefficients as intended at M = 1.00. However, for the configurations tested the M = 1.05 indentations were practically as effective as the M = 1.20 indentations at M = 1.20 and as the M = 1.00 re-indentation (basic wing) at M = 1.00. Thus this M = 1.05 design is close to the best compromise design for the test Mach number range and for symmetrical body contouring. The M = 1.05 body indentation for the modified wing resulted in the largest reduction in zero-lift drag coefficient (0.0100 at M = 1.05). The corresponding reduction for the basic-wing model was somewhat less, although the basic-wing model generally had slightly lower drag coefficients.

The general superiority of the M = 1.05 indentations at supersonic speeds is also evident in the maximum lift-drag ratios presented in figure 25. All indentations improved the lift-drag ratios at supersonic test speeds in comparison with the values with the Sears-Haack body. The comparison between the lift-drag ratios for the two wings has been discussed previously.

The effect of the M = 1.05 and M = 1.20 body indentations on the lift-curve slopes at low angles of attack where the curves are linear are shown in figure 26. The M = 1.20 indentations resulted in an increase in lift-curve slope at the higher supersonic speeds, but a decrease at M = 1.00 and all subsonic speeds. The M = 1.05 indentations resulted in greater decreases in lift-curve slope at most subsonic speeds, but also greater increases at all supersonic test Mach numbers including Mach numbers near 1.

The effect on the variation of aerodynamic-center position due to the M = 1.05 and M = 1.20 indentations was primarily a delay in the rear-ward shift of the aerodynamic-center position with Mach number, as shown in figure 27; however, the indented models had the largest shift in going from subsonic to supersonic speeds.

SUMMARY OF RESULTS

The main results of this investigation are as follows:

1. The indentations designed for the modified wing with a thickened leading edge were as effective in reducing the wave drag as those for the basic wing, particularly at zero lift and at the design Mach number of the indentation.

2. At transonic speeds the zero-lift drag coefficients for the two wings were similar; however, at Mach numbers near 1.2 the basic-wing models consistently had drag coefficients which were lower than modified-wing models with the Sears-Haack body or with indentations designed for the same Mach number.

3. The M = 1.05 indentations were practically as effective as the M = 1.20 indentations at M = 1.20 and as the M = 1.00 indentation (basic wing) at M = 1.00. Thus for the configurations tested the M = 1.05 design is probably the best compromise design for the test Mach number range.

4. For similar or thinner wings and similar body sizes relative to the wings, the wing volume exposed by indentation of the body may be neg-lected in designing indentations for a supersonic Mach number; however, this additional wing volume was included in all the wave-drag computations.

5. The experimental wave-drag coefficients were adequately predicted in each case at all supersonic Mach numbers.

Ames Aeronautical Laboratory
    National Advisory Committee for Aeronautics
        Moffett Field, Calif., Nov. 26, 1956

APPENDIX A

SYMBOLS

A   aspect ratio, $\dfrac{2b}{(1+\lambda)c_\sigma}$

a   dimensionless parameter, $\dfrac{1}{1 - \dfrac{\tan \Omega_{TE}}{\tan \Omega_{LE}}}$ or

$$\left(\frac{x}{c}\right)_{ref} + \frac{A}{4}\left(\frac{1+\lambda}{1-\lambda}\right)(\tan \Lambda_{ref} - \tan \psi)$$

b   model span

C_D drag coefficient

C_{D_O} zero-lift drag coefficient

ΔC_{D_O} rise of C_{D_O} above subsonic level (M ~ 0.8)

C_L lift coefficient

C_m pitching-moment coefficient about $\dfrac{\overline{c}}{4}$ for the basic wing

C_p pressure coefficient, $\dfrac{p-p_\infty}{q}$

c   local chord of wing measured parallel to the plane of symmetry

c_O local chord, c, at intersection of area cut with leading or trailing edge, whichever is the greater distance from the center line
(The edges are considered as extending to their point of intersection.)

$\overline{c}$ mean aerodynamic chord of the total basic wing

c' local chord of the design airfoil sections

e   perpendicular distance from c_O to center line

$\left(\dfrac{L}{D}\right)_{max}$ maximum lift-drag ratio

M   free-stream Mach number

N   number of terms or harmonics used in the theoretical computations
          of wave drag

p   local static pressure on the model

p_∞ free-stream static pressure

q   free-stream dynamic pressure

R   Reynolds number

r   perpendicular distance from edge of body to center line; radius
          of body

S   projection of S_S on a plane perpendicular to x axis

S_S area formed by cutting configurations with planes tangent to the
          Mach cone

S_W total wing area including the region within the body

$S(\xi)$ at ξ, the cross-sectional wing area projected on a plane
          perpendicular to the x axis

t   local wing thickness

$\left[\dfrac{t}{c}\right]$ normalized thickness-chord ratio, $\dfrac{t/c}{(t/c)_{\sigma_{max}}}$

X   planes tangent to the Mach cone

x,y,z   Cartesian coordinates as conventional body axes

x'   distance from the wing leading edge to a point in the wing-chord
          plane measured in the x direction

y'   distance from c_0 to a point in the wing-chord plane measured in
          the negative y direction

α angle of attack

γ constant ratio of thicknesses, $\dfrac{t_\tau}{t_\sigma}$ at a given percent chord

η nondimensionalized variable of integration, $\left(\dfrac{y'}{c_0}\right) \tan \Omega_{LE}$

          (integration from wing extremities to plan-form center line)

η_B limit of integration, at the body, $\eta_e - \eta_r$

η_T limit of integration, at the wing tip, equals $\eta_e - \eta_{b/2}$ for $\eta_{b/2} < \eta_e$ and 0 for $\eta_{b/2} \geq \eta_e$

θ angle between the z axis and the intersection of the cutting plane X with the yz plane

Λ_{LE} leading-edge sweep

Λ_{TE} trailing-edge sweep

Λ_{ref} reference percent-chord-line sweep

λ taper ratio, $\dfrac{c_T}{c_\sigma}$

ξ distance in the x direction measured from the intersection of the configuration center line and the wing leading edge

ψ angle in the xy plane between the intercept of the cutting planes X with the xy plane and the positive y axis, $\arctan(\sqrt{M^2-1} \cos \theta)$

Ω_{LE} sheared-wing leading-edge sweep, $\arctan(\tan \Lambda_{LE} - \tan \psi)$

Ω_{TE} sheared-wing trailing-edge sweep, $\arctan(\tan \Lambda_{TE} - \tan \psi)$

Subscripts

i   indentation

max   maximum value

ref   reference percent chord line

σ body center-line location

τ wing tip location

APPENDIX B

COMPUTATION OF WING CROSS-SECTIONAL AREAS

AND RE-INDENTATIONS

A wing cross-sectional-area computation procedure applicable to wings of any sweep and any normal taper ratio ($0 \leq \lambda \leq 1$) is presented. The procedure is, to a large extent, based on the work of Jarmolow and Vandrey, reference 9. The equations are written primarily for wings with straight-line surface elements along a constant-percent-chord location. The airfoil section at the center of the wing may be similar or different from the tip airfoil section. An equation is also presented for a wing with linear thickness-ratio variations.

Indentation formulas which include the added wing area due to the indentation (re-indentation) are written for a Mach number of 1.00 and for supersonic Mach numbers. These equations are approximations, but are considered entirely satisfactory for thin wings and for indentations that are not too abrupt.

COMPUTATION OF WING CROSS-SECTIONAL AREAS

General Area Equation for Wings With Linear Variation
of Physical Thickness

The general equation in nondimensionalized form, which is derived later in this appendix, is:

$$\frac{S(\xi)}{c_\sigma{}^2} = K \left(\frac{c_0}{c_\sigma}\right)_\xi \int_{\eta_1}^{\eta_2} f_1(\eta) \left\{ 1 - [1 - \lambda f_2(\eta)] \frac{\eta_e{}^{-\eta}}{\eta_{b/2}} \right\} d\eta \qquad (1)$$

where

$$K = \frac{(t/c)_{\sigma_{max}}}{\tan \Omega_{LE}}$$

$$f_1(\eta) = \left[\frac{t}{c}\right]_\sigma = \text{normalized thickness-chord ratio along center-line chord}$$
(varies with percent chord, a function of η)

$$f_2(\eta) = \frac{[t/c]_T}{[t/c]_\sigma}$$

$\left[\dfrac{t}{c}\right]_T$ = normalized thickness-chord ratio along tip chord (varies with percent chord, a function of η)

The equation gives the wing cross-sectional area at each station ξ, along the center line; η is the variable; for each ξ, c_0 is a constant; however, c_0 is a function of ξ.

Equation (1) can be used for any Mach number. For Mach number 1.00 the wing plan form is handled directly; however, for Mach numbers greater than 1, the symbol, tan Ω_{LE} includes the effect of "shearing" the $M > 1$ wing to an equivalent $M = 1$ wing. (See following discussion and definitions in fig. 28 and Appendix A.)

For Mach number 1.00, the wing-area cuts are perpendicular to the x axis (fig. 28(a)). One computation of wing cross-sectional area at each station, ξ, is all that is needed. For Mach numbers greater than 1.00, the Mach planes will no longer cut the wing perpendicular to the x axis. If the wing is considered to lie within the xy plane, for Mach numbers greater than 1.00, the Mach planes tangent to the Mach cone will cut the wing not only at the angle, $\psi = \arctan\sqrt{M^2-1}$, but also at smaller angles, $\psi = \arctan\sqrt{M^2-1}\cos\theta$, (due to planes tangent to the Mach cone along a line not in the xy plane). In order to compute the complete drag for one Mach number, $M > 1$, the areas at various roll angles θ should be computed. (See ref. 4.)

The equations have been worked out for planes cutting a wing perpendicular to the x axis. For $M = 1.00$, then, the cutting planes are in the proper position. For Mach numbers greater than 1.00, the shearing technique of reference 9 was used to make all cutting planes perpendicular to the x axis. The wings can be sheared such that the resulting area perpendicular to the x axis is an area equivalent to the projection of the oblique cut on the yz plane. Thus, the procedure is to shear the wings and compute the area perpendicular to the x axis as in the $M = 1.00$ case. The shearing is defined in figure 28(b). This shearing will also affect the wing plan-form parameter a since a is a function of the angles shown. The sheared wing will have a new leading-edge angle,

$$\Omega_{LE} = \arctan(\tan\Lambda_{LE} - \tan\psi)$$

and a new trailing-edge angle

$$\Omega_{TE} = \arctan(\tan\Lambda_{TE} - \tan\psi)$$

For $M = 1.00$, tan ψ is zero. Note that tan ψ is a function of the Mach number and the cosine of the roll angle, and as $\cos\theta$ changes from plus to minus, tan ψ will also change.

In this analysis the wing thickness has been considered as lying in the xy plane. This concept introduces an error in the vertical direction for Mach numbers greater than 1.00. However, this error is considered insignificant for thin wings ($(t/c)_{max}$ = 0.06 or less).

The equation for computing areas for wings with linear spanwise variation in thickness along constant-percent-chord lines will be developed from the simple area integral equation. With this linear thickness variation the wing surface is composed of straight-line elements. The cross-sectional area at one longitudinal station, ξ, may be written as

$$S(\xi) = \int t \, dy'$$ (2)

where y' is taken in the opposite direction to y and is measured from the spanwise station at which the chord length is c_0. One may write a new variable of integration, η, by nondimensionalizing y' as follows:

$$\eta = \frac{y'}{c_0} \tan \Omega_{LE}$$ (3)

For $M = 1.00$ cuts $\eta = \frac{y'}{c_0} \tan \Lambda_{LE}$ which is similar to the notation of reference 9.

The thickness, t, at any point on the wing plan form will be expressed as a function of the thickness at the center of the wing, t_σ, and the thickness at the tip, t_T; and t_T and t_σ will be the thickness on the percent-chord line passing through this point (fig. 28(a)). At any percent-chord station:

$$t = t_\sigma - (t_\sigma - t_T) \frac{\Delta y'}{b/2}$$

where, from equation (3) and figure 28,

$$\frac{\Delta y'}{b/2} = \frac{e - y'}{b/2} = \frac{\eta_e - \eta}{\eta_{b/2}}$$

and thus

$$t = t_\sigma - (t_\sigma - t_T) \frac{\eta_e - \eta}{\eta_{b/2}}$$ (4)

The chord, c, at any point can be expressed as a function of the chord, c_0, located at the intersection of the area cut and the outer edge of the wing (extended if necessary), figure 28, and as a function of the tangents at the leading and trailing edges.

$$c = c_0 + y'(\tan \Lambda_{LE} - \tan \Lambda_{TE}) = c_0\left(1 + \frac{\eta}{a}\right) \tag{5}$$

Note that a change in $\tan \psi$ does not affect the chord, c. An expression for the <u>ratio</u> <u>of</u> <u>thickness</u> <u>to</u> <u>chord</u> can be obtained by combining equations (4) and (5) and introducing c_σ.

$$\frac{t}{c} = \frac{c_\sigma}{c_0[1+(\eta/a)]}\left[\frac{t_\sigma}{c_\sigma} - \left(\frac{t_\sigma}{c_\sigma} - \frac{t_T}{c_\sigma}\right)\frac{\eta_e - \eta}{\eta_{b/2}}\right]$$

and since

$$\frac{t_T}{c_\sigma}\frac{c_T}{c_T} = \frac{t_T}{c_T}\frac{c_T}{c_\sigma} = \frac{t_T}{c_T}\lambda$$

then

$$\frac{t}{c} = \frac{c_\sigma}{c_0[1+(\eta/a)]}\left[\frac{t_\sigma}{c_\sigma} - \left(\frac{t_\sigma}{c_\sigma} - \lambda\frac{t_T}{c_T}\right)\frac{\eta_e - \eta}{\eta_{b/2}}\right] \tag{6}$$

The <u>normalized</u> <u>thickness</u> <u>ratio</u> is the ratio of thickness-to-chord ratio at <u>any point</u>, to the <u>maximum</u> thickness-to-chord ratio at the center line; the normalized thickness ratio will range between 0 and 1 unless the tip airfoil section has the greater maximum thickness-to-chord ratio. By definition,

$$\left[\frac{t}{c}\right] = \frac{t/c}{(t/c)_{\sigma_{max}}} \tag{7}$$

then

$$\left[\frac{t}{c}\right]_T = \frac{(t/c)_T}{(t/c)_{\sigma_{max}}} \; ; \quad \left[\frac{t}{c}\right]_\sigma = \frac{(t/c)_\sigma}{(t/c)_{\sigma_{max}}} \; ; \text{ etc.}$$

$$\left[\frac{t}{c}\right] = \frac{c_\sigma}{c_o}\left(\left[\frac{t}{c}\right]_\sigma - \left\{\left[\frac{t}{c}\right]_\sigma - \lambda\left[\frac{t}{c}\right]_T\right\}\frac{\eta_e - \eta}{\eta_{b/2}}\right)\frac{1}{1+(\eta/a)}$$

then from definitions given with equation (1),

$$\left[\frac{t}{c}\right] = \frac{c_\sigma}{c_o}f_1(\eta)\left\{1-[1-\lambda f_2(\eta)]\frac{\eta_e-\eta}{\eta_{b/2}}\right\}\frac{1}{1+(\eta/a)} \tag{8}$$

The final equation (eq. (1)) is obtained by substituting equations (3), (5), (7), and (8) in equation (2) and nondimensionalizing with the center-line chord,

$$\frac{S(\xi)}{c_o^2} = \frac{(c_o/c_\sigma)_\xi(t/c)_{\sigma_{max}}}{\tan\Omega_{LE}}\int_{\eta_1}^{\eta_2}f_1(\eta)\left\{1-[1-\lambda f_2(\eta)]\frac{\eta_e-\eta}{\eta_{b/2}}\right\}d\eta$$

which is equation (1). This will give the nondimensionalized cross-sectional area at station, ξ, for the particular Mach number and θ determining Ω_{LE}.

For convenience in computing, $\tan\Lambda_{LE}$, $\tan\Lambda_{TE}$ and a can be defined in terms of a reference angle, such as that used in a wing design.

$$\tan\Lambda_{LE} = \frac{4}{A}\left(\frac{x'}{c}\right)_{ref}\left(\frac{1-\lambda}{1+\lambda}\right)+\tan\Lambda_{ref} \tag{9a}$$

$$\tan\Lambda_{TE} = \frac{-4}{A}\left[1-\left(\frac{x'}{c}\right)_{ref}\right]\left(\frac{1-\lambda}{1+\lambda}\right)+\tan\Lambda_{ref} \tag{9b}$$

$$a = \left(\frac{x'}{c}\right)_{ref}+\frac{A}{4}\left(\frac{1+\lambda}{1-\lambda}\right)(\tan\Lambda_{ref}-\tan\psi) \tag{9c}$$

The $\tan\Omega_{LE}$ and $\tan\Omega_{TE}$ can also be expressed in terms of a. This may be a convenient form since the limits for η are given, as they were originally derived in reference 9, in these terms:

$$\tan\Omega_{LE} = \frac{4(1-\lambda)a}{(1+\lambda)A} \tag{10a}$$

$$\tan\Omega_{TE} = \frac{4(1-\lambda)(a-1)}{(1+\lambda)A} \tag{10b}$$

Application of equation (1).- For certain types of thickness variation, the general equation can be simplified considerably.

Case I: For the most general case, the thickness distribution at the root chord can be different from the thickness distribution at the tip chord. There is _linear_ _variation_ _in_ _the_ _physical_ _thickness_ along a constant-percent-chord line. This means that $f_1(\eta)$ and $f_2(\eta)$ remain variables.

Case II: A simplification in case I is possible when the root and tip sections are the same type but have different ratios of $(t/c)_{max}$, that is,

$$\left(\frac{t_T}{t_\sigma}\right)_{x'/c} = \gamma, \text{ a constant}$$

and

$$\left(\frac{t_T}{t_\sigma}\right)_{x'/c} \neq \frac{c_T}{c_\sigma}$$

therefore

$$f_2(\eta) = \frac{\gamma}{\lambda}$$

For this situation equation (1) reduces to:

$$\frac{S(\xi)}{c_\sigma^2} = \frac{(c_0/c_\sigma)_\xi (t/c)_{\sigma_{max}}}{\tan \Omega_{LE}} \int_{\eta_1}^{\eta_2} f_1(\eta)\left[1-(1-\gamma)\frac{\eta_e-\eta}{\eta_{b/2}}\right]d\eta \qquad (11)$$

Case III: A further simplification of case II is possible when the streamwise airfoils at the root and tip are similar, that is, the thickness distribution is the same at the root and the tip.

$$\left(\frac{t_T}{t_\sigma}\right)_{x'/c} = \frac{c_T}{c_\sigma} = \lambda$$

therefore

$$f_2(\eta) = 1$$

The equation for the normalized thickness ratio, (8), becomes:

$$\left[\frac{t}{c}\right] = \frac{c_\sigma}{c_o} f_1(\eta)\left[1-(1-\lambda)\frac{\eta_e-\eta}{\eta_{b/2}}\right]\frac{1}{1+(\eta/a)}$$

and from equations (3), (5), and (10)

$$\left[1-(1-\lambda)\frac{\eta_e-\eta}{\eta_{b/2}}\right] = \frac{c_o}{c_\sigma}\left(1+\frac{\eta}{a}\right)$$

therefore

$$\left[\frac{t}{c}\right] = f_1(\eta)$$

Equation (1) reduces to (see eqs. (2) and (5)):

$$\frac{S(\xi)}{c_\sigma{}^2} = \frac{(t/c)_{\sigma_{max}}(c_o/c_\sigma)_\xi{}^2}{\tan \Omega_{LE}}\int_{\eta_1}^{\eta_2}f_1(\eta)\left(1+\frac{\eta}{a}\right)d\eta \qquad (12)$$

With only a slight alteration in equation (1), a different type of wing can be handled, a wing with <u>linear</u> variation <u>in thickness-chord ratio</u> which may be called case IV. For this wing, the ratio of thickness to chord (rather than the thickness itself) will be linear. The equation for ratio of thickness to chord may be defined as:

$$\frac{t}{c} = \left(\frac{t}{c}\right)_\sigma-\left[\left(\frac{t}{c}\right)_\sigma-\left(\frac{t}{c}\right)_\tau\right]\frac{\eta_e-\eta}{\eta_{b/2}}$$

and the normalized thickness ratio (eq. (8)) becomes:

$$\left[\frac{t}{c}\right] = \left[\frac{t}{c}\right]_\sigma-\left\{\left[\frac{t}{c}\right]_\sigma-\left[\frac{t}{c}\right]_\tau\right\}\frac{\eta_e-\eta}{\eta_{b/2}} = f_1(\eta)\left\{1-\left[1-f_2(\eta)\right]\frac{\eta_e-\eta}{\eta_{b/2}}\right\}$$

and the equation for the nondimensionalized area becomes:

$$\frac{S(\xi)}{c_\sigma{}^2} = \frac{(c_o/c_\sigma)_\xi{}^2(t/c)_{\sigma_{max}}}{\tan \Omega_{LE}}\int_{\eta_1}^{\eta_2}f_1(\eta)\left\{1-[1-f_2(\eta)]\frac{\eta_e-\eta}{\eta_{b/2}}\right\}\left(1+\frac{\eta}{a}\right)d\eta$$

$$(13)$$

In general, equations for the streamwise shapes of the wing at the root and the tip will not be available; if plots of these shapes, $[t/c]_\sigma = f_1(\eta)$ and $[t/c]_\tau = [t/c]_\sigma f_2(\eta)$, are given, approximate or mechanical integrating methods can be used. However, if the streamwise shapes at the root and tip are expressible in equation form as functions of η, the area can be found by direct integration.

$\xi = \eta_e c_0$

$x' = \eta c_0$

Sketch (a)

$\xi = \eta_e c_0 + c_0$

$x' = \eta c_0 + c_0$

Sketch (b)

For variations in wing plan form, the primary change in form of the equation will be in the limits of integration. Two symbols take on a different meaning for wings with certain sweeps. For area cuts intersecting a sweptback leading edge (extended if necessary), ξ and x' are measured in the x direction from the leading edge to the intersection of the leading edge with c_0 (sketch (a)). For area cuts intersecting a sweptforward trailing edge, ξ and x' are measured in the x direction from the leading edge to the intersection of the trailing edge with c_0 (sketch (b)). Note that for the sweptforward leading edge, η becomes negative. In both of the above cases, the leading and trailing edges are considered as extending to their point of intersection in order to define the limits of integration for some of the area cuts. For the cuts where this is necessary c_0 will lie beyond the wing tip. Thus the following two sets of equations are needed: one for the sweptback leading edge (set 1) and another for the sweptforward trailing edge (set 2). Set 2 can be obtained from set 1 by replacing x' in set 1 by $x'-c_0$ and by replacing ξ in set 1 by $\xi-c_0$, thus obtaining equivalent-meaning values for ηc_0 and $\eta_e c_0$ in terms of ξ and x'.

<u>SET 1[1]</u>
(Sweptback leading edge)

$$c_0/c_\sigma = 1-(\xi/ac_\sigma)$$

$$\eta_e = \frac{\xi/c_\sigma}{1-(\xi/ac_\sigma)}$$

$$\eta_{b/2} = \frac{[(b/2)/c_\sigma](\tan \Omega_{LE})}{1-(\xi/ac_\sigma)}$$

$$\eta_r = \frac{r/c_\sigma(\tan \Omega_{LE})}{1-(\xi/ac_\sigma)}$$

$$\eta_B = \eta_e - \eta_r$$

$$\eta_T = \eta_e - \eta_{b/2} \quad \text{for} \quad \eta_{b/2} < \eta_e$$

$$= 0 \quad \text{for} \quad \eta_{b/2} \geq \eta_e$$

$$\frac{x'}{c} = \frac{\eta}{1+(\eta/a)}$$

<u>SET 2[1]</u>
(Sweptforward trailing edge)

$$c_0/c_\sigma = [1-(\xi/ac_\sigma)] \div [1-(1/a)]$$

$$\eta_e = \frac{(\xi/c_\sigma)-1}{1-(\xi/ac_\sigma)}$$

$$\eta_{b/2} = \frac{[(b/2)/c_\sigma]\tan \Omega_{LE}[1-(1/a)]}{1-(\xi/ac_\sigma)}$$

$$\eta_r = \frac{(r/c_\sigma)\tan \Omega_{LE}[1-(1/a)]}{1-(\xi/ac_\sigma)}$$

$$\eta_B = \eta_e - \eta_r$$

$$\eta_T = \eta_e - \eta_{b/2} \quad \text{for} \quad \eta_{b/2} < \eta_e$$

$$= 0 \quad \text{for} \quad \eta_{b/2} \geq \eta_e$$

$$\frac{x'}{c} = \frac{\eta+1}{1+(\eta/a)}$$

When the wing cross-sectional area cut coincides with the unswept percent chord line, equation (1) becomes indeterminate. The following two equations, (14) for linear physical thickness and (14a) for linear thickness ratio, can be used for computing the wing cross-sectional area:

$$\frac{S(\xi)}{c_\sigma^2} = \frac{(t/c)_{\sigma_{max}}[(b/2)-r]}{2c_\sigma} \left(\left\{ \left[\frac{t}{c}\right]_\sigma + \lambda\left[\frac{t}{c}\right]_T \right\} - \frac{r}{b/2}\left\{ \left[\frac{t}{c}\right]_\sigma - \lambda\left[\frac{t}{c}\right]_T \right\} \right)_{\left(\frac{x'}{c} = \frac{\xi}{c_\sigma}\right)}$$

(14)
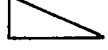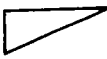
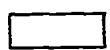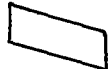[1]Originally derived in reference 9.

$$\frac{S(\xi)}{c_\sigma{}^2} = \frac{(t/c)_{\sigma_{max}}[(b/2)-r]}{6c_\sigma} \left(\left\{ \left[\frac{t}{c}\right]_\sigma (2+\lambda) + \left[\frac{t}{c}\right]_\tau (2\lambda+1) \right\} - \right.$$

$$\frac{r}{b/2} \left\{ \left[\frac{t}{c}\right]_\sigma (4-\lambda) - \left[\frac{t}{c}\right]_\tau (2\lambda+1) \right\} +$$

$$\left. \frac{2r^2}{(b/2)^2} \left\{ \left[\frac{t}{c}\right]_\sigma (1-\lambda) - \left[\frac{t}{c}\right]_\tau (1-\lambda) \right\} \right) \qquad (14a)$$

$$\left(\frac{x'}{c} = \frac{\xi}{c_\sigma} \right)$$

The following tables of plan forms indicate the differences that occur in the area solution for the various wings. (The quantity a is used as an indicator of the sheared sweep of the leading and trailing edges, Ω_{LE} and Ω_{TE}, respectively, since it is a function of both of these.)

Equations for Wings of Different Plan Forms

For wings with taper: $0 \leq \lambda < 1$				
a	LE	TE	Equations	Wing shape diagram
$\infty > a > 1$	Sweptback	Sweptback	Set 1 and eq. (1)	
$a = 1$	Sweptback	Unswept	Set 1 and eq. (1)	
$1 > a > 0$	Sweptback	Sweptforward		
	When $\xi/c_\sigma < a$		Set 1 and eq. (1)	Upper part
	$\xi/c_\sigma = a$		Eq. (14)	Dividing line
	$\xi/c_\sigma > a$		Set 2 and eq. (1)	Lower part
$a = 0$	Unswept	Sweptforward		
	(Indeterminate in this form: Turn wing over and handle same as second case.)			
$0 > a > -\infty$	Sweptforward	Sweptforward	Set 2 and eq. (1)	

For wings with no taper: $\lambda = 1$, $a = \infty$			
Tan Ω_{LE}	Ω_{LE}, Ω_{TE}	Equations	Wing shape diagram
Tan $\Omega_{LE} > 0$	Sweptback	Set 1 and eq. (1)	
Tan $\Omega_{LE} = 0$	Unswept	Eq. (14)	
Tan $\Omega_{LE} < 0$	Sweptforward	Set 2 and eq. (1)	

NOTE: The above tables apply for wings with <u>linear</u> <u>physical</u> <u>thickness</u> on a constant-percent-chord line; these tables may also be used for wings with <u>linear</u> <u>thickness</u> <u>ratio</u> on a constant-percent-chord line (see variation in thickness, case IV) if equation (13) is substituted for equation (1) and equation (14a) for equation (14).

Limits of integration (fig. 28(c)) are determined from the geometry of the wing. The limit at the outer edge of a wing will be, η_1.

$$\eta_1 = \eta_T \tag{15}$$

$$\eta_T = 0 \quad \text{when} \quad \eta_e \leq \eta_{b/2}$$

$$\eta_T = \eta_e - \eta_{b/2} \quad \text{when} \quad \eta_e > \eta_{b/2}$$

Limit at the inner edge of the wing will be, η_2. For some wing sweeps there will be a maximum value for η which will be called η_{max} (fig. 28(c)).

$$\eta_{max} = \frac{y'_{max}}{c_0} \tan \Omega_{LE}$$

Maximum values for η

λ	tan Ω_{LE} and tan Ω_{TE}	η_{max}
< 1	Sweptback	$\dfrac{a}{a-1}$
< 1	Sweptforward	-1
$= 1$	Sweptback	$+1$
$= 1$	Sweptforward	-1
	All others	∞

$$\eta_2 = \eta_{max} \qquad \text{when} \quad \eta_e \geq \eta_{max}$$

$$\eta_2 = \eta_e \qquad \text{when} \quad \eta_e < \eta_{max}$$

When there is no maximum value (η_{max} is infinite), $\eta_2 = \eta_e$. For the cross-sectional area of the wings with a body, use η_B in place of η_e. If the cross-sectional area of the wings with an indented body is desired, use η_{B_i}.

For the computation of wing cross-sectional area with a body (with or without indentation) the change in the general equation will be in the limits of integration. For this condition, only the part of the wing outside the body need be considered. This means a limit of integration to correspond with the edge at the body will be needed,[2] η_B.

Sketch (c)

$$\eta_B c_0 = (e-r)(\tan \Omega_{LE})$$
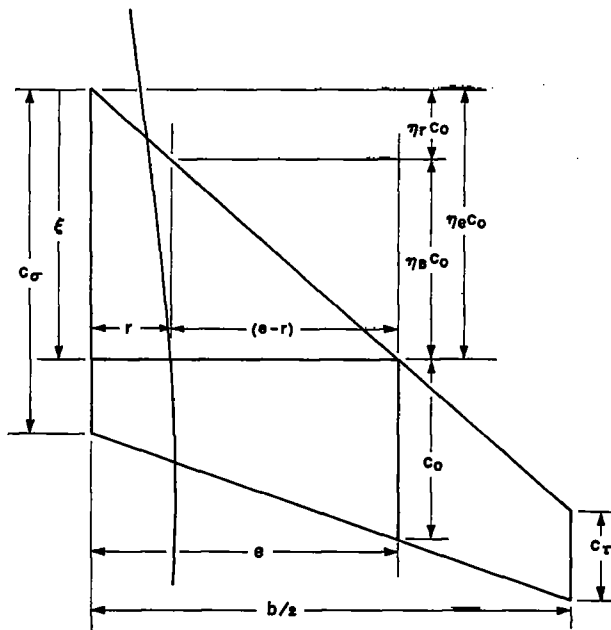
$$\eta_B = \frac{e}{c_0}(\tan \Omega_{LE}) - \frac{r}{c_0}(\tan \Omega_{LE})$$

$$\eta_B = \eta_e - \eta_r \tag{17}$$

---

[2]Since the wing is thin, the curvature at the body in the yz plane will be ignored.

ADDED WING CROSS-SECTIONAL AREA DUE TO INDENTATION; $\Delta S(\xi)$

Let η_{B_i} equal the limits of integration on an indented body.

$$\frac{\Delta S(\xi)}{c_\sigma^2} = \frac{(c_0/c_\sigma)_\xi (t/c)_{\sigma_{max}}}{\tan \Omega_{LE}} \int_{\eta_B}^{\eta_{B_i}} f_1(\eta) \left\{ 1-[1-\lambda f_2(\eta)] \frac{\eta_e - \eta}{\eta_{b/2}} \right\} d\eta \qquad (18)$$

Sketch (d)
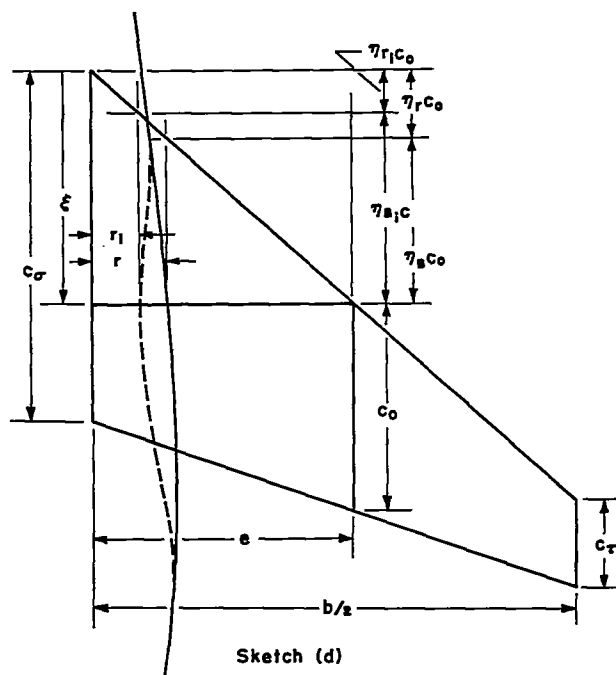
In order to compute r_i easily an approximation of $\Delta S(\xi)$ is needed in terms of r_i.

$$\frac{\Delta S(\xi)}{c_\sigma^2} \approx \frac{(c_0/c_\sigma)_\xi (t/c)_{\sigma_{max}}}{\tan \Omega_{LE}} f_1(\eta) \left\{ 1-[1-\lambda f_2(\eta)] \frac{\eta_e - \eta}{\eta_{b/2}} \right\}_{\eta=\eta_B} \left(\eta_{B_i} - \eta_B \right)$$

$$\eta_{B_i} - \eta_B = (\eta_e - \eta_{r_i}) - (\eta_e - \eta_r) = \eta_r - \eta_{r_i}$$

$$\frac{\Delta S(\xi)}{c_\sigma{}^2} \approx \frac{(c_\sigma/c_\sigma)_\xi (t/c)_{\sigma_{max}}}{\tan \Omega_{LE}} f_1(\eta)\left\{1-[1-\lambda f_2(\eta)]\frac{\eta_e{}^{-\eta}}{\eta_{b/2}}\right\}_{\eta=\eta_B} \frac{(r-r_1)(\tan \Omega_{LE})}{(c_o)_\xi}$$

$$\Delta S(\xi) \approx c_\sigma \left(\frac{t}{c}\right)_{\sigma_{max}} f_1(\eta)\left\{1-[1-\lambda f_2(\eta)]\frac{\eta_e{}^{-\eta}}{\eta_{b/2}}\right\}_{\eta=\eta_B} (r-r_1) \qquad (19)$$

Let

$$G = c_\sigma \left(\frac{t}{c}\right)_{\sigma_{max}} f_1(\eta)\left\{1-[1-\lambda f_2(\eta)]\frac{\eta_e{}^{-\eta}}{\eta_{b/2}}\right\}_{\eta=\eta_B} \qquad (20)$$

$$\Delta S(\xi) \approx G(r-r_1) \qquad (21)$$

COMPUTATION OF THE RE-INDENTATION

The total cross-sectional area of the exposed wing with the re-indented body is equal to the difference in cross-sectional area between the original body and the re-indented body. Let

$S_B(\xi,r)$ = cross-sectional area of the original body, at ξ.

$S_{B_1}(\xi,r_1)$ = cross-sectional area of the re-indented body, at ξ.

$S_E(\xi,r)$ = cross-sectional area of the exposed wing (with the original body) at ξ.

$S_{E_1}(\xi,r_1)$ = cross-sectional area of the exposed wing (with the re-indented body) at ξ.

The exposed wing cross-sectional area is:

$$S_{E_i}(\xi,r_i) = S_E(\xi,r)+\Delta S(\xi) = S_B(\xi,r)-S_{B_i}(\xi,r_i)$$

$$S_E(\xi,r)+\Delta S(\xi) \approx S_E(\xi,r)+G(r-r_i)$$

Solve for the unknown r_i; this is the general approximate formula for re-indentation:

$$S_{B_i}(\xi,r_i)-Gr_i \approx S_B(\xi,r)-S_E(\xi,r)-rG \tag{22}$$

For a body of revolution at $M = 1.0$ the cross-sectional area of the body becomes:

$$S_B(\xi,r) = \pi r^2 \qquad S_{B_i}(\xi,r_i) = \pi r_i^2$$

Substituting in equation (22):

$$\pi r_i^2-Gr_i \approx \pi r^2-S_E(\xi,r)-rG$$

$$r_i \approx \frac{G\pm\sqrt{G^2-4\pi[-\pi r^2+S_E(\xi,r)+rG]}}{2\pi}$$

when $G \rightarrow 0$; $S_E(\xi,r) \rightarrow 0$; $r_i \rightarrow r$

$$r_i \approx \frac{G}{2\pi} + \sqrt{\left(\frac{G}{2\pi}\right)^2+r^2-\frac{rG}{\pi}-\frac{S_E(\xi,r)}{\pi}} \tag{23}$$

Note: When $\dfrac{\xi-C_\sigma}{\tan\Omega_{TE}}$ is greater than r, that is, aft of the trailing-edge juncture, G equals 0; hence equation (23) reduces to

$$r_i = \sqrt{\frac{\pi r^2-S_E(\xi,r)}{\pi}} \tag{24}$$

An approximation of the re-indentation was made for $M = 1.2$ (body of revolution) by using in equation (23) the average exposed wing cross-sectional area, $S_{E_A}(\xi,r)$, (i.e., the average of the areas at the various angles of θ for $M = 1.2$) in place of the exposed wing area, $S_E(\xi,r)$. Thus, the re-indentation was made on the plane perpendicular to the x axis and $\Delta S(\xi)$ was evaluated in this plane. For greater accuracy in evaluating the wing areas (S_{E_A} and the final wing areas), the body, as well as the wings, was sheared for each θ angle.

REFERENCES

1. Graham, David, and Evans, William T.: Investigation of the Effects of an Airfoil Section Modification on the Aerodynamic Characteristics at Subsonic and Supersonic Speeds of a Thin Swept Wing of Aspect Ratio 3 in Combination With a Body. NACA RM A55D11, 1955.

2. Jones, Robert T.: Theory of Wing-Body Drag at Supersonic Speeds. NACA RM A53H18a, 1953.

3. Whitcomb, Richard T., and Fischetti, Thomas L.: Development of a Supersonic Area Rule and an Application to the Design of a Wing-Body Combination Having High Lift-to-Drag Ratios. NACA RM L53H31a, 1953.

4. Holdaway, George H., and Mersman, William A.: Application of Tchebichef Form of Harmonic Analysis to the Calculation of Zero-Lift Wave Drag of Wing-Body-Tail Combinations. NACA RM A55J28, 1956.

5. Spiegel, Joseph M., and Lawrence, Leslie F.: A Description of the Ames 2- by 2-Foot Transonic Wind Tunnel and Preliminary Evaluation of Wall Interference. NACA RM A55I21, 1956.

6. Holdaway, George H.: Additional Comparisons Between Computed and Measured Transonic Drag-Rise Coefficients at Zero Lift for Wing-Body-Tail Configurations. NACA RM A55F06, 1955.

7. Boyd, John W., Migotsky, Eugene, and Wetzel, Benton E.: A Study of Conical Camber for Triangular and Sweptback Wings. NACA RM A55G19, 1955.

8. Friedman, Morris D., and Cohen, Doris: Arrangement of Fusiform Bodies to Reduce Wave Drag at Supersonic Speeds. NACA Rep. 1236, 1955.

9. Jarmolow, K., and Vandrey, F.: An Exact Method for the Rapid Calculation of the Area Distributions of Wings of Trapezoidal Geometry Based on a New Interpretation of the Area Rule. Eng. Rep. No. 7689, Glenn L. Martin Co., Aug. 24, 1955.

TABLE I.- COORDINATES OF THE AIRFOIL SECTIONS

[All coordinates are referred to the chord of the NACA 64A006 section and are in terms of percent of that chord. Asterisks indicate coordinates that are identical to those of the basic wing. The 64A006 sections are perpendicular to their own quarter chord line, which is swept 39.45°. (Sweep of streamwise quarter chord line is 40.60°.)]

Sections normal to 39.45° sweep line			Streamwise sections		
Station	Basic wing (64A006)	Modified wing	Station	Basic wing	Modified wing
-1.50		0	-2.03		0
-1.25		.733	-1.69		.705
-1.00		.988	-1.35		.948
-.75		1.173	-1.01		1.123
-.25		1.455	.34		1.395
.00	0	1.573	.00	0	1.505
.25	---	1.675	.34	---	1.603
.50	.485	1.765	.672	.464	1.685
.75	.585	1.843	1.008	.559	1.750
1.25	.739	1.980	1.677	.705	1.893
2.5	1.016	2.211	3.340	.965	2.098
5.0	1.399	2.500	6.624	1.317	2.356
7.5	1.684	2.677	9.845	1.571	2.501
10	1.919	2.800	13.02	1.775	2.585
15	2.283	2.947	19.21	2.077	2.679
20	2.557	3.004	25.20	2.289	2.690
25	2.757	2.996	30.99	2.428	2.637
30	2.896	2.995	36.62	2.511	2.598
35	2.977	2.999	42.05	2.541	2.558
40	2.999	3.000	47.32	2.520	2.520
45	2.945	*	52.44	2.438	*
50	2.825		57.41	2.302	
55	2.653		62.22	2.132	
60	2.438		66.90	1.931	
65	2.188		71.45	1.709	
70	1.907		75.87	1.468	
75	1.602		80.17	1.216	
80	1.285		84.35	.963	
85	.967		88.42	.715	
90	.649		92.38	.474	
95	.331		96.24	.238	
100	.013		100.00	.009	
Leading-edge radius	.246	1.190		.167	.810
Center of leading-edge radius	x = 0.246	x = -0.310		x = 0.167	x = -1.22

TABLE II.- RADII OF BODIES INDENTED FOR EACH WING FOR DIFFERENT DESIGN MACH NUMBERS, INCHES

Body station x, in.	Sears-Haack body	Basic-wing bodies				Modified-wing bodies		
		M = 1.00 re-indentation	M = 1.05	M = 1.20	M = 1.20 re-indentation	M = 1.05	M = 1.20	M = 1.20 re-indentation
0 ↓ 34.88	0 ↓ 4.00 }	Radii the same for all bodies. See figure 3 for body shape and equation.					(a)	(a)
35.38	4.03	4.03	4.03	4.03ᵃ	4.03ᵃ	4.03	4.01	4.01
36.05	4.06	4.06	4.06	4.04	4.04	4.06ᵃ	4.01	4.01
37.05	4.10	4.10	4.10ᵃ	4.05	4.05	4.08	3.99	3.99
38.39	4.15	4.15ᵃ	4.12	4.04	4.04	4.07	3.93	3.91
40.06	4.21	4.14	4.11	4.00	3.99	4.00	3.82	3.78
41.73	4.27	4.09	4.08	3.94	3.90	3.90	3.70	3.63
43.39	4.32	4.00	4.01	3.81	3.76	3.78	3.54	3.42
45.06	4.36	3.89	3.91	3.68	3.59	3.66	3.41	3.26
46.73	4.40	3.76	3.78	3.55	3.42	3.52	3.31	3.14
48.40	4.43	3.61	3.64	3.44	3.27	3.38	3.23	3.03
50.07	4.46	3.45	3.51	3.38	3.18	3.26	3.19	2.98
51.74	4.48	3.27	3.67	3.33	3.13	3.14	3.15	2.93
53.41	4.49	3.11	3.24	3.29	3.08	3.02	3.12	2.91
55.08	4.50	2.98	3.13	3.28	3.10	2.93	3.17	2.99
56.75	4.50	2.90	3.07	3.38	3.26	2.90	3.26	3.12
58.42	4.49	2.86	3.10	3.51	3.42	2.95	3.40	3.31
60.08	4.48	2.89	3.17	3.60	3.53	3.04	3.50	3.44
61.75	4.47	2.97	3.27	3.69	3.66	3.17	3.60	3.57
63.42	4.44	3.08	3.42	3.76	3.74	3.34	3.68	3.66
65.09	4.42	3.26	3.61	3.82	3.82	3.54	3.75	3.75
66.76	4.38	3.49	3.75	3.86	3.86	3.70	3.80	3.80
68.43	4.34	3.69	3.85	3.89	3.89	3.80	3.84	3.84
70.10	4.29	3.85	3.91	3.90	3.90	3.86	3.85	3.85
71.77	4.24	3.85	3.94	3.89	3.89	3.90	3.85	3.85
73.44	4.18	4.02	3.95	3.88	3.88	3.92	3.85	3.85
75.11	4.11	4.06	3.94	3.85	3.85	3.93	3.82	3.82
76.77	4.04	4.04	3.92	3.81	3.81	3.91	3.80	3.80
78.44	3.96	3.96	3.88	3.76	3.76	3.87	3.74	3.74
80.11	3.88	3.88	3.82	3.71	3.71	3.83	3.69	3.69
81.78	3.79	3.79	3.76	3.65	3.65	3.76	3.63	3.63
83.45	3.69	3.69	3.68	3.57	3.57	3.68	3.56	3.56
84.79	3.60	3.60	3.60	3.51	3.51	3.60	3.50	3.50
85.50	3.55	3.55	3.55	3.48	3.48	3.55	3.46	3.46
86.63	3.47	3.47	3.47	3.42	3.42	3.47	3.40	3.40
87.75	3.39	3.39	3.39	3.35	3.35	3.39	3.34	3.34
88.88	3.31	3.31	3.31	3.26	3.26	3.31	3.26	3.26
90.00	3.22	3.22	3.22	3.18	3.18	3.22	3.18	3.18

ᵃStart of the indentation.

TABLE III.- ZERO-LIFT PRESSURE COEFFICIENTS, C_p

(a) Body pressure coefficients; basic wing with Sears-Haack body

ξ/c_j	θ / M = 0.90 Top 0°	Side -90°	M = 0.95 Top 0°	Side -90°	M = 1.00 Top 0°	Side -90°	M = 1.05 Top 0°	Side -90°	M = 1.10 Top 0°	Side -90°	M = 1.20 Top 0°	Side -90°
-1.295	0.100	0.098	0.110	0.117	0.147	0.145	0.167	0.163	0.164	0.164	0.135	0.135
-1.035	---	.027	---	.036	---	.060	---	.082	---	.080	---	.075
-.775	-.003	-.006	.004	-.004	.030	.030	.045	.043	.048	.035	.041	.035
-.5	-.012	-.027	-.024	-.030	-.007	-.012	-.003	.009	.018	.005	.009	.004
-.3	.000	.000	.020	-.010	.025	.020	.040	.020	.050	.030	.050	.030
-.2	-.035	-.020	-.035	-.025	.020	.005	.055	.030	.045	.040	.050	.030
-.1	-.080	-.080	-.115	-.105	-.100	-.110	-.045	-.060	-.040	-.055	-.020	-.045
-.05	---	-.005	---	-.010	---	-.155	---	-.110	---	-.100	---	-.080
0	-.065	.240	-.055	.250	-.160	.200	-.110	.215	-.100	.205	-.075	.180
.05	---	-.003	---	.010	---	.025	---	.020	---	.055	---	.055
.1	-.040	-.073	-.020	-.070	-.040	-.055	-.075	-.050	-.060	-.025	-.050	.000
.2	-.020	-.035	-.010	-.030	.050	.025	-.050	-.090	-.030	-.080	-.040	-.060
.3	.030	-.005	.050	.015	.100	.080	.005	-.040	.010	-.025	.007	-.055
.4	.050	.035	.065	.050	.115	.100	.090	.075	.100	.090	.080	.065
.5	.010	.010	.020	-.005	.065	.050	.050	.020	.060	.040	.060	.035
.6	.080	.060	.100	.080	.155	.130	.140	.110	.145	.135	.120	.095
.7	.010	-.020	.015	-.010	.075	.060	.090	.075	.145	.125	.130	.120
.8	-.080	-.080	-.120	-.120	-.055	-.055	-.040	-.030	.030	.030	.030	.030
.9	-.090	-.055	-.180	-.165	-.115	-.100	-.100	-.080	-.020	-.010	-.015	-.010
.95	---	-.020	---	-.090	---	-.110	---	-.060	---	-.025	---	-.015
1.00	-.060	.020	-.130	-.010	-.155	-.075	-.125	-.040	-.050	-.015	-.050	-.015
1.05	---	.030	---	.020	---	-.065	---	-.060	---	-.005	---	-.020
1.1	-.030	.000	-.030	.010	-.125	-.050	-.155	-.075	-.110	-.030	-.090	-.045
1.2	-.025	-.020	-.015	-.007	-.110	-.100	-.110	-.080	-.090	-.060	-.070	-.015
1.3	---	-.020	---	-.010	---	-.135	---	-.070	---	-.070	---	-.060
1.4	-.020	-.020	-.010	-.010	-.135	-.140	-.090	-.090	-.080	-.080	-.065	-.070
1.6	-.025	-.025	-.020	-.020	-.005	-.020	-.095	-.080	-.080	-.090	-.055	-.050
1.8	-.090	-.040	-.050	-.045	-.020	-.005	-.080	-.080	-.095	-.100	-.095	-.095

(b) Body pressure coefficients; modified wing with Sears-Haack body

ξ/c_j	Top 0°	Side -90°	Top 0°	Side -90°	Top 0°	Side -90°	Top 0°	Side -90°	Top 0°	Side -90°	Top 0°	Side -90°
-.3	.035	.035	.020	.010	.075	.010	.030	-.030	.007	-.015	-.007	-.137
-.2	.027	.055	.014	.035	.077	.040	.107	.010	.057	-.020	-.030	-.110
-.1	.008	.098	-.003	.100	.052	.137	.085	.103	.116	-.025	.100	-.035
-.05	---	.287	---	.295	---	.325	---	.335	---	.285	---	.190
0	-.021	.150	-.045	.162	.005	.190	.040	.247	.065	.270	.082	.283
.05	---	.000	---	.000	---	.024	---	.130	---	.120	---	.135
.1	-.050	-.045	-.080	-.020	-.041	-.040	-.010	.068	.020	.067	.043	.090
.2	-.075	-.075	-.110	-.090	-.073	-.085	-.045	.000	-.009	.005	.012	.035
.3	-.097	-.087	-.133	-.112	-.097	-.103	-.065	-.045	-.026	-.025	-.012	.003
.4	-.118	-.100	-.162	-.123	-.115	-.109	-.090	-.060	-.040	-.040	-.033	-.020
.5	-.135	-.135	-.212	-.170	-.150	-.120	-.130	-.103	-.070	-.055	-.055	-.040
.6	-.090	-.187	-.250	-.225	-.175	-.175	-.157	-.140	-.098	-.103	-.075	-.082
.7	-.055	-.167	-.227	-.255	-.195	-.205	-.170	-.175	-.120	-.130	-.095	-.125
.8	-.047	-.130	-.145	-.273	-.210	-.220	-.160	-.205	-.135	-.140	-.114	-.130
.9	.005	-.067	-.050	-.285	-.170	-.230	-.110	-.200	-.107	-.145	-.107	-.127
.95	---	-.020	---	-.172	---	-.220	---	-.180	---	-.140	---	-.120
1.00	.025	.037	.007	-.030	-.123	-.195	-.066	-.130	-.066	-.107	-.088	-.105
1.05	---	.070	---	.035	---	-.167	---	-.060	---	-.045	---	-.040
1.1	.027	.035	.019	.015	-.065	-.130	-.030	-.090	-.055	-.050	-.043	-.050
1.2	.027	.007	.010	-.010	.050	-.015	-.085	-.132	-.085	-.072	-.060	-.067
1.3	---	-.005	---	-.026	---	.040	---	-.100	---	-.108	---	-.080
1.4	.022	.012	.000	-.030	.040	.047	-.060	-.067	-.055	-.055	-.070	-.065
1.6	---	.026	---	.022	---	-.106	---	-.060	---	-.065	---	-.055
1.8	---	.010	---	-.007	---	-.010	---	-.055	---	-.068	---	-.062

[1]See figure 6 for the definition of the notation.

TABLE III.- ZERO-LIFT PRESSURE COEFFICIENTS, C_p - Continued

(c) Body pressure coefficients; basic wing with M = 1.05 indented body

ξ'/c_j (θ)	M = 0.90 Top 0°	M = 0.90 Side -90°	M = 0.95 Top 0°	M = 0.95 Side -90°	M = 1.00 Top 0°	M = 1.00 Side -90°	M = 1.05 Top 0°	M = 1.05 Side -90°	M = 1.10 Top 0°	M = 1.10 Side -90°	M = 1.20 Top 0°	M = 1.20 Side -90°
-1.295	0.100	0.098	0.110	0.117	0.147	0.145	0.167	0.163	0.164	0.164	0.135	0.135
-1.035	---	.027	---	.036	---	.060	---	.082	---	.080	---	.075
-.775	-.003	-.006	.004	-.004	.030	.030	.045	.043	.048	.035	.041	.035
-.5	-.012	-.027	-.024	-.030	-.007	-.012	-.003	.009	.018	.005	.009	.004
-.3	-.015	-.010	-.030	-.030	-.015	-.030	-.015	.000	.010	.020	-.005	.020
-.2	-.035	-.030	-.045	-.035	-.005	-.015	.000	.010	.020	.020	.000	.000
-.1	-.060	-.045	-.075	-.065	-.050	-.055	-.035	-.025	-.015	-.020	-.025	-.020
-.05	---	-.025	---	-.050	---	-.100	---	-.080	---	-.070	---	-.040
0	-.095	.220	-.110	.220	-.185	.195	-.150	.210	-.120	.200	-.110	.175
.05	---	.000	---	.000	---	.010	---	.057	---	.080	---	.065
.1	-.125	-.070	-.145	-.080	-.155	-.050	-.130	-.030	-.070	.010	-.095	-.010
.2	-.130	-.145	-.170	-.170	-.125	-.120	-.125	-.120	-.065	-.085	-.080	-.095
.3	-.100	-.125	-.105	-.135	-.095	-.136	-.125	-.135	-.065	-.095	-.075	-.110
.4	-.050	-.100	-.085	-.115	-.065	-.115	-.110	-.125	-.055	-.075	-.070	-.100
.5	-.025	-.060	-.060	-.090	-.025	-.070	-.090	-.090	-.025	-.035	-.045	-.070
.6	.045	.000	.025	-.005	.030	.000	-.020	-.040	.035	.015	-.010	-.030
.7	.085	.055	.075	.040	.090	.055	.065	.030	.110	.080	.070	.040
.8	.085	.070	.070	.055	.095	.070	.080	.060	.145	.120	.100	.080
.9	.070	.060	.060	.035	.090	.065	.080	.055	.150	.130	.110	.095
.95	---	.045	---	.010	---	.045	---	.048	---	.120	---	.090
1.00	-.015	.020	-.040	-.030	.020	.025	.000	.040	.070	.100	.080	.080
1.05	---	-.015	---	-.060	---	-.010	---	.010	---	.050	---	.055
1.1	-.065	-.050	-.085	-.080	-.055	-.055	-.100	-.065	-.040	-.015	-.040	.000
1.2	-.095	.080	-.110	-.090	-.170	-.110	-.140	-.095	-.100	-.060	-.085	-.045
1.3	---	-.080	---	-.090	---	-.155	---	-.110	---	-.090	---	-.070
1.4	-.075	-.077	-.080	-.080	-.175	-.155	-.150	-.120	-.120	-.110	-.085	-.080
1.6	-.060	-.060	-.075	-.075	-.080	-.080	-.140	-.117	-.125	-.120	-.090	-.085
1.8	-.040	-.040	-.050	-.050	-.025	-.025	-.170	-.090	-.105	-.100	-.110	-.090

(d) Body pressure coefficients; modified wing with M = 1.05 indented body

ξ'/c_j (θ)	M = 0.90 Top 0°	M = 0.90 Side -90°	M = 0.95 Top 0°	M = 0.95 Side -90°	M = 1.00 Top 0°	M = 1.00 Side -90°	M = 1.05 Top 0°	M = 1.05 Side -90°	M = 1.10 Top 0°	M = 1.10 Side -90°	M = 1.20 Top 0°	M = 1.20 Side -90°
-.3	-.060	-.065	-.065	-.055	-.030	-.025	-.050	-.040	-.020	-.020	-.020	-.020
-.2	-.070	-.050	-.050	-.040	-.010	.010	-.020	-.025	-.020	-.005	-.010	-.010
-.1	-.115	-.020	-.115	-.015	-.060	.010	-.050	-.030	-.050	-.035	-.045	-.050
-.05	---	.010	---	.020	---	.000	---	-.060	---	-.115	---	-.110
0	-.170	.175	-.160	.195	-.150	.235	-.200	.210	-.175	.180	-.155	.160
.05	---	-.205	---	-.180	---	-.095	---	-.090	---	-.090	---	-.055
.1	-.160	-.225	-.175	-.220	-.110	-.250	-.140	-.190	-.115	-.160	-.090	-.145
.2	-.130	-.175	-.155	-.200	-.095	-.260	-.125	-.185	-.090	-.200	-.065	-.205
.3	-.100	-.120	-.120	-.135	-.090	-.140	-.125	-.170	-.100	-.125	-.085	-.135
.4	-.070	-.080	-.085	-.080	-.080	-.100	-.120	-.135	-.095	-.100	-.100	-.105
.5	-.045	-.055	-.040	-.050	-.040	-.050	-.095	-.100	-.075	-.080	-.075	-.085
.6	.010	.000	.030	.000	.050	.010	-.030	-.045	-.025	-.040	-.010	-.050
.7	.090	.040	.100	.050	.120	.075	.100	.030	.070	.050	.090	.040
.8	.100	.045	.105	.050	.125	.095	.145	.055	.095	.090	.130	.065
.9	.075	.040	.070	.035	.100	.085	.140	.057	.080	.100	.125	.070
.95	---	.000	---	-.010	---	.050	---	.040	---	.090	---	.065
1.00	-.020	-.025	.005	-.030	.055	.025	.100	.020	.040	.070	.095	.050
1.05	---	-.040	---	-.040	---	-.005	---	-.015	---	.005	---	.035
1.1	-.060	-.050	-.045	-.050	-.025	-.030	.000	-.030	-.040	-.030	.010	.025
1.2	-.080	-.065	-.085	-.055	-.100	-.075	-.080	-.060	-.105	-.070	-.060	-.020
1.3	---	-.070	---	-.065	---	-.110	---	-.090	---	-.110	---	-.060
1.4	-.087	-.070	-.100	-.070	-.140	-.105	-.130	-.110	-.140	-.120	-.085	-.075
1.6	-.080	-.060	-.090	-.060	-.045	-.035	-.130	-.110	-.130	-.100	-.095	-.090
1.8	-.030	-.030	-.030	-.030	.010	.010	-.080	-.075	-.080	-.065	-.095	-.075

TABLE III.- ZERO-LIFT PRESSURE COEFFICIENTS, C_p - Continued

(e) Body pressure coefficients; basic wing with M = 1.20 indented body

ξ'/c_j θ	M = 0.90 Top 0°	M = 0.90 Side -90°	M = 0.95 Top 0°	M = 0.95 Side -90°	M = 1.00 Top 0°	M = 1.00 Side -90°	M = 1.05 Top 0°	M = 1.05 Side -90°	M = 1.10 Top 0°	M = 1.10 Side -90°	M = 1.20 Top 0°	M = 1.20 Side -90°
-1.295	0.100	0.098	0.110	0.117	0.147	0.145	0.167	0.163	0.164	0.164	0.135	0.135
-1.035	---	.027	---	.036	---	.060	---	.082	---	.080	---	.075
-.775	-.003	-.006	.004	-.004	.030	.030	.045	.043	.048	.035	.041	.035
-.5	-.012	-.027	-.024	-.030	-.007	-.012	-.003	.009	.018	.005	.009	.004
-.3	-.055	-.036	-.044	-.042	-.030	-.024	-.010	-.008	-.007	-.015	-.009	-.015
-.2	-.016	-.038	-.010	-.042	.010	-.004	.019	-.017	.015	.021	.005	-.023
-.1	-.040	-.003	-.023	.000	.017	.046	-.020	-.020	-.012	-.027	-.017	-.032
-.05	---	.037	---	.061	---	.099	---	.000	---	-.031	---	-.030
0	-.005	.258	-.020	.274	.062	.319	-.007	-.287	-.027	.260	-.026	.215
.05	---	.085	---	.100	---	.150	---	.150	---	.150	---	.125
.1	-.016	.016	.005	.037	.056	.090	.055	.092	.051	.097	-.020	.082
.2	-.037	-.064	-.010	-.050	.035	.020	.042	.044	-.179	.045	.050	.036
.3	-.081	-.105	-.057	-.090	-.010	-.030	.007	.005	.040	.017	.030	.010
.4	-.102	-.150	-.083	-.133	-.027	-.070	-.012	-.047	.025	-.006	.013	-.015
.5	-.134	-.196	-.123	-.183	-.068	-.110	-.058	-.090	-.010	-.031	-.015	-.041
.6	-.160	-.236	-.153	-.226	-.100	-.160	-.075	-.125	-.027	-.096	-.022	-.067
.7	-.191	-.255	-.197	-.256	-.149	-.197	-.120	-.170	-.042	-.118	-.055	-.103
.8	-.147	-.176	-.230	-.273	-.181	-.218	-.150	-.185	-.083	-.123	-.088	-.115
.9	-.091	-.110	-.223	-.276	-.176	-.236	-.142	-.185	-.085	-.125	-.082	-.123
.95	---	-.058	---	-.240	---	-.227	---	-.183	---	-.123	---	-.125
1.00	-.048	.005	---	-.110	-.203	-.150	-.120	-.137	-.123	-.100	-.117	-.115
1.05	---	.027	---	-.016	---	-.100	---	-.072	---	-.055	---	-.050
1.1	---	.004	-.223	.001	---	-.116	---	-.100	---	-.090	---	-.077
1.2	-.058	-.007	-.027	.024	-.210	-.116	-.137	-.090	-.191	-.051	-.134	-.067
1.3	---	-.014	---	.034	---	-.107	---	-.065	---	-.045	---	-.058
1.4	-.048	-.018	-.019	.017	-.127	-.106	-.075	-.060	-.102	-.050	-.085	-.055
1.6	-.048	-.022	-.031	-.003	.013	.017	-.095	-.071	-.107	-.094	-.083	-.062
1.8	-.049	-.027	-.042	-.030	.024	.019	-.076	-.078	-.083	-.083	-.092	-.070

(f) Body pressure coefficients; modified wing with M = 1.20 indented body

ξ'/c_j	M = 0.90 Top 0°	M = 0.90 Side -90°	M = 0.95 Top 0°	M = 0.95 Side -90°	M = 1.00 Top 0°	M = 1.00 Side -90°	M = 1.05 Top 0°	M = 1.05 Side -90°	M = 1.10 Top 0°	M = 1.10 Side -90°	M = 1.20 Top 0°	M = 1.20 Side -90°
-.3	-.030	-.020	-.045	-.030	-.025	.000	-.010	.010	-.005	.020	.005	.020
-.2	-.170	-.020	-.220	-.030	-.140	.010	-.090	.020	-.075	.025	-.055	.020
-.1	-.110	.000	-.080	-.010	-.290	-.065	-.235	-.100	-.205	-.110	-.170	-.055
-.05	---	.020	---	.010	---	-.155	---	-.160	---	-.170	---	-.135
0	-.070	.240	-.095	.250	-.030	.175	-.045	.215	-.080	.210	-.130	.160
.05	---	-.060	---	-.020	---	.000	---	.010	---	.030	---	.040
.1	-.025	-.200	-.035	-.207	.035	-.155	-.010	-.160	-.020	-.140	-.055	-.085
.2	.000	-.050	.005	-.055	.070	.020	.005	-.090	.025	-.105	.005	-.100
.3	.020	.000	.030	.000	.090	.065	.030	.005	.060	.015	.041	.000
.4	.025	.020	.055	.025	.105	.095	.075	.060	.090	.075	.070	.055
.5	.020	.040	.055	.042	.110	.115	.095	.085	.120	.105	.095	.090
.6	.010	.050	.015	.040	.080	.105	.080	.090	.120	.115	.110	.110
.7	-.080	-.010	-.140	-.015	-.060	.050	-.045	.060	.020	.090	.025	.110
.8	-.075	-.110	-.185	-.180	-.122	-.195	-.110	-.070	-.045	-.015	-.030	-.010
.9	-.070	-.080	-.205	-.190	-.160	-.125	-.150	-.115	-.085	-.045	-.070	-.045
.95	---	-.055	---	-.180	---	-.140	---	-.115	---	-.050	---	-.055
1.00	.035	-.010	-.120	-.120	-.170	-.095	-.140	-.100	-.090	-.060	-.080	-.060
1.05	---	.035	---	-.030	---	-.020	---	-.030	---	.000	---	.000
1.1	.185	.005	.200	-.040	-.160	-.070	-.105	-.085	-.080	-.055	-.050	-.030
1.2	.185	-.040	.200	-.045	-.180	-.150	-.120	-.100	-.120	-.085	-.105	-.070
1.3	---	-.030	---	-.030	---	-.155	---	-.095	---	-.087	---	-.070
1.4	-.025	-.025	-.045	-.040	-.005	-.025	-.095	-.080	-.100	-.070	-.090	-.070
1.6	-.045	-.030	-.070	-.060	.000	-.010	-.035	-.045	-.085	-.060	-.060	-.070
1.8	-.035	-.025	-.030	.030	.070	-.145	.035	-.100	-.065	-.075	-.040	-.060

TABLE III.- ZERO-LIFT PRESSURE COEFFICIENTS, C_p - Concluded

x'/c	M=0.90 0.18	0.51	0.89	M=0.95 0.18	0.51	0.89	M=1.00 0.18	0.51	0.89	M=1.05 0.18	0.51	0.89	M=1.10 0.18	0.51	0.89	M=1.20 0.18	0.51	0.89
(g) Wing pressure coefficients; basic wing with Sears-Haack body																		
0.000	0.570	0.495	0.490	0.600	0.510	0.490	0.625	0.540	0.520	0.635	0.560	0.550	0.650	0.600	0.580	0.660	0.610	0.495
.0125	.015	---	---	.320	---	---	.110	---	---	.110	---	---	.100	---	---	.090	---	---
.025	-.011	-.080	---	.094	-.078	---	.081	-.011	---	.080	-.001	---	.065	.031	---	.070	.005	---
.05	-.027	-.109	-.175	.030	-.102	-.169	.060	-.041	-.132	.058	-.030	-.091	.056	.015	-.062	.046	-.012	-.021
.10	-.055	-.143	-.205	-.024	-.129	-.223	.025	-.075	-.165	.027	-.057	-.112	.039	-.013	-.068	.018	-.031	-.042
.20	-.100	-.189	-.240	-.071	-.161	-.291	-.022	-.120	-.219	-.011	-.084	-.151	.017	-.048	-.103	-.013	-.050	-.067
.30	-.140	-.222	-.240	-.110	-.200	-.339	-.062	-.161	-.268	-.045	-.120	-.203	-.011	-.077	-.160	-.027	-.070	-.101
.40	-.174	-.251	-.215	-.150	-.250	-.371	-.109	-.202	-.314	-.084	-.162	-.265	-.045	-.113	-.220	-.049	-.100	-.147
.50	-.215	-.267	-.180	-.200	-.303	-.400	-.151	-.240	-.358	-.125	-.212	-.311	-.088	-.162	-.270	-.080	-.140	-.197
.60	-.266	-.228	-.130	-.250	-.345	-.421	-.198	-.275	-.400	-.171	-.246	-.340	-.120	-.193	-.308	-.113	-.179	-.238
.70	-.270	-.154	-.070	-.290	-.349	-.006	-.233	-.300	-.439	-.205	-.259	-.400	-.142	-.204	-.328	-.141	-.190	-.270
.80	-.180	-.073	-.000	-.302	-.250	.077	-.255	-.308	-.449	-.211	-.260	-.377	-.155	-.203	-.325	-.155	-.187	-.276
.90	-.099	.010	.100	-.275	.030	.134	-.250	-.239	-.185	-.190	-.203	-.100	-.147	-.147	-.180	-.148	-.175	---
(h) Wing pressure coefficients; modified wing with Sears-Haack body																		
.000	---	.498	.535	---	.490	.507	---	.520	.545	---	.520	.570	---	.570	.578	---	.600	.605
.0125	-.015	---	---	.009	---	---	.062	---	---	.060	---	---	.052	---	---	.160	---	---
.025	-.137	-.285	---	-.125	-.315	---	-.070	-.295	---	-.070	-.295	---	-.042	-.225	---	.015	-.125	---
.05	-.154	-.270	-.435	-.135	-.317	-.532	-.082	-.305	-.495	-.082	-.305	-.397	-.060	-.263	-.385	-.015	-.200	-.220
.10	-.158	-.235	-.332	-.127	-.270	-.410	-.075	-.212	-.378	-.075	-.212	-.355	-.040	-.190	-.340	-.010	-.155	-.225
.20	-.133	-.180	-.248	-.117	-.210	-.337	-.072	-.165	-.274	-.030	-.165	-.250	-.025	-.105	-.210	-.007	-.090	-.260
.30	-.110	-.160	-.209	-.112	-.197	-.318	-.075	-.150	-.248	-.040	-.150	-.205	-.025	-.077	-.152	-.010	-.060	-.110
.40	-.120	-.167	-.131	-.130	-.217	-.355	-.080	-.163	-.275	-.055	-.165	-.220	-.035	-.085	-.167	-.020	-.060	-.095
.50	-.157	-.170	-.112	-.160	-.250	-.287	-.122	-.200	-.310	-.100	-.200	-.255	-.075	-.125	-.222	-.040	-.080	-.145
.60	-.180	-.142	-.085	-.210	-.287	-.065	-.170	-.240	-.340	-.145	-.235	-.295	-.110	-.163	-.255	-.065	-.115	-.180
.70	-.170	-.105	-.035	-.260	-.295	.025	-.205	-.260	-.368	-.182	-.260	-.305	-.135	-.175	-.275	-.100	-.135	-.205
.80	-.130	-.040	.022	-.285	-.140	.062	-.242	-.255	-.350	-.207	-.254	-.315	-.150	-.190	-.293	-.135	-.145	-.230
.90	-.065	.035	.095	-.230	.045	.115	-.227	-.203	-.200	-.190	-.205	.150	-.140	-.170	.220	-.125	-.125	.290
(i) Wing pressure coefficients; basic wing with M=1.05 indented body																		
.000	---	.510	.495	---	.525	.515	---	.525	.540	---	.530	.500	---	.555	.545	---	.600	.595
.0125	-.115	---	---	-.105	---	---	-.075	---	---	-.075	---	---	-.040	---	---	-.035	---	---
.025	-.140	-.045	---	-.155	-.045	---	-.140	-.075	---	-.130	-.035	---	-.105	.015	---	-.100	.000	---
.05	-.120	-.075	-.140	-.165	-.065	-.125	-.135	-.085	-.180	-.135	-.040	-.090	-.090	-.020	-.050	-.120	-.035	-.075
.10	-.115	-.090	-.155	-.115	-.095	-.145	-.125	-.095	-.175	-.120	-.095	-.115	-.075	-.055	-.065	-.100	-.080	-.078
.20	-.090	-.120	-.195	-.090	-.120	-.195	-.125	-.125	-.195	-.130	-.130	-.157	-.085	-.090	-.105	-.103	-.105	-.095
.30	-.045	-.135	-.205	-.055	-.145	-.275	-.045	-.145	-.240	-.125	-.160	-.210	-.045	-.118	-.155	-.065	-.120	-.145
.40	-.015	-.145	-.195	-.015	-.155	-.330	.000	-.160	-.275	-.035	-.195	-.280	.025	-.137	-.215	-.037	-.133	-.195
.50	.005	-.150	-.160	.010	-.165	-.305	.025	-.160	-.290	.005	-.210	-.315	.030	-.150	-.262	.020	-.165	-.235
.60	.020	-.135	-.125	.005	-.160	-.125	.030	-.140	-.310	.025	-.185	-.340	.085	-.130	-.305	.055	-.185	-.275
.70	.015	-.100	-.075	-.003	-.130	-.035	.030	-.115	-.350	.025	-.140	-.345	.085	-.095	-.315	.055	-.160	-.295
.80	.007	-.050	-.015	-.020	-.075	.035	.020	-.125	-.030	.018	-.085	-.200	.070	-.050	-.240	.025	-.100	-.290
.90	.000	.010	.050	-.025	-.005	.110	.021	-.030	.155	.020	.015	.220	.000	.065	.265	.025	-.025	.350
(j) Wing pressure coefficients; modified wing with M=1.05 indented body																		
.000	---	.510	.485	---	.525	.515	---	.535	.525	---	.530	.535	---	.560	.560	---	.600	.600
.0125	-.075	---	---	-.045	---	---	-.015	---	---	.000	---	---	.040	---	---	.085	---	---
.025	-.245	-.215	---	-.220	-.220	---	-.190	-.290	---	-.175	-.300	---	-.145	-.235	---	-.090	-.230	---
.05	-.275	-.215	-.345	-.270	-.235	-.345	-.245	-.325	-.400	-.235	-.345	-.420	-.215	-.375	-.410	-.180	-.350	-.350
.10	-.235	-.180	-.315	-.240	-.190	-.290	-.210	-.235	-.340	-.215	-.300	-.395	-.210	-.320	-.415	-.180	-.330	-.390
.20	-.140	-.135	-.230	-.160	-.135	-.240	-.155	-.155	-.240	-.165	-.215	-.295	-.170	-.195	-.275	-.175	-.235	-.363
.30	-.080	-.115	-.187	-.090	-.110	-.245	-.110	-.110	-.205	-.125	-.170	-.240	-.120	-.125	-.200	-.115	-.135	-.310
.40	-.055	-.110	-.140	-.050	-.100	-.270	-.090	-.095	-.215	-.110	-.145	-.240	-.080	-.110	-.200	-.055	-.075	-.220
.50	-.045	-.115	-.115	-.035	-.115	-.160	-.080	-.095	-.242	-.100	-.150	-.255	-.080	-.125	-.220	-.065	-.100	-.205
.60	-.025	-.115	-.100	-.015	-.125	-.095	-.025	-.100	-.260	-.060	-.140	-.265	-.050	-.120	-.245	-.075	-.180	-.200
.70	.000	-.095	-.065	.000	-.120	-.035	.020	-.095	-.235	-.025	-.120	-.250	.020	-.080	-.235	-.010	-.175	-.205
.80	-.035	-.055	-.007	-.025	-.080	.020	.015	-.080	-.015	-.030	-.085	-.180	.015	-.055	-.215	-.015	-.095	-.225
.90	-.035	.005	.060	-.025	.000	.100	.015	-.040	.160	-.015	-.045	.280	.035	.025	.260	.025	-.045	.345
(k) Wing pressure coefficients; basic wing with M=1.20 indented body																		
.000	---	.313	.490	---	.550	.495	---	.565	.500	---	.540	.530	---	.570	.560	---	.600	.575
.0125	-.080	---	---	-.080	---	---	.008	---	---	-.55	---	---	-.060	---	---	-.050	---	---
.025	-.050	-.018	---	-.060	-.005	---	-.025	.060	---	-.120	-.015	---	-.110	-.015	---	-.090	.020	---
.05	-.028	-.035	-.140	-.040	-.020	-.135	-.045	.040	-.045	-.050	-.030	-.055	-.055	-.035	-.025	-.075	-.015	-.035
.10	-.040	-.060	-.155	-.030	-.050	-.155	-.025	.010	-.085	-.005	-.045	-.080	.000	-.035	-.050	-.018	.065	.055
.20	-.050	-.085	-.195	-.030	-.070	-.195	.005	-.030	-.135	-.010	-.060	-.105	.040	.015	-.075	-.005	-.090	-.085
.30	-.035	-.116	-.215	-.030	-.105	-.270	.000	-.050	-.185	.010	-.090	-.140	.060	-.030	-.110	.018	-.095	-.120
.40	-.085	-.145	-.175	-.095	-.145	-.325	-.025	-.080	-.260	-.015	-.100	-.185	.050	-.060	-.160	.060	-.065	-.150
.50	-.105	-.165	-.150	-.155	-.195	-.345	-.095	-.140	-.300	-.085	-.115	-.235	-.010	-.065	-.200	-.015	-.090	-.185
.60	-.050	-.150	-.132	-.165	-.215	-.120	-.135	-.155	-.350	-.120	-.120	-.297	-.050	-.065	-.250	-.040	-.105	-.210
.70	-.020	-.105	-.110	-.080	-.230	.015	-.122	-.185	-.425	-.098	-.155	-.350	.031	-.095	-.275	.012	-.070	-.245
.80	-.040	-.045	.015	-.062	-.115	.090	-.068	-.190	-.325	-.060	-.165	-.315	-.002	-.110	-.245	.014	-.075	-.240
.90	-.050	.025	.100	-.100	.040	.150	-.120	-.120	.020	-.120	-.195	.195	-.004	-.095	.317	.000	-.070	.400
(l) Wing pressure coefficients; modified wing with M=1.20 indented body																		
.000	---	.535	.525	---	.540	.515	---	.580	.540	---	.550	.595	---	.580	.575	---	.600	.595
.0125	-.085	---	---	-.045	---	---	-.020	---	---	-.010	---	---	.020	---	---	-.115	---	---
.025	-.250	-.250	---	-.225	-.255	---	-.205	-.175	---	-.205	-.275	---	-.160	-.310	---	-.200	-.220	---
.05	-.270	-.240	-.435	-.260	-.250	-.445	-.245	-.180	-.340	-.260	-.295	-.395	-.225	-.370	-.370	-.200	-.325	-.345
.10	-.165	-.185	-.320	-.200	-.195	-.395	-.175	-.140	-.265	-.230	-.205	-.320	-.200	-.225	-.307	-.200	-.310	-.365
.20	-.090	-.130	-.250	-.085	-.143	-.300	-.020	-.087	-.210	-.120	-.180	-.210	-.135	-.090	-.180	-.050	-.230	-.335
.30	-.030	-.105	-.190	.025	-.120	-.285	.020	-.060	-.205	-.040	-.085	-.165	-.030	-.040	-.110	-.005	-.090	-.280
.40	-.015	-.110	-.110	.025	-.105	-.340	.030	-.065	-.245	-.005	-.078	-.200	.020	-.037	-.140	.015	-.060	-.150
.50	-.025	-.130	-.100	-.030	-.125	-.320	.030	-.100	-.290	.000	-.060	-.240	.010	-.045	-.175	.025	-.075	-.160
.60	-.045	-.130	-.090	-.035	-.220	-.165	-.025	-.150	-.315	-.000	-.122	-.265	.040	-.060	-.210	.025	-.095	-.180
.70	-.080	-.110	-.055	-.085	-.250	-.010	-.030	-.190	-.320	-.020	-.155	-.280	.040	-.100	-.230	-.040	-.090	-.190
.80	-.110	-.055	-.000	-.185	-.185	.042	-.130	-.190	-.280	-.115	-.175	-.290	-.055	-.125	-.235	-.050	-.095	-.200
.90	-.070	.020	.065	-.190	-.015	.105	-.135	-.130	.150	-.120	-.145	.215	-.065	-.115	.273	---	-.100	.365

PLAN

Flexible walls

Model support system

13.71

13.92

Air flow

Dimensions in feet

Nozzle
36.75

Test section
33.75

Slotted wall detail
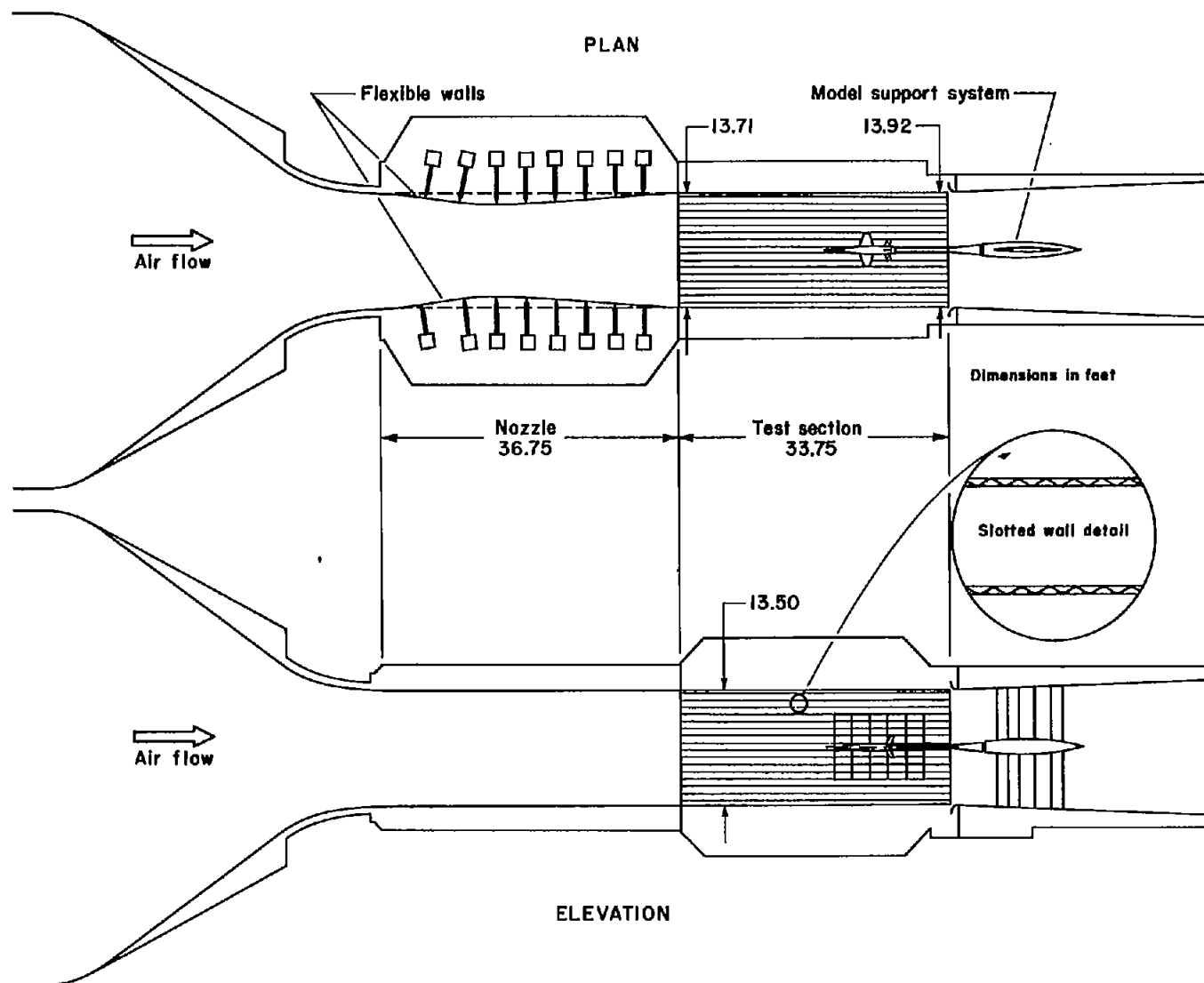
13.50

Air flow

ELEVATION

Figure 1.- Two views of the high-speed region of the Ames 14-foot transonic wind tunnel.

A-20417.2

Figure 2.- Rear view of test section and model support system of the
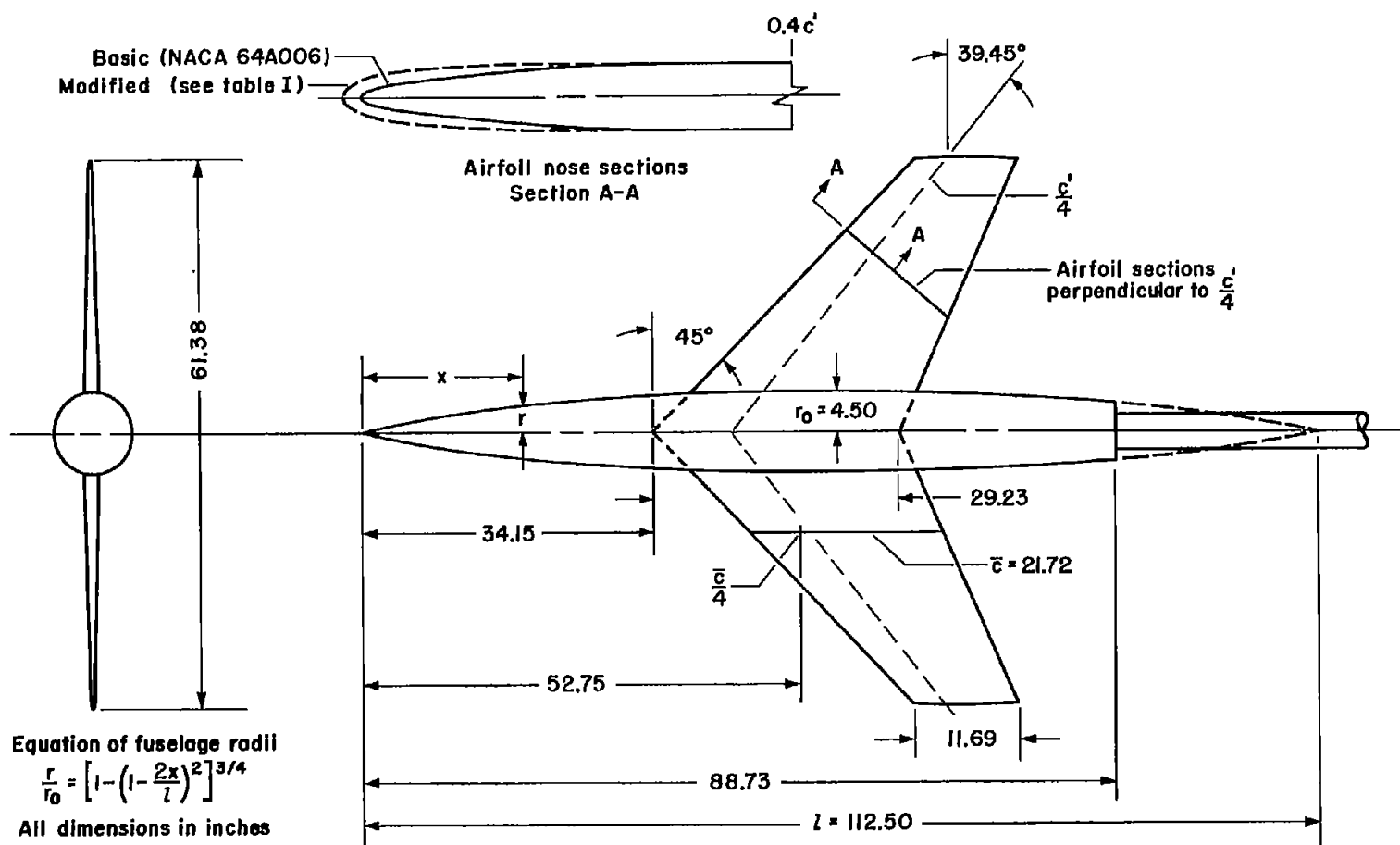Ames 14-foot transonic wind tunnel.

Basic (NACA 64A006)
Modified (see table I)

0.4c'

Airfoil nose sections
Section A-A

39.45°

$\dfrac{c'}{4}$

A

A

Airfoil sections
perpendicular to $\dfrac{c'}{4}$

61.38

45°

x

r

$r_0 = 4.50$

29.23

$\bar{c} = 21.72$

34.15

$\dfrac{\bar{c}}{4}$

52.75

11.69

Equation of fuselage radii

$$\dfrac{r}{r_0} = \left[1 - \left(1 - \dfrac{2x}{l}\right)^2\right]^{3/4}$$

All dimensions in inches

88.73

$l = 112.50$

Figure 3.- Two-view drawing of the basic aspect-ratio-3 wing with the fineness-ratio-12.5
Sears-Haack body, and sketch of the modified wing section.
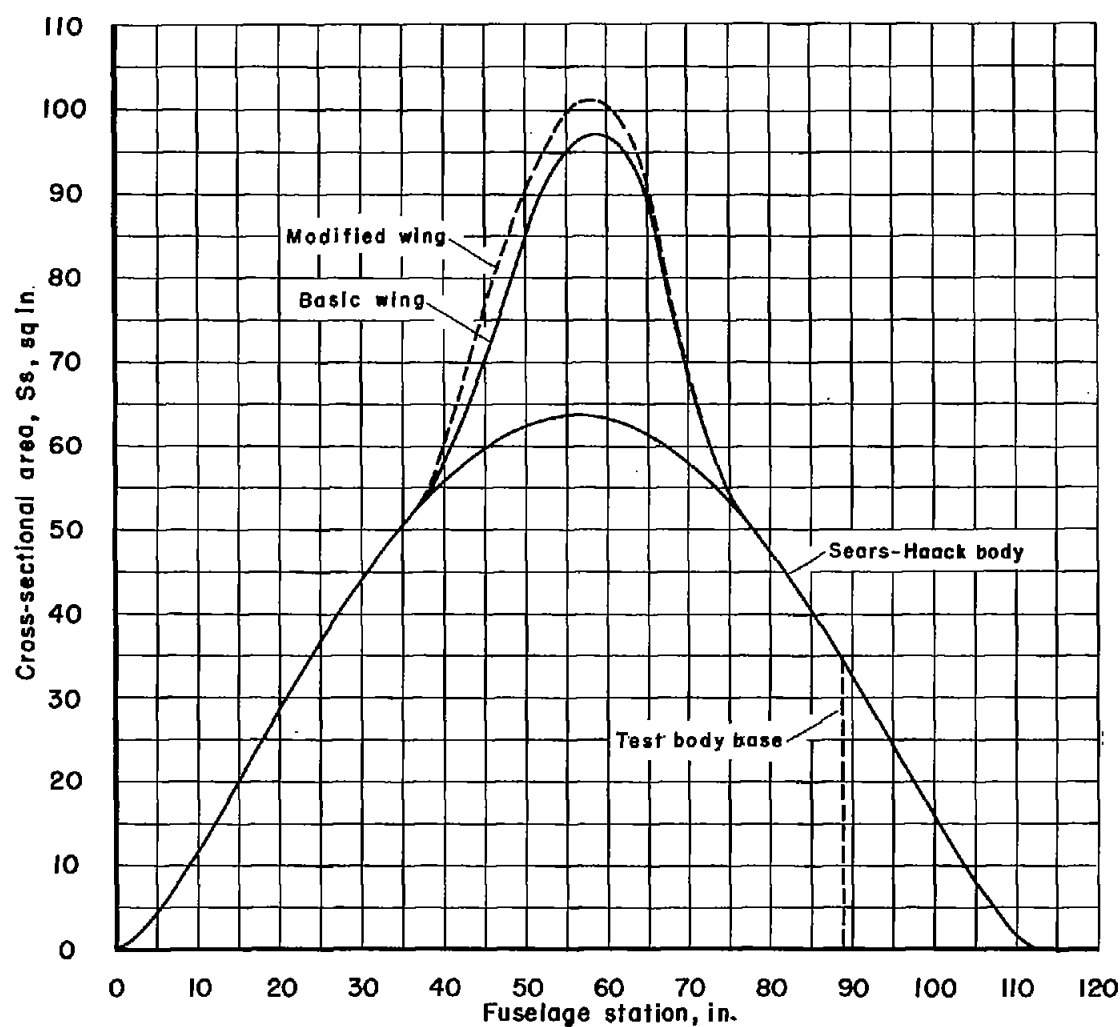
(a) Sears-Haack body; basic and modified wings.

Figure 4.- Cross-sectional area distributions for the bodies and wing-body combinations (M = 1.00).
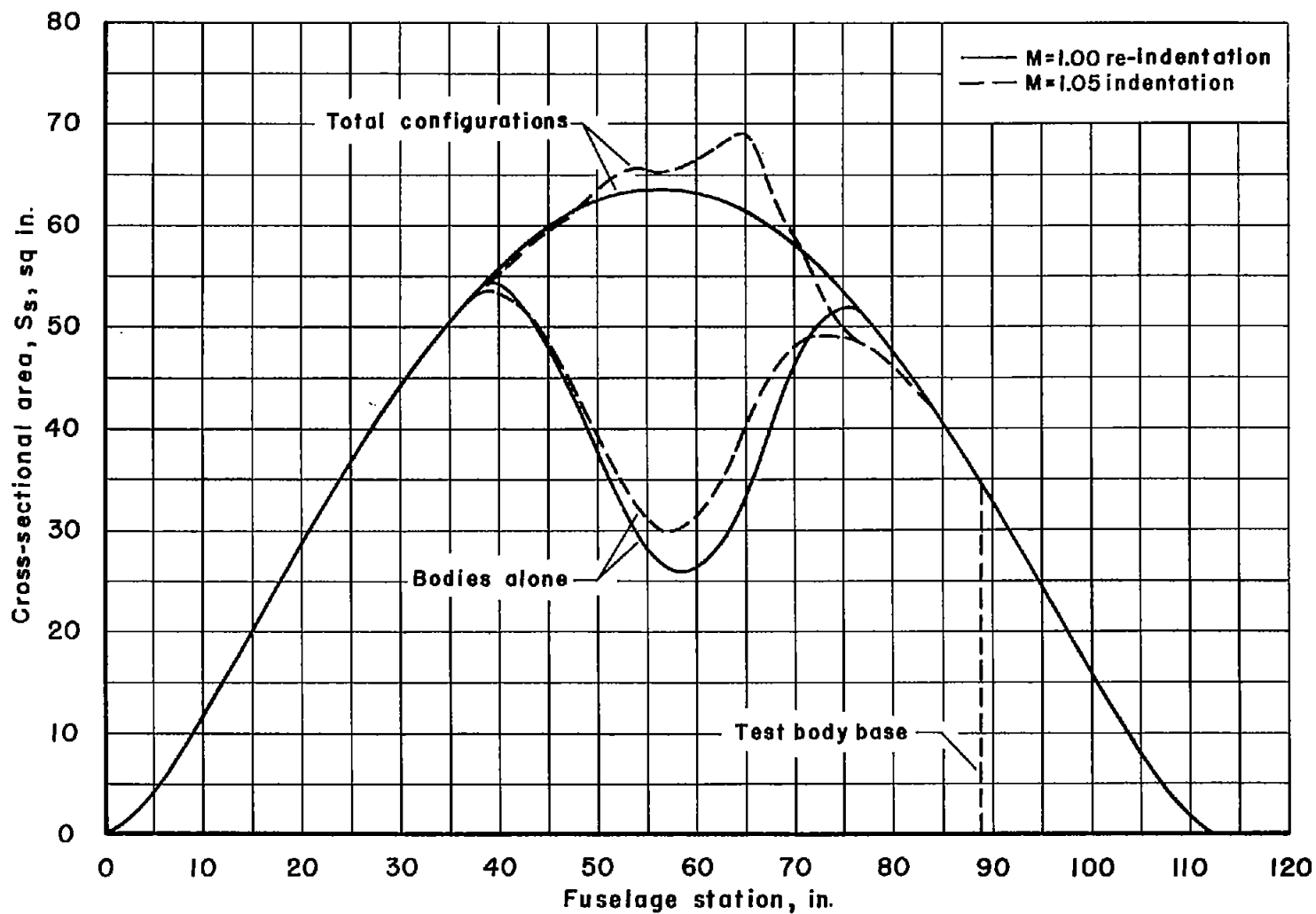
(b) Body indentations for M = 1.00 and M = 1.05, basic wing.

Figure 4.- Continued.
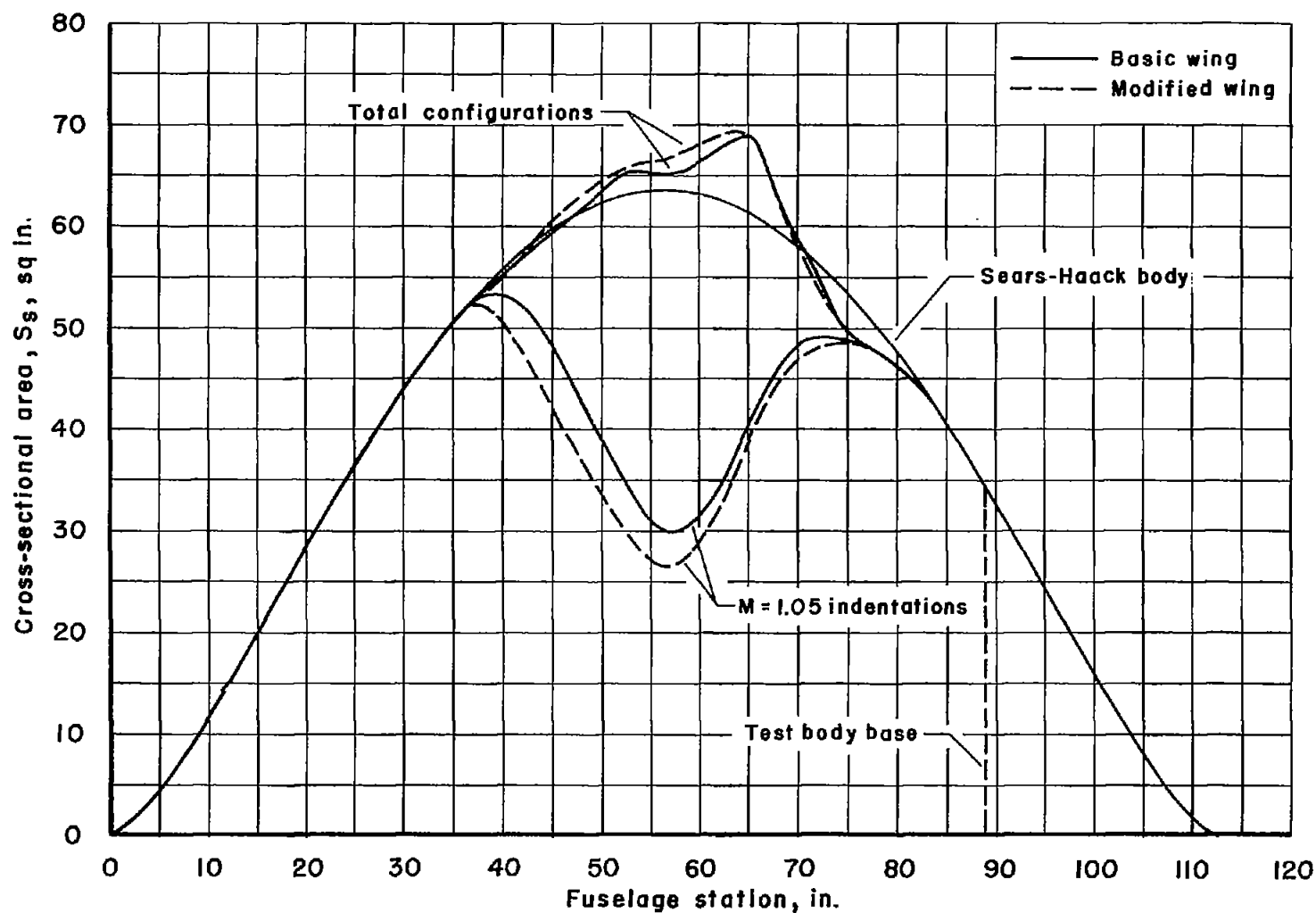
(c) Body indentations for M = 1.05, basic and modified wings.
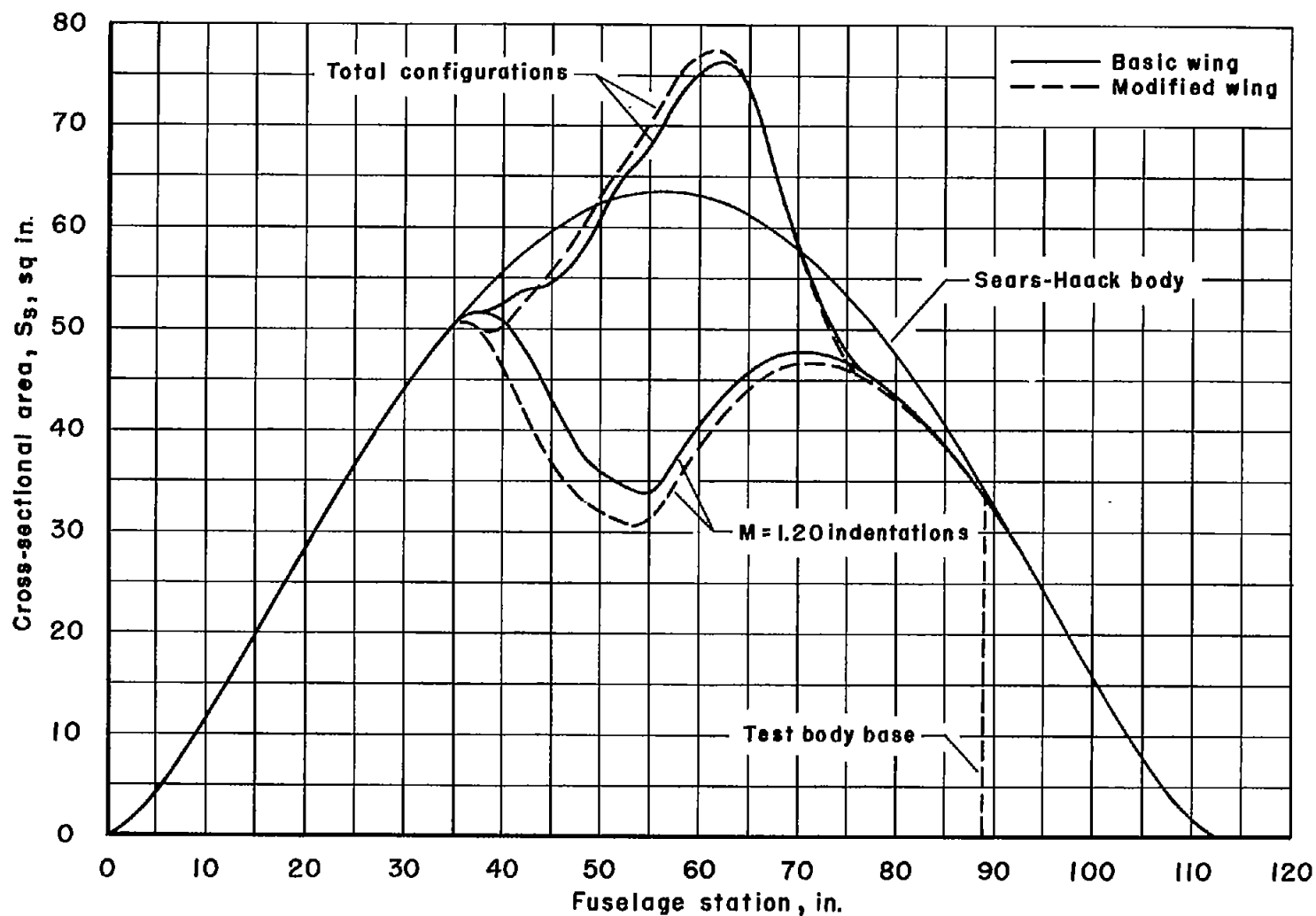
Figure 4.- Continued.

(d) Body indentations for M = 1.20, basic and modified wings.
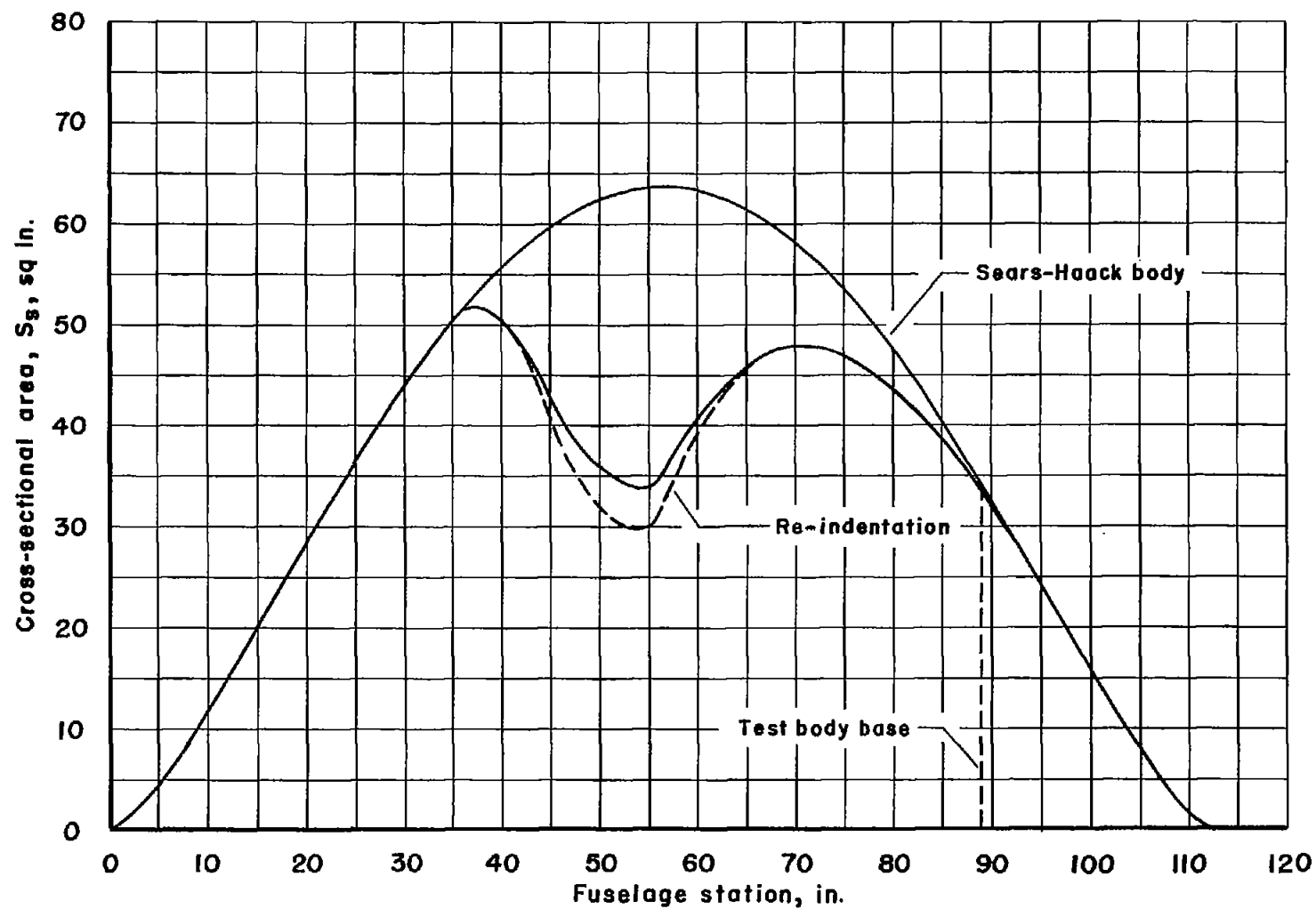
Figure 4.- Continued.

(e) Body indentation and re-indentation for M = 1.20, basic wing.

Figure 4.- Continued.
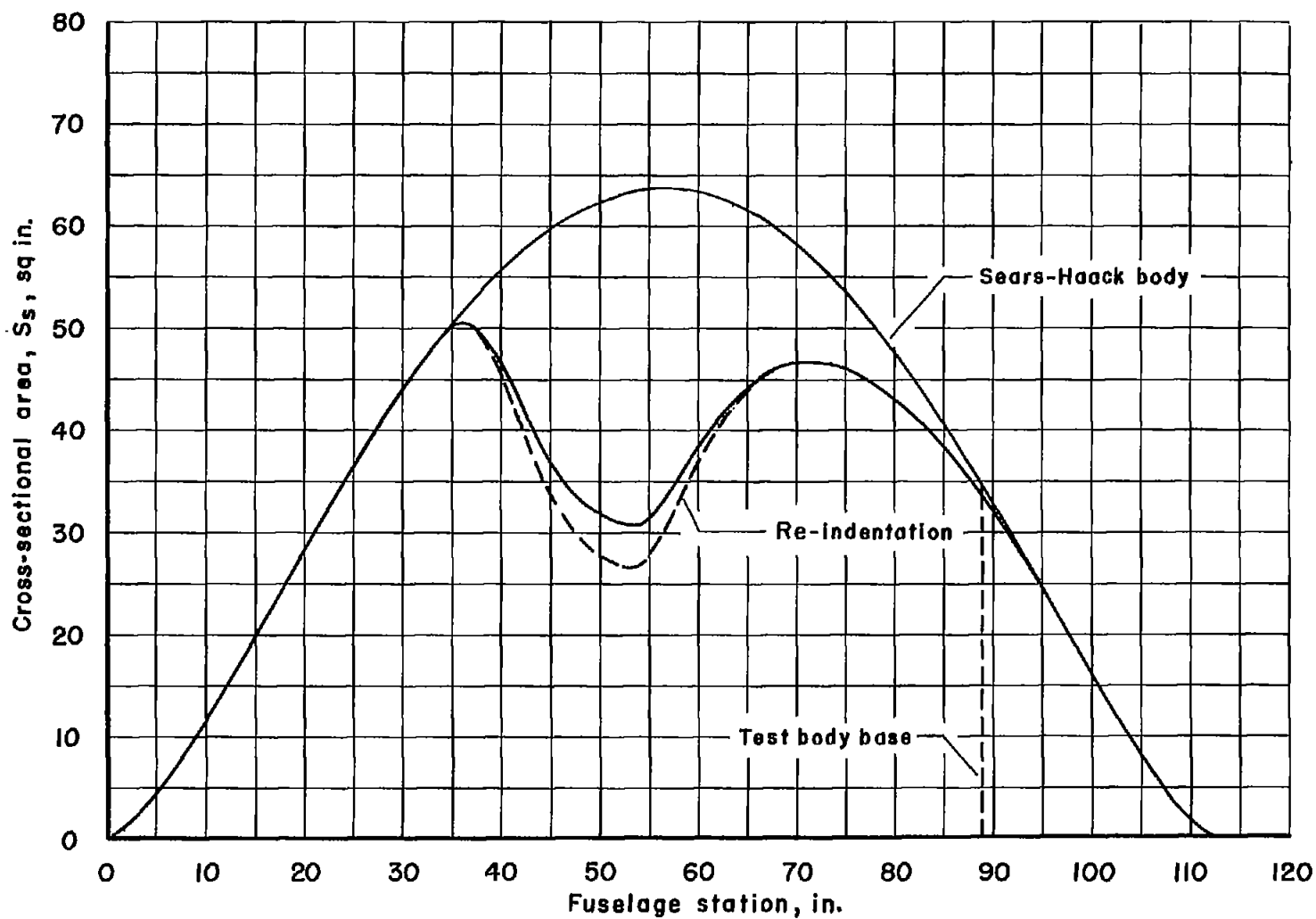
(f) Body indentation and re-indentation for M = 1.20, modified wing.

Figure 4.- Concluded.
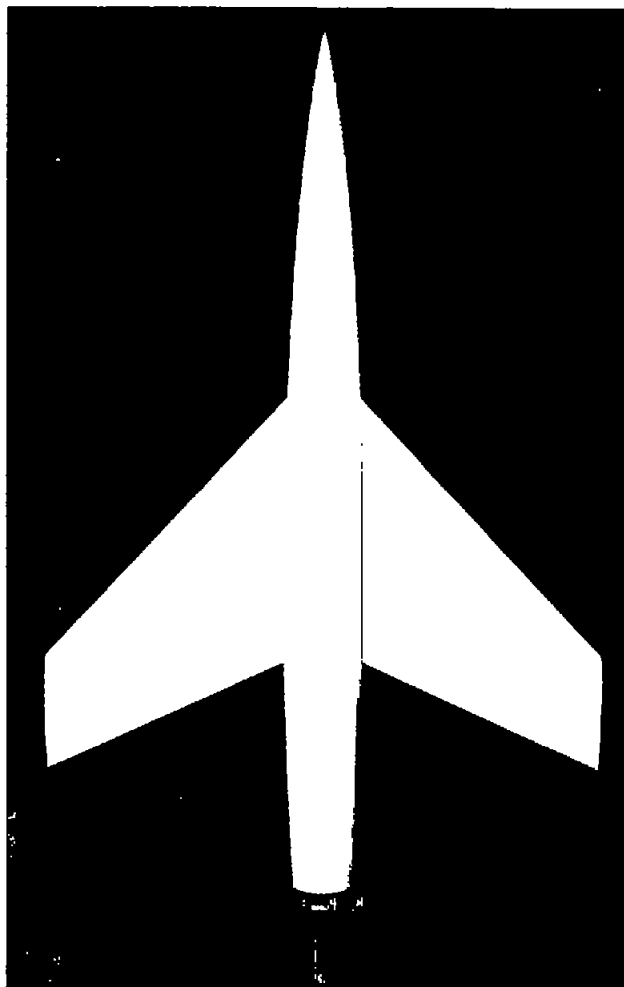
A-21320
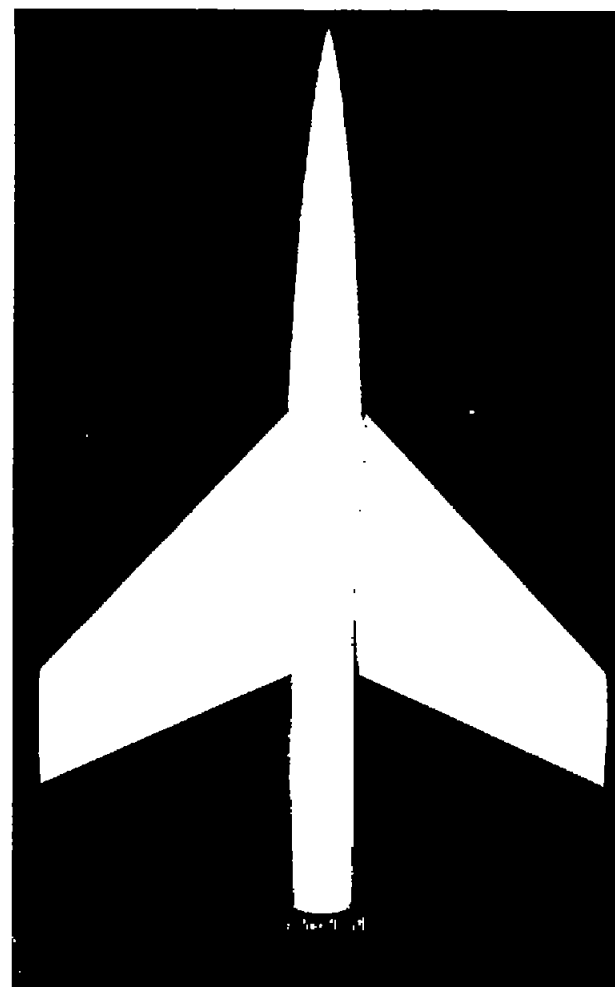
A-21321

(a) The modified wing with Sears-Haack body.   (b) The basic wing with M = 1.20 re-indented body.

Figure 5.- Representative photographs of the models.

Pressure station	x inches	ξ'/c_j
1	4.2	-1.295
2	7.43	-1.035
3	17.44	-.775
4	24.85	-.5
5	30.24	-.3
6	32.94	-.2
7	35.63	-.1
8	36.98	-.05
9	38.33	0
10	39.68	.05
11	41.03	.1
12	43.72	.2
13	46.42	.3
14	49.11	.4
15	51.81	.5
16	54.51	.6
17	57.20	.7
18	59.90	.8
19	62.59	.9
20	63.94	.95
21	65.29	1.0
22	66.64	1.05
23	67.99	1.1
24	70.68	1.2
25	73.38	1.3
26	76.07	1.4
27	81.47	1.6
28	86.86	1.8
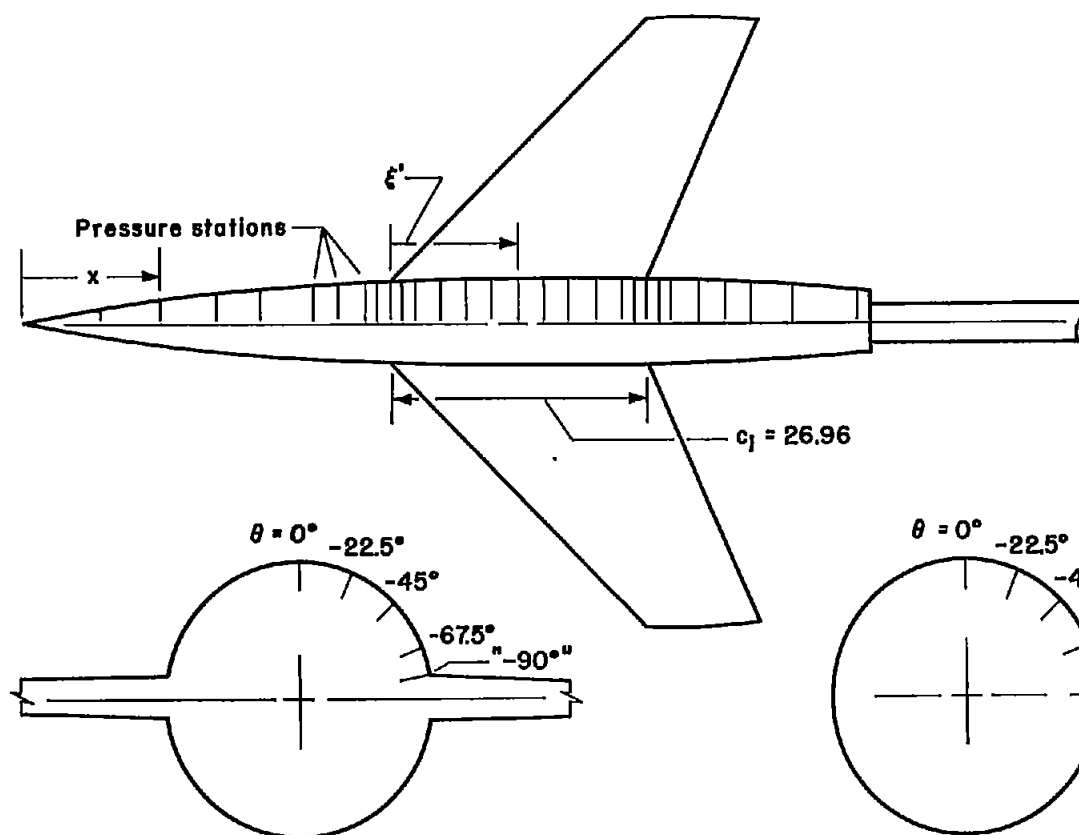
Body section showing pressure stations around the body in the region of the wing.

Body section showing pressure stations around the body.

(a) Body pressure orifices.

Figure 6.- Location of pressure orifices on all models.
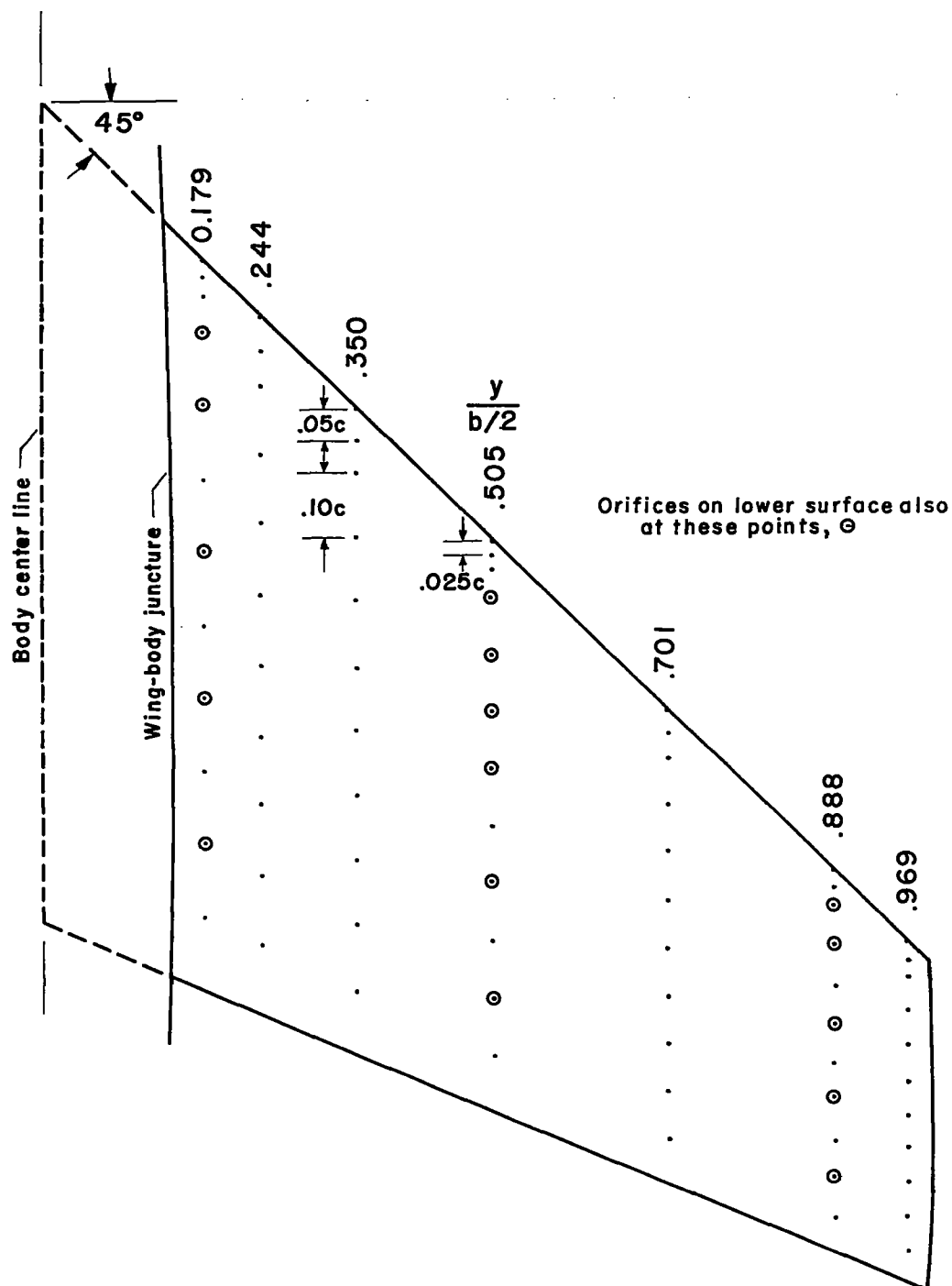
(b) Wing pressure orifices.

Figure 6.- Concluded.
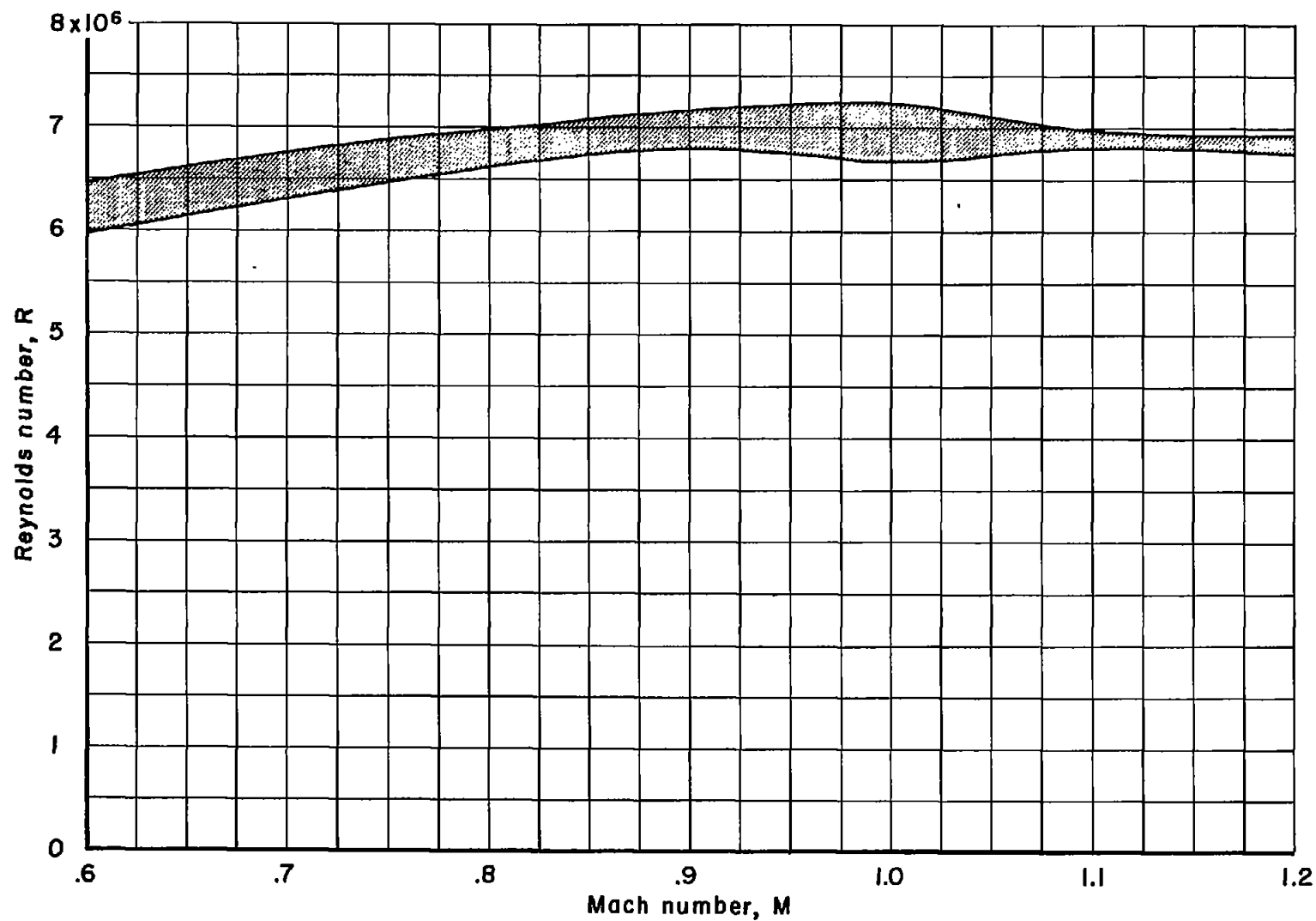
Figure 7.- Reynolds number variation for the tests based on the mean aerodynamic chord of the basic wing.
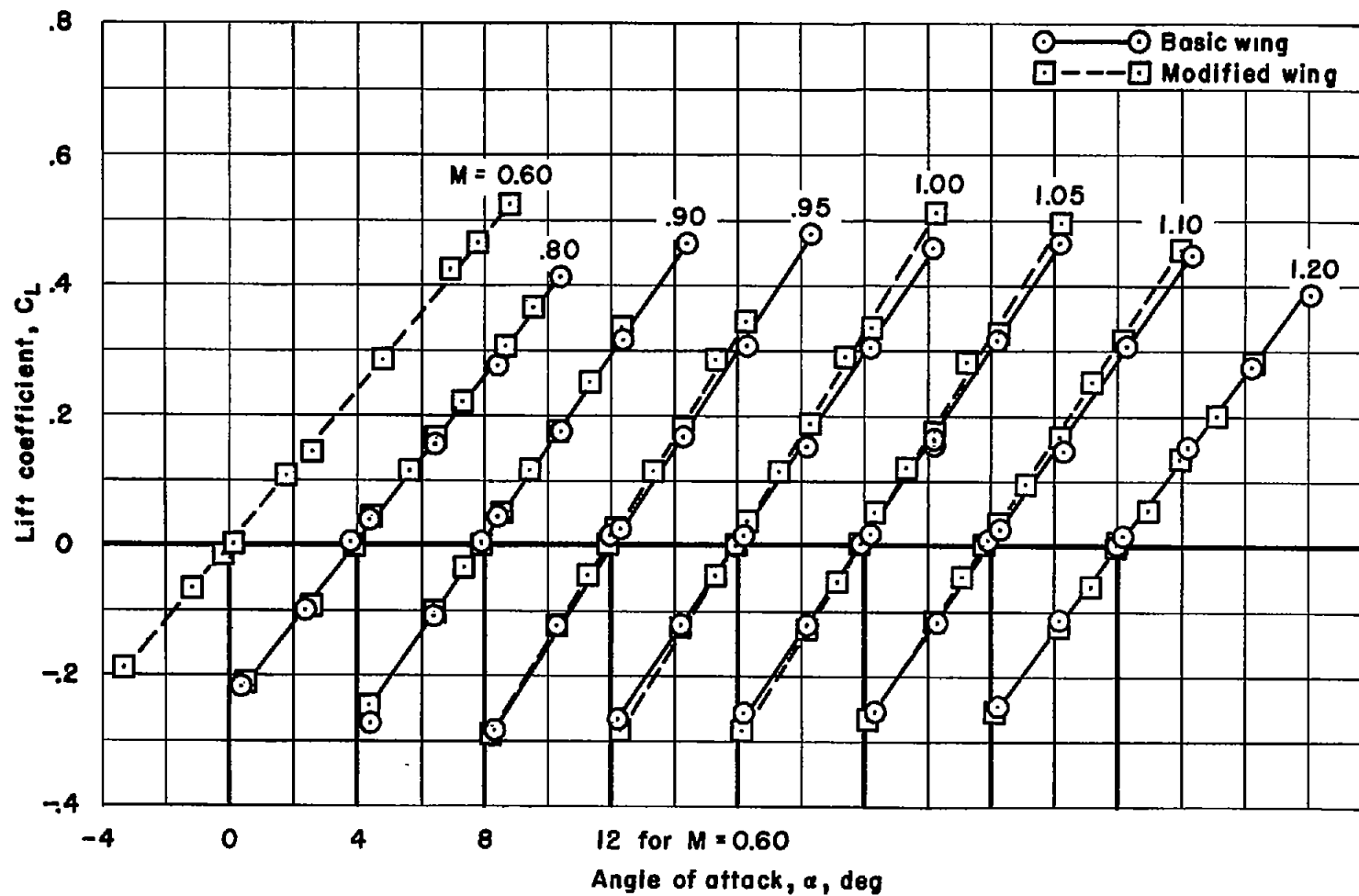
(a) C_L vs. α; Sears-Haack body.

Figure 8.- Aerodynamic characteristics of the basic- and modified-wing models with the Sears-Haack body.
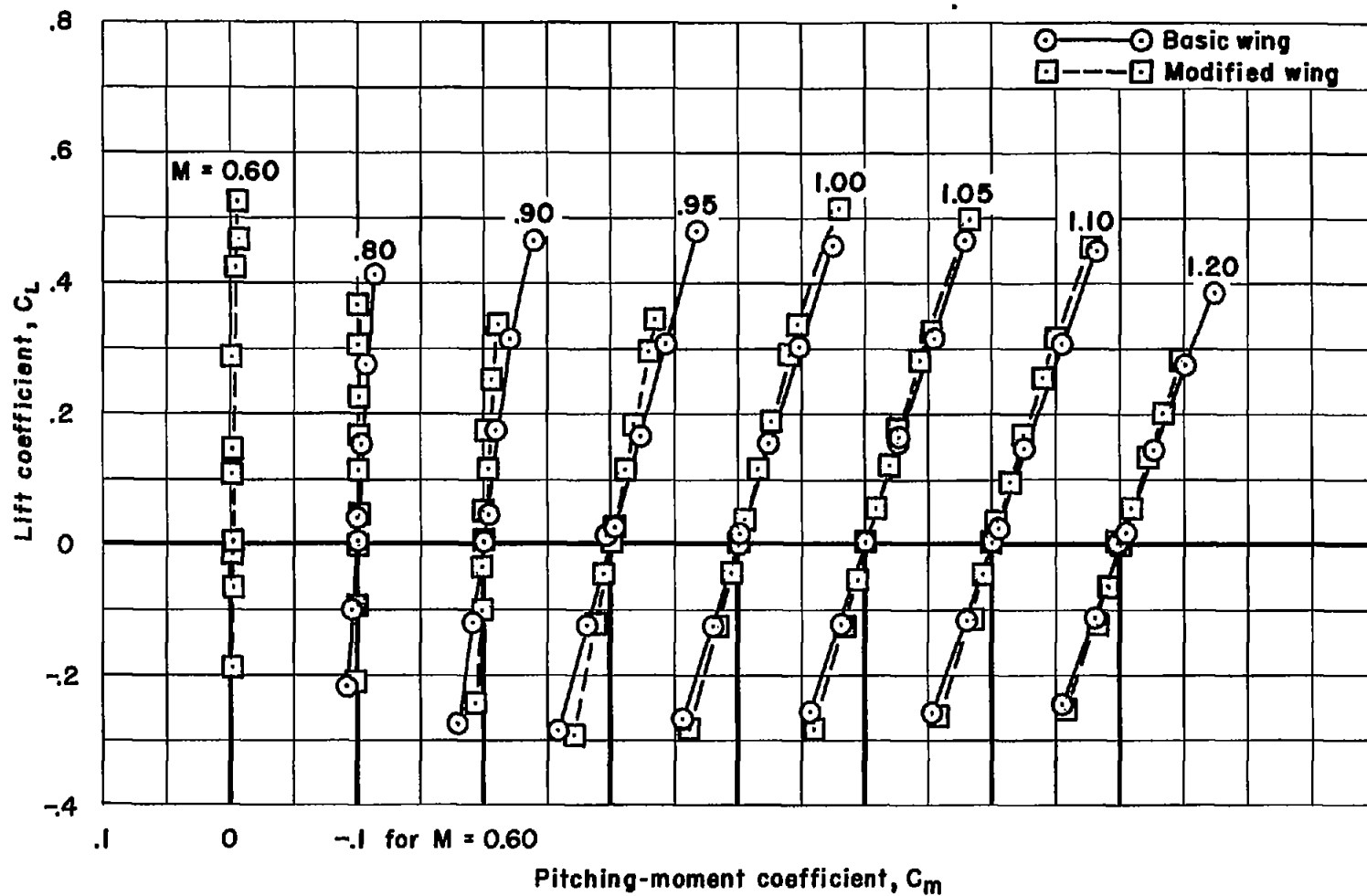
(b) C_L vs. C_m; Sears-Haack body.

Figure 8.- Continued.
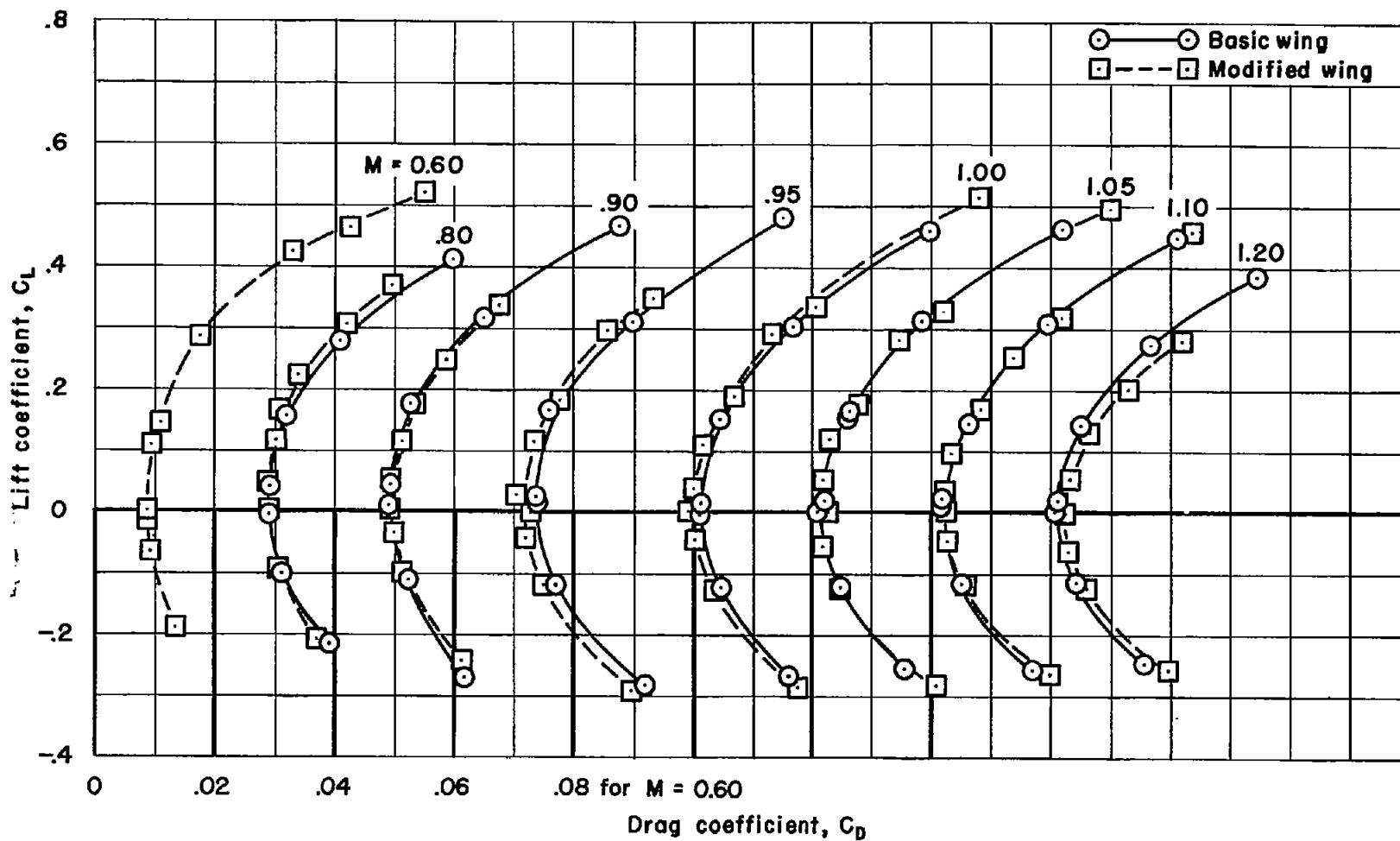
(c) C_L vs. C_D; Sears-Haack body.

Figure 8.- Concluded.
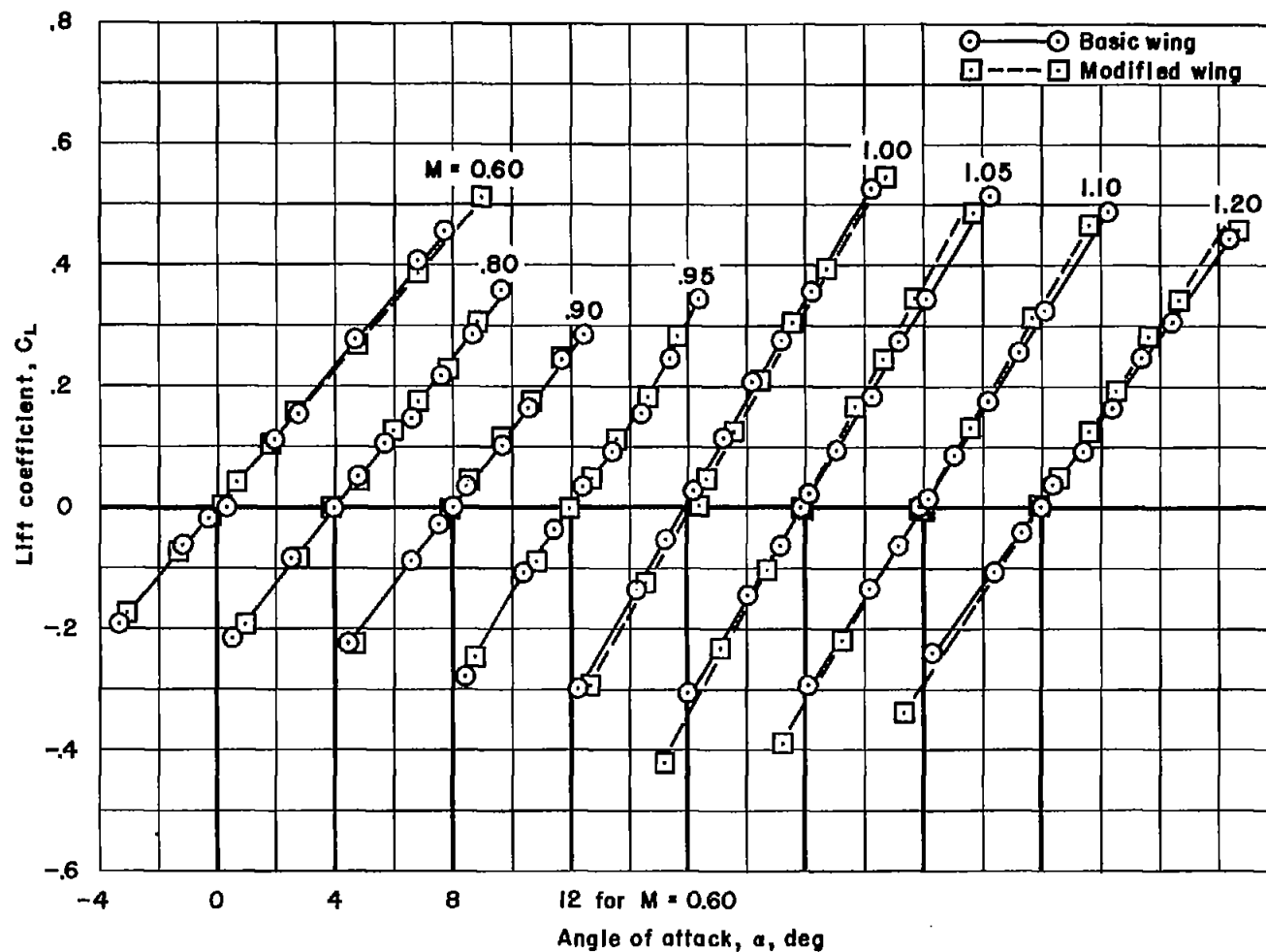
(a) C_L vs. α; M = 1.05 body indentations.

Figure 9.- Aerodynamic characteristics of the basic- and modified-wing models with bodies indented for M = 1.05.
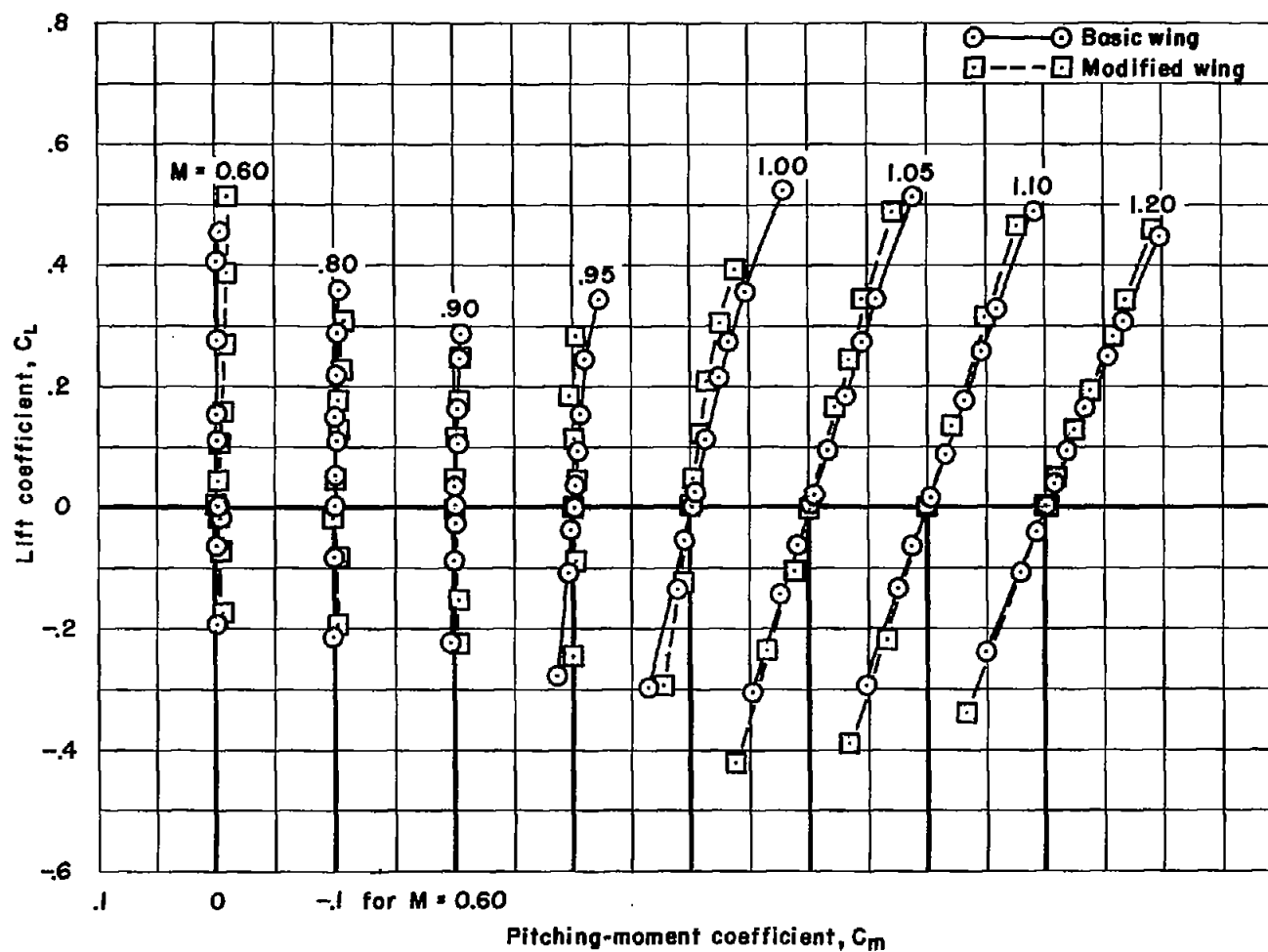
(b) C_L vs. C_m; M = 1.05 body indentations.

Figure 9.- Continued.
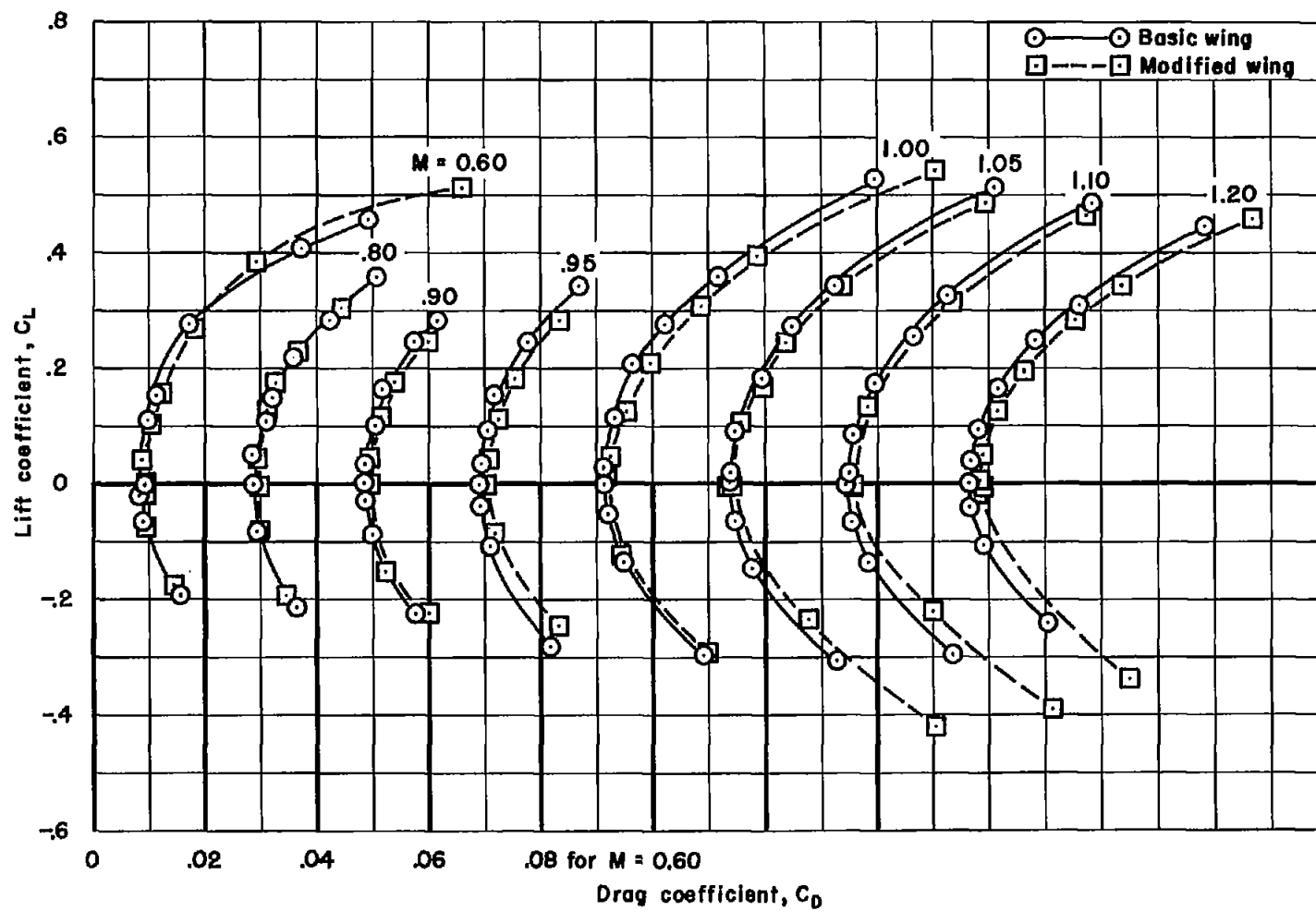
(c) C_L vs. C_D; M = 1.05 body indentations.

Figure 9.- Concluded.
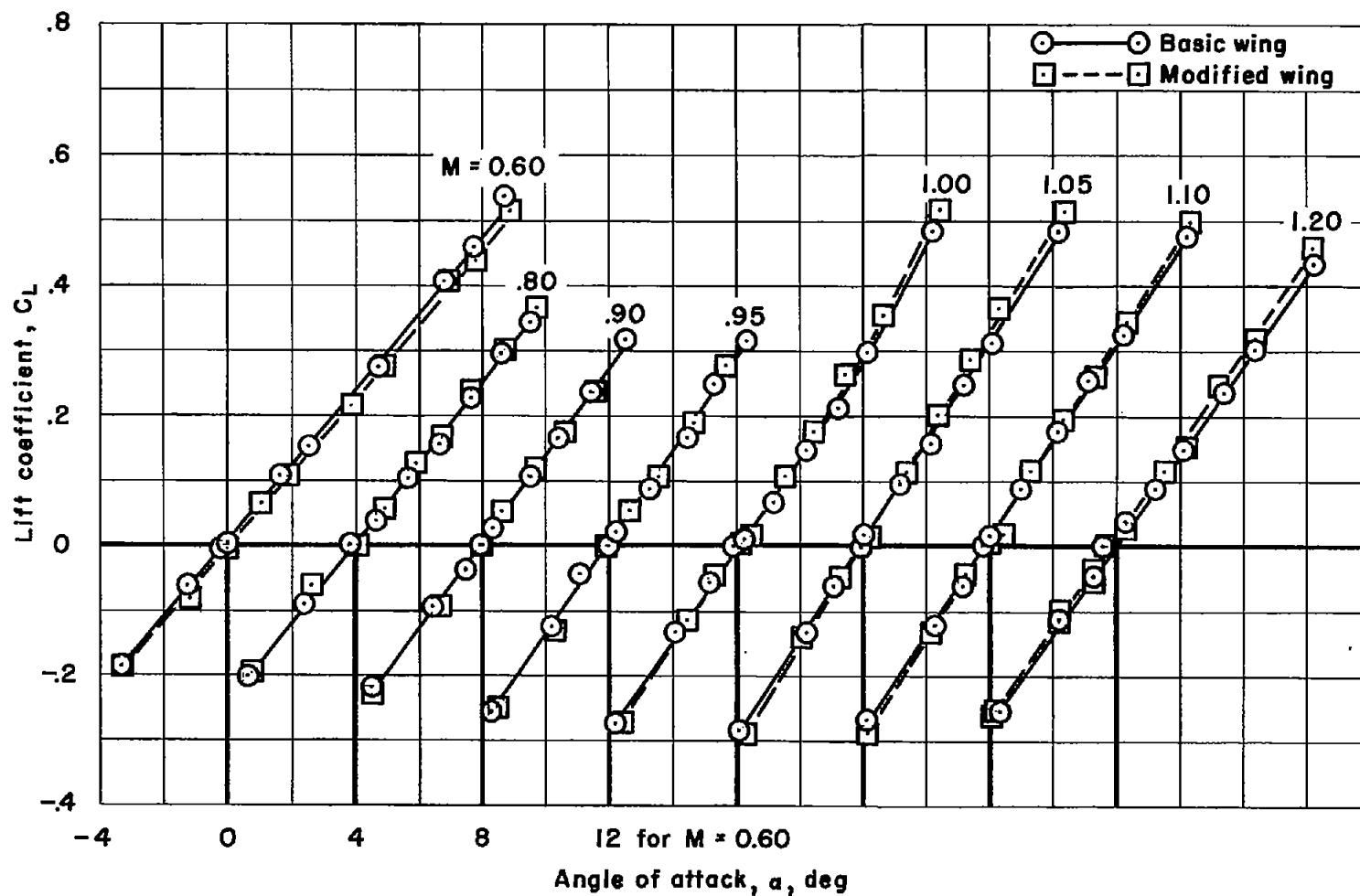
(a) C_L vs. α; M = 1.20 body indentations.

Figure 10.- Aerodynamic characteristics of the basic- and modified-wing models with bodies indented for M = 1.20.
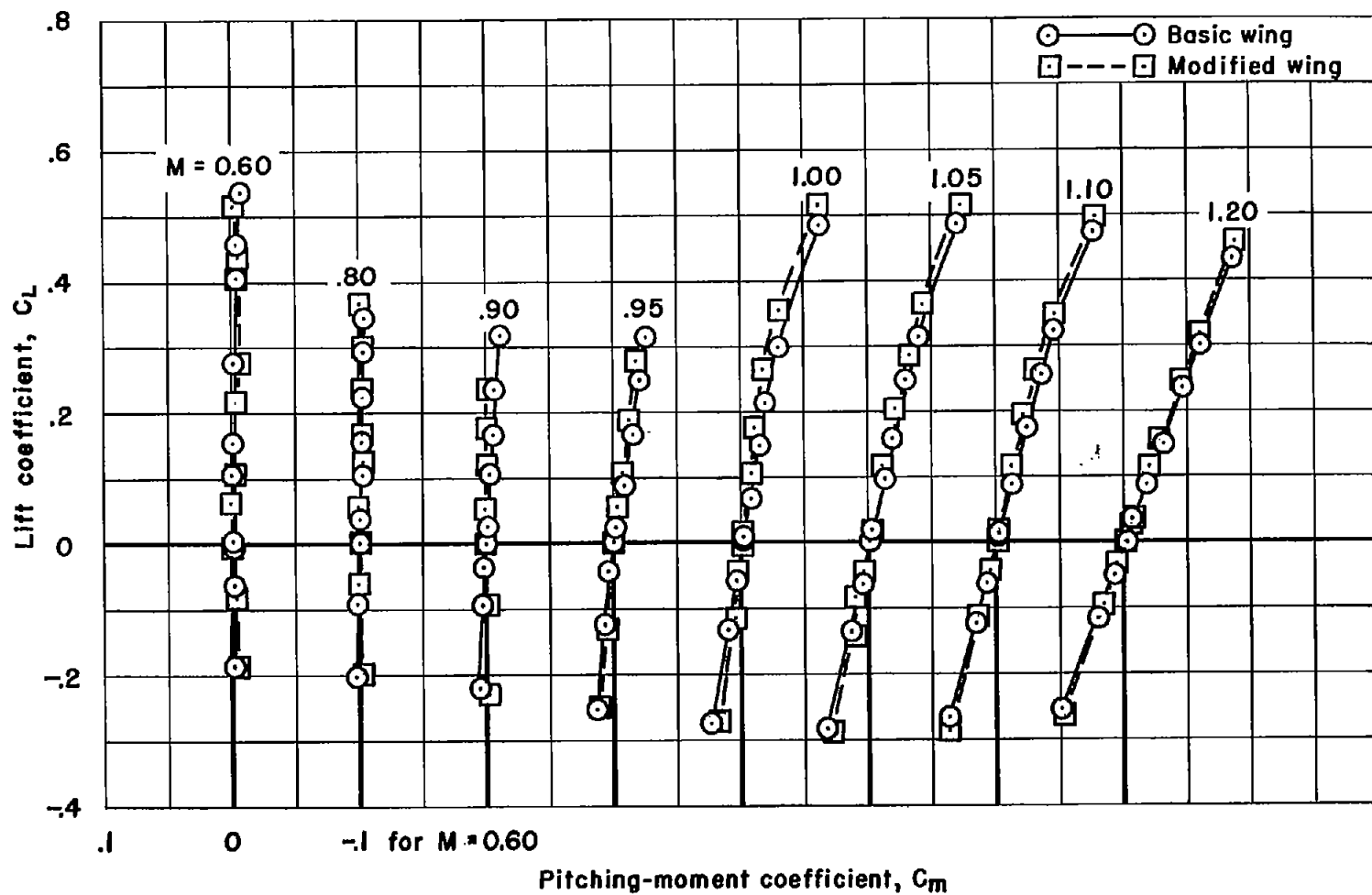
(b) C_L vs. C_m; M = 1.20 body indentations.

Figure 10.- Continued.
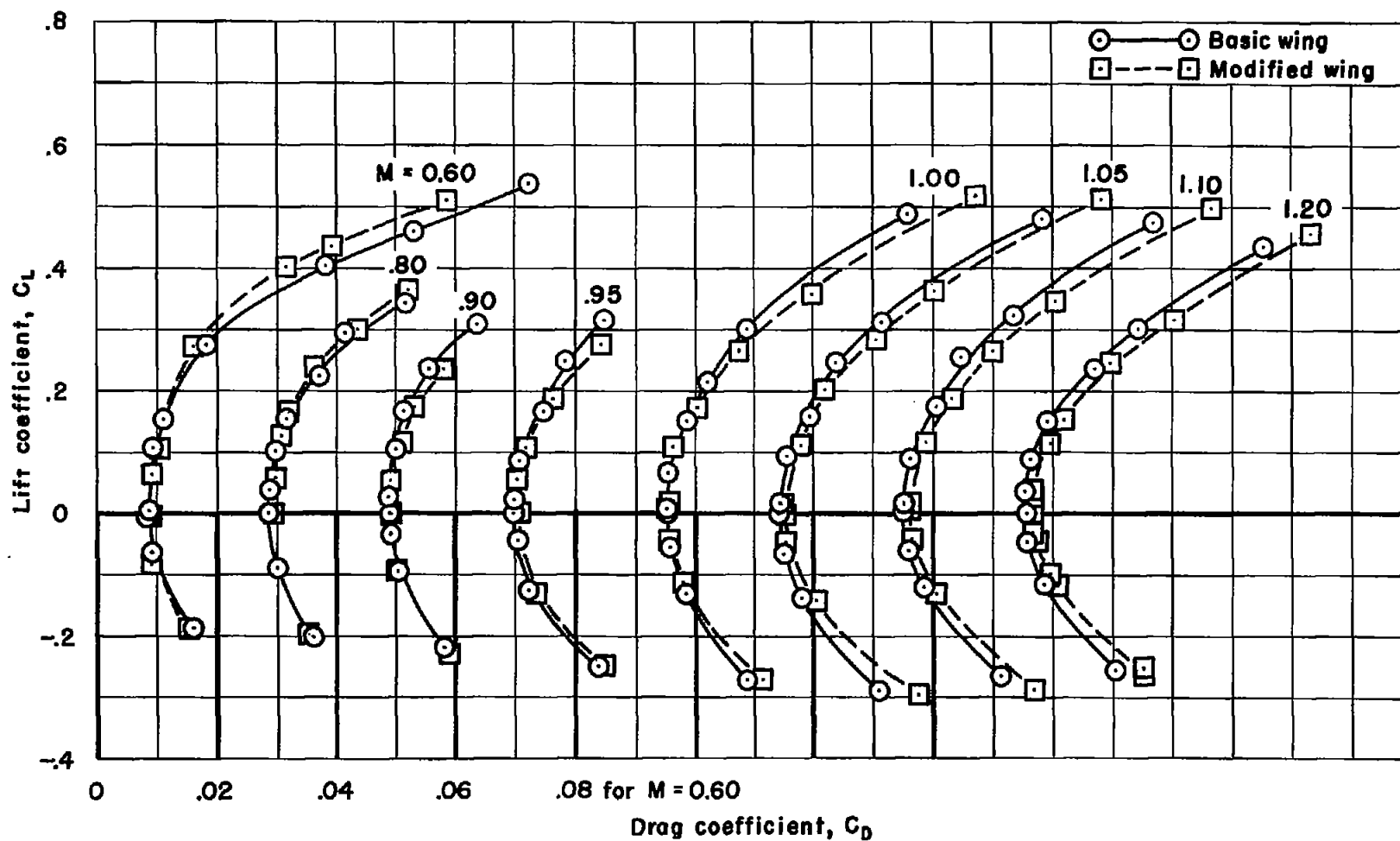
(c) C_L vs. C_D; M = 1.20 body indentations.

Figure 10.- Concluded.
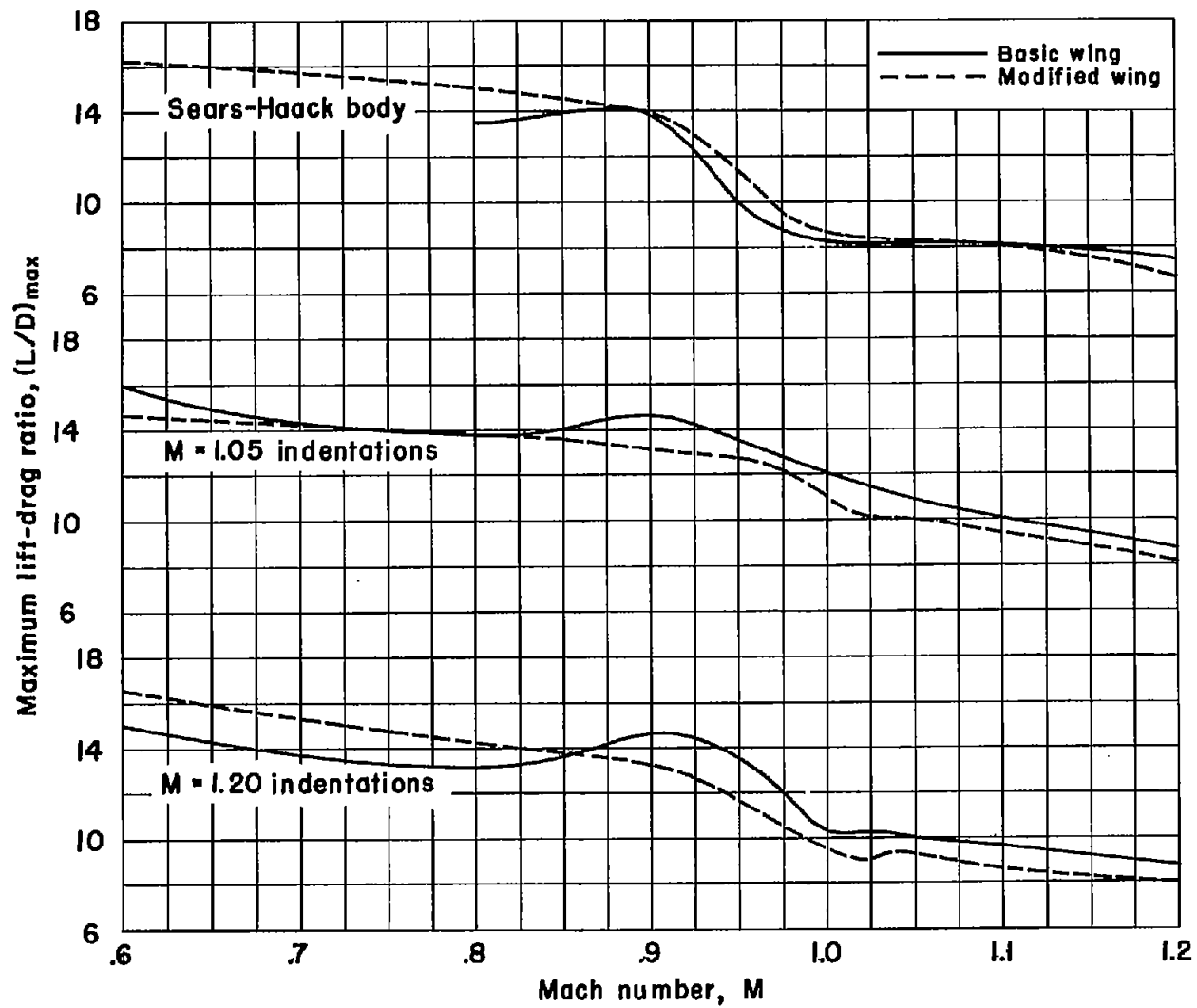
Figure 11.- Maximum lift-drag ratios for the basic- and modified-wing models with various bodies.
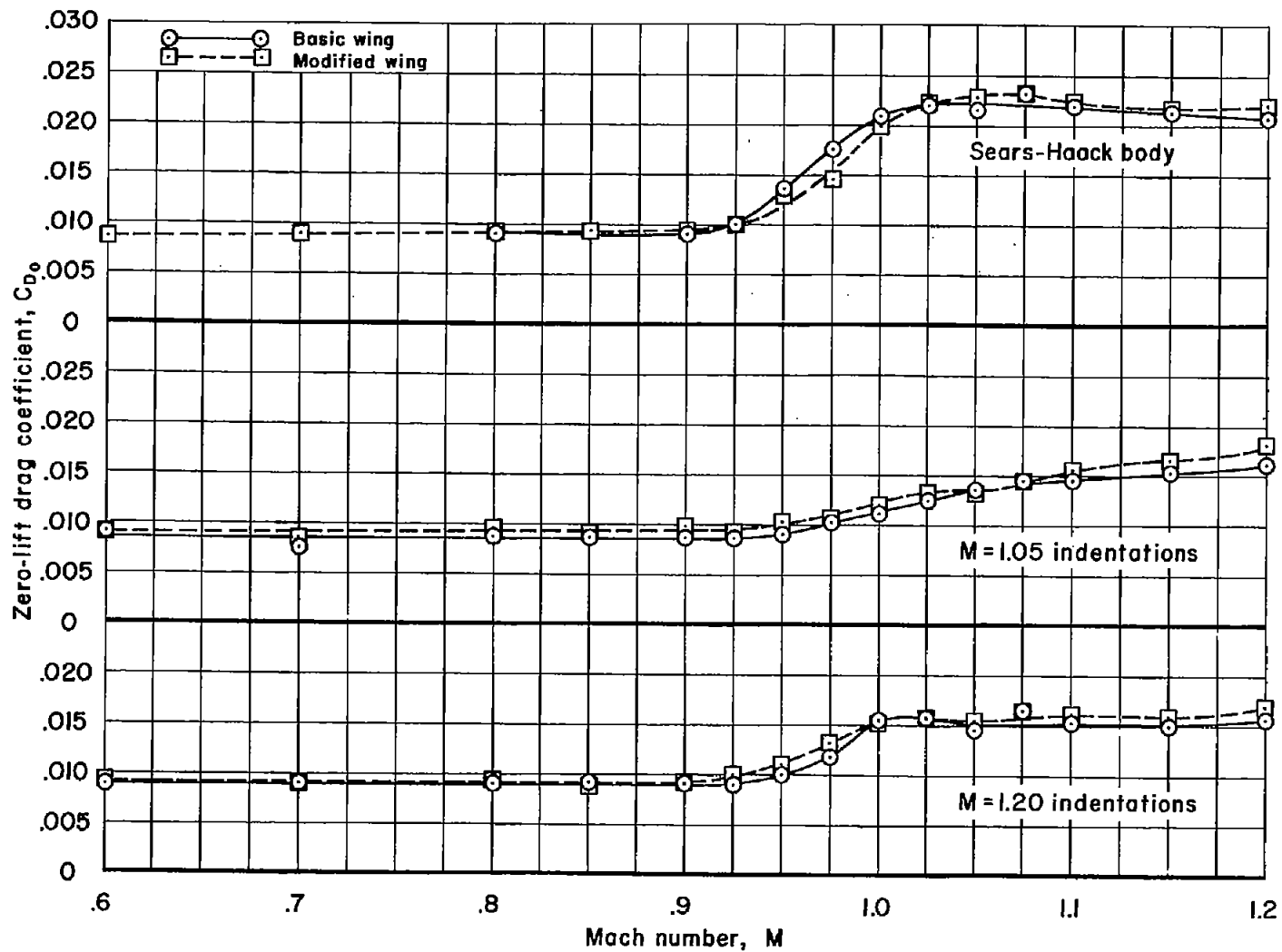
Figure 12.- Zero-lift drag coefficients for the basic- and modified-wing models with various bodies.
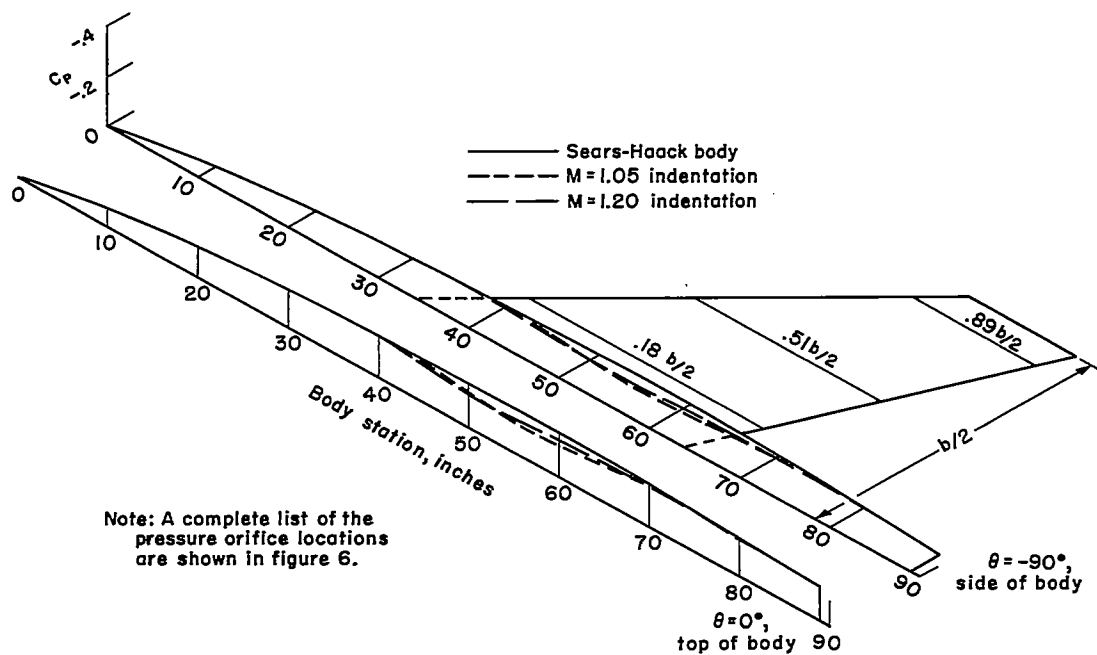
Figure 13.- Regions of wing and body represented by the pressure curves of figure 14.

(a) M = 0.90.
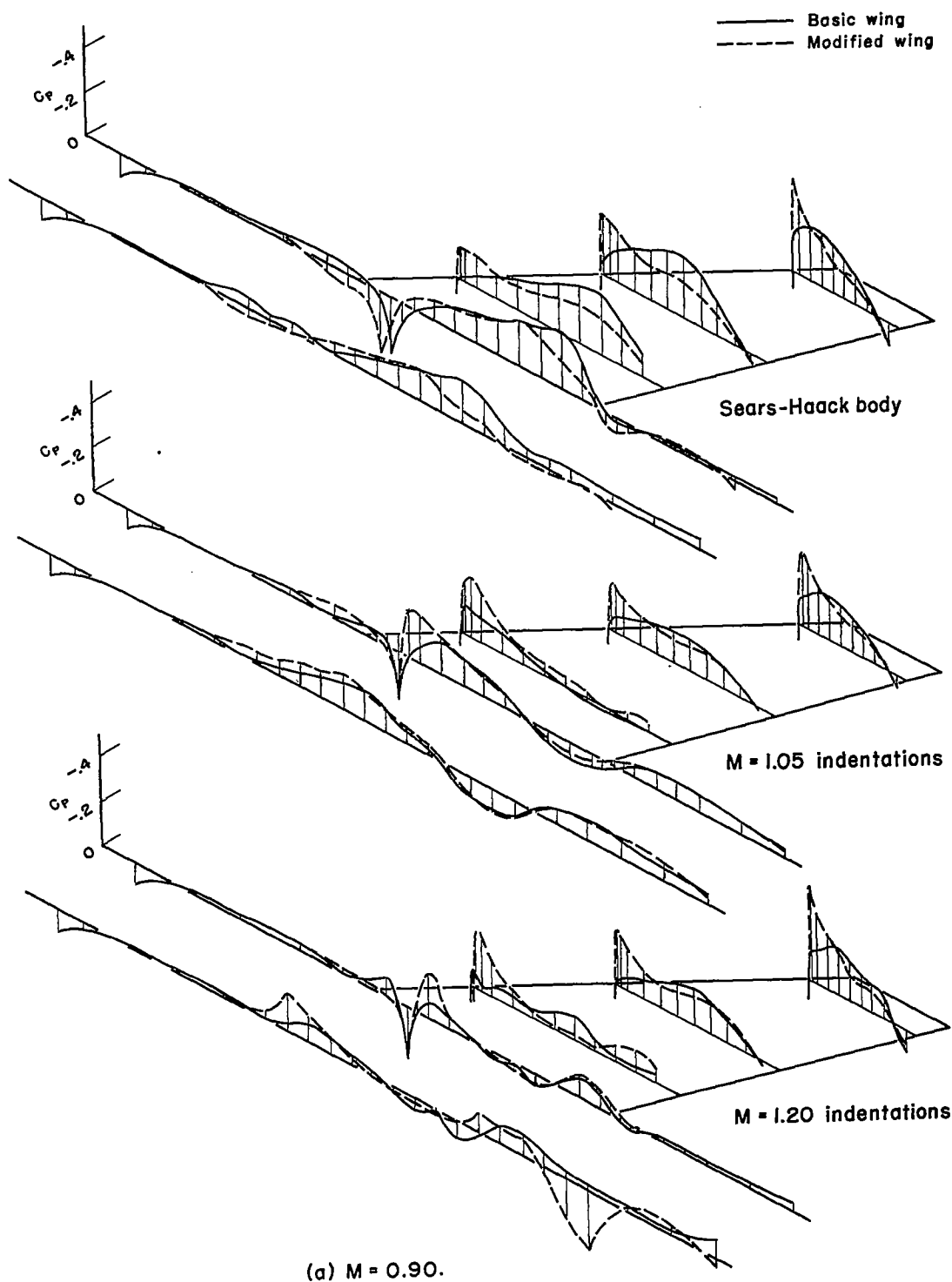
Figure 14.- Representative zero-lift pressure distributions.
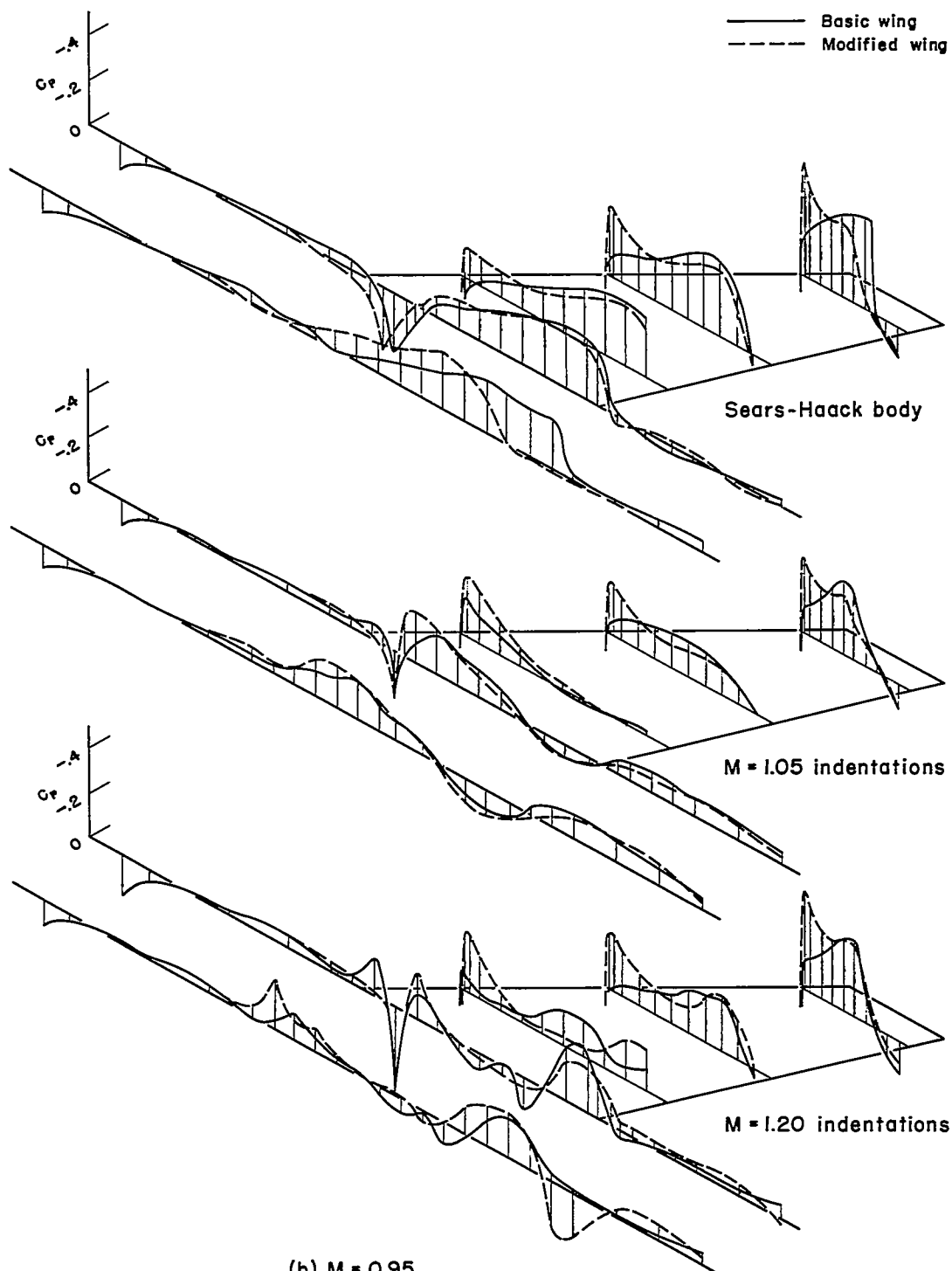
(b) M = 0.95.

Figure 14.- Continued.

Basic wing
Modified wing

-.4
C_p -.2
0

Sears-Haack body

-.4
C_p -.2
0

M = 1.05 indentations

-.4
C_p -.2
0

M = 1.20 indentations

(c) M = 1.00.

Figure 14.- Continued.

(d) M = 1.05.

Figure 14.- Continued.

Basic wing
Modified wing

Sears-Haack body

M = 1.05 indentations

M = 1.20 indentations
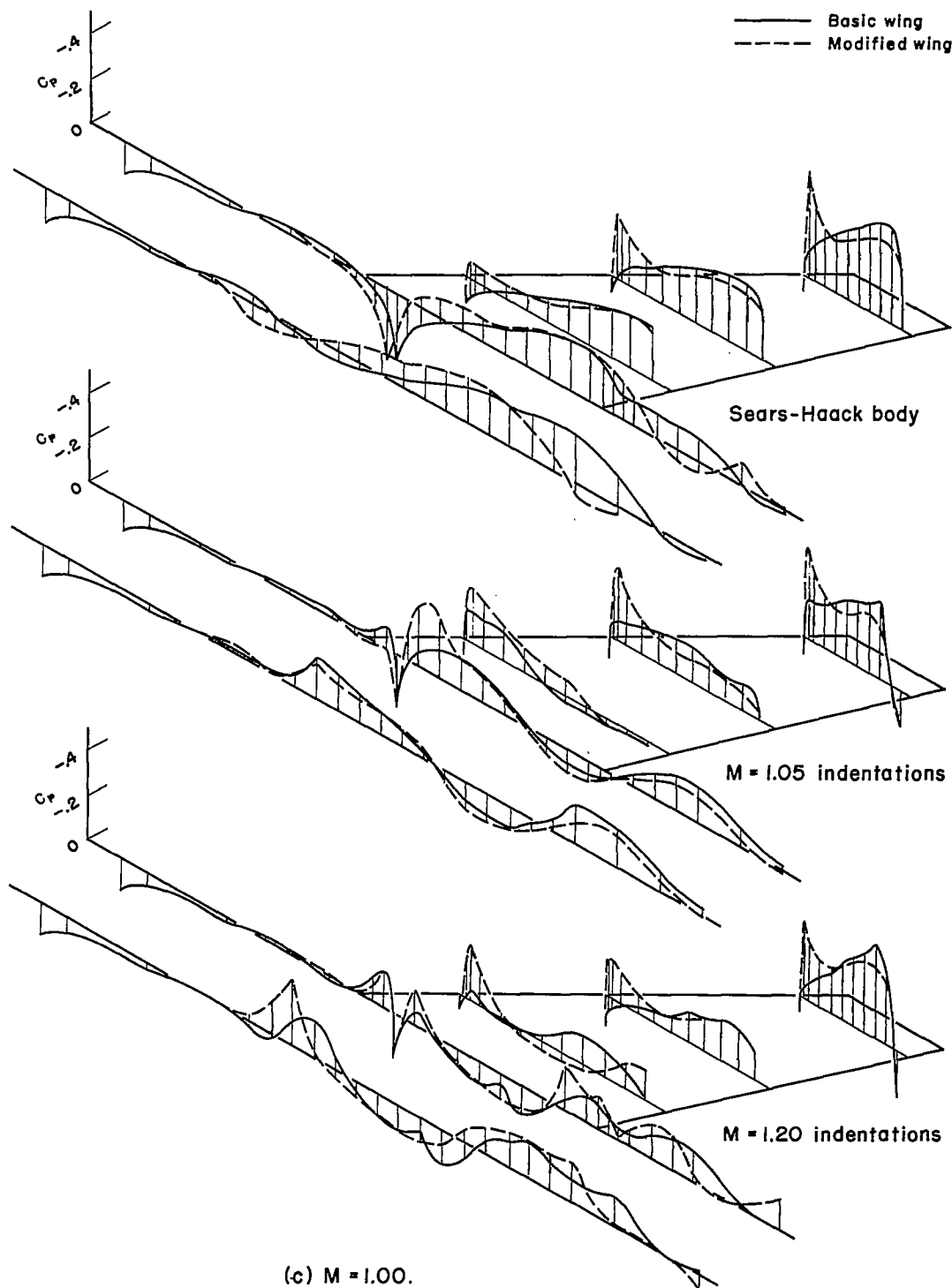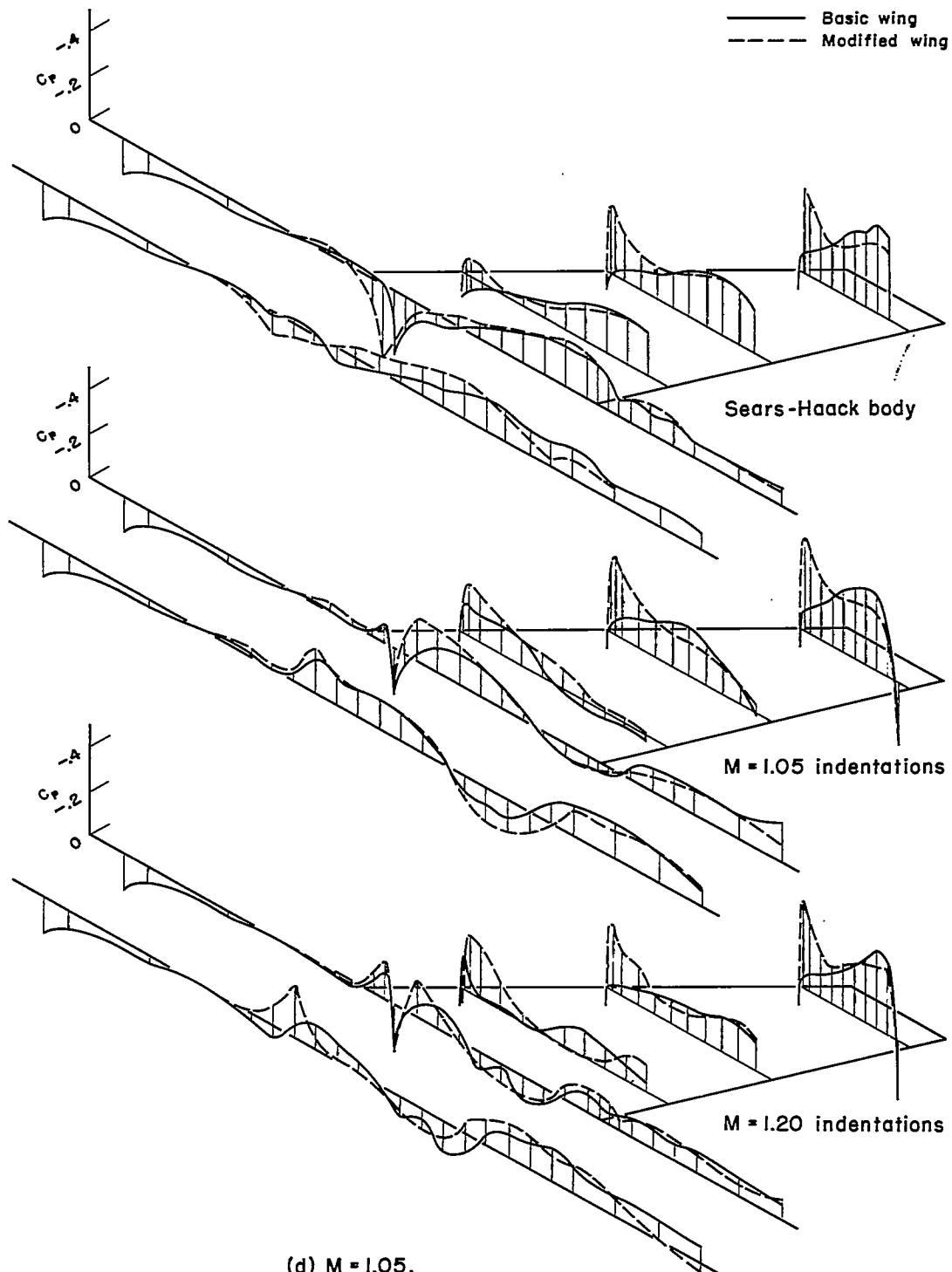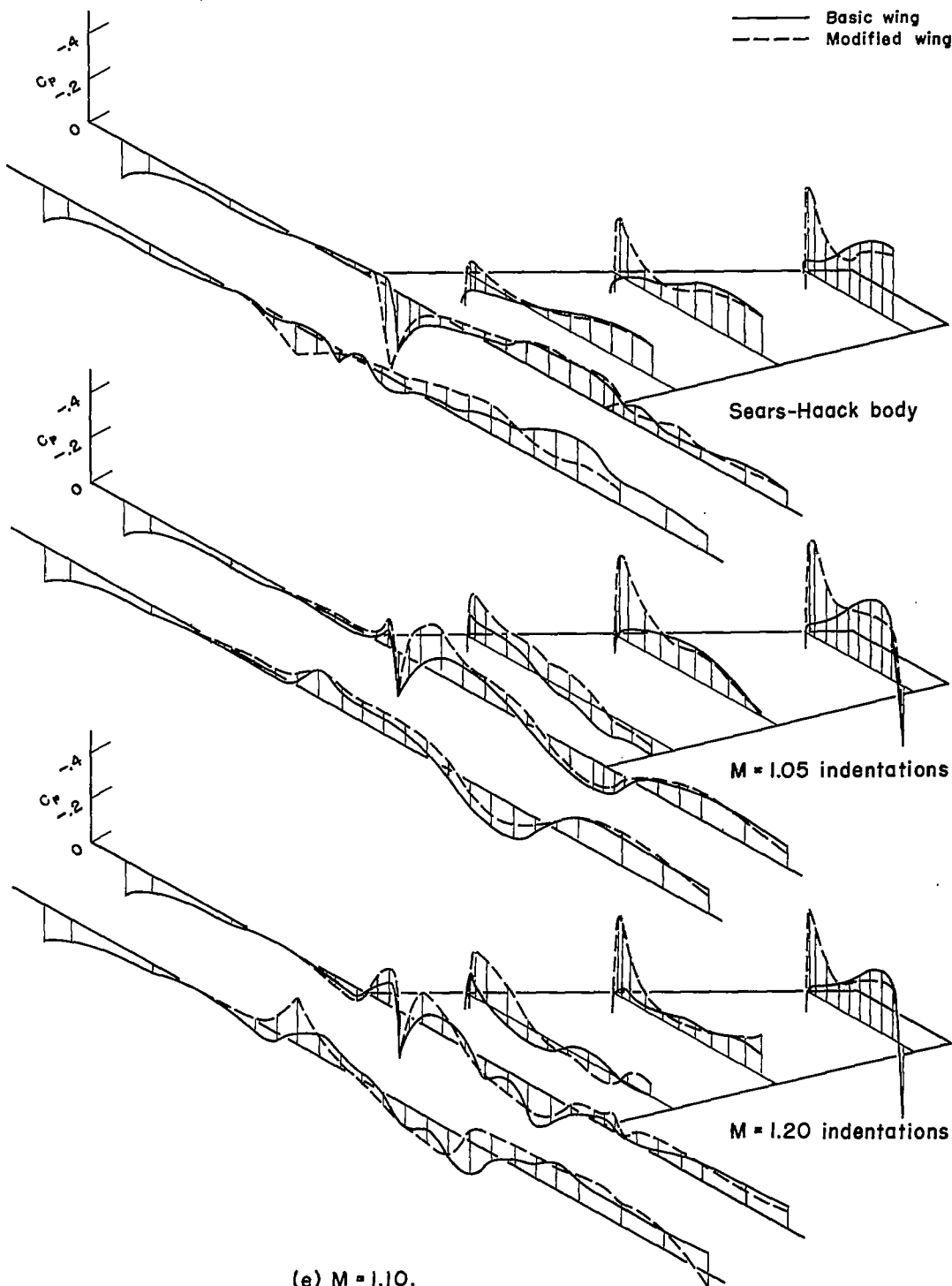
(e) M = 1.10.

Figure 14.- Continued.

(f) M = 1.20.
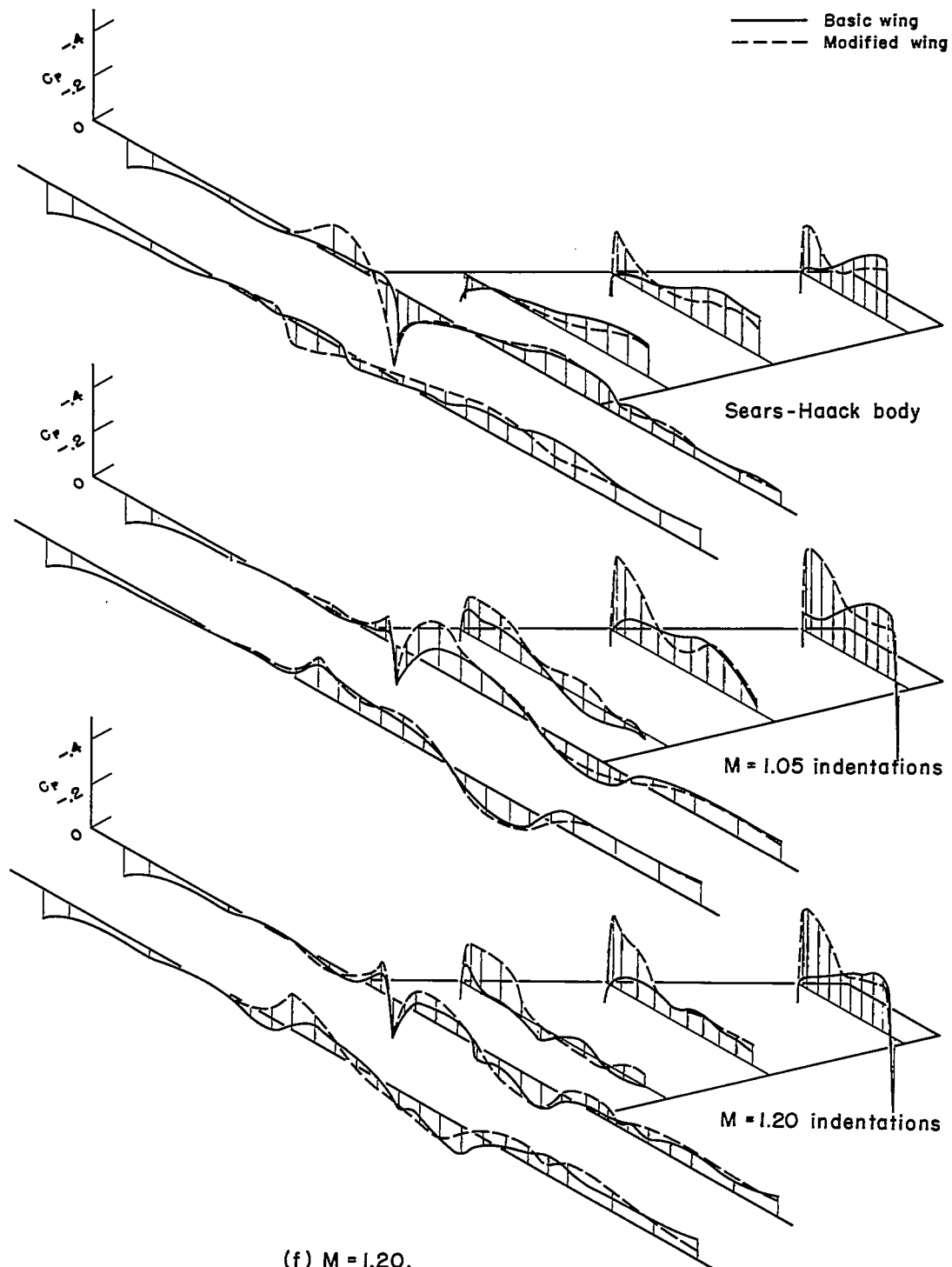
Figure 14.- Concluded.
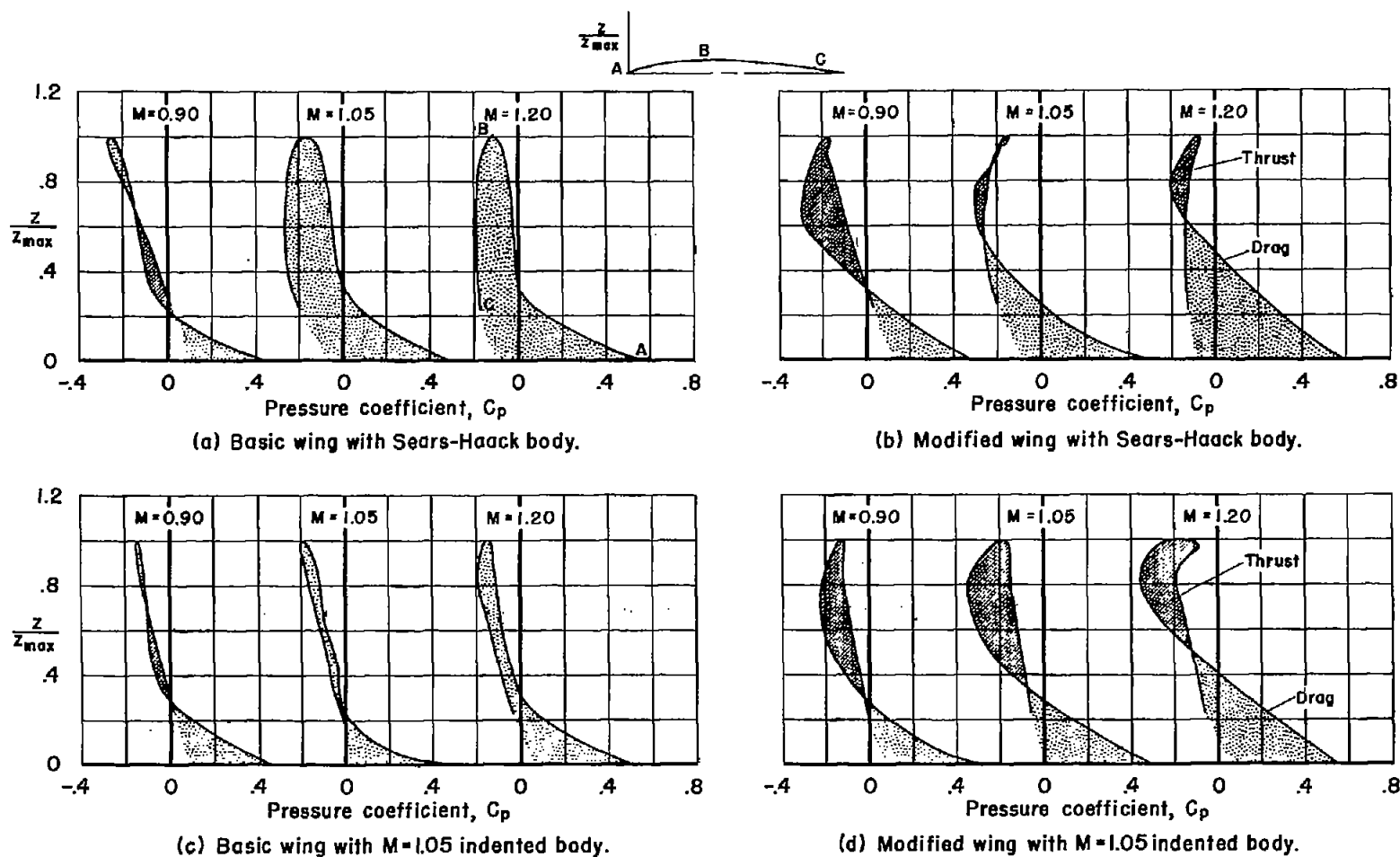
Figure 15.- Zero-lift pressure coefficients for the mid-semispan station (see fig. 13) and the upper surface of each wing plotted to illustrate the thrust and drag components of the streamwise airfoil sections.
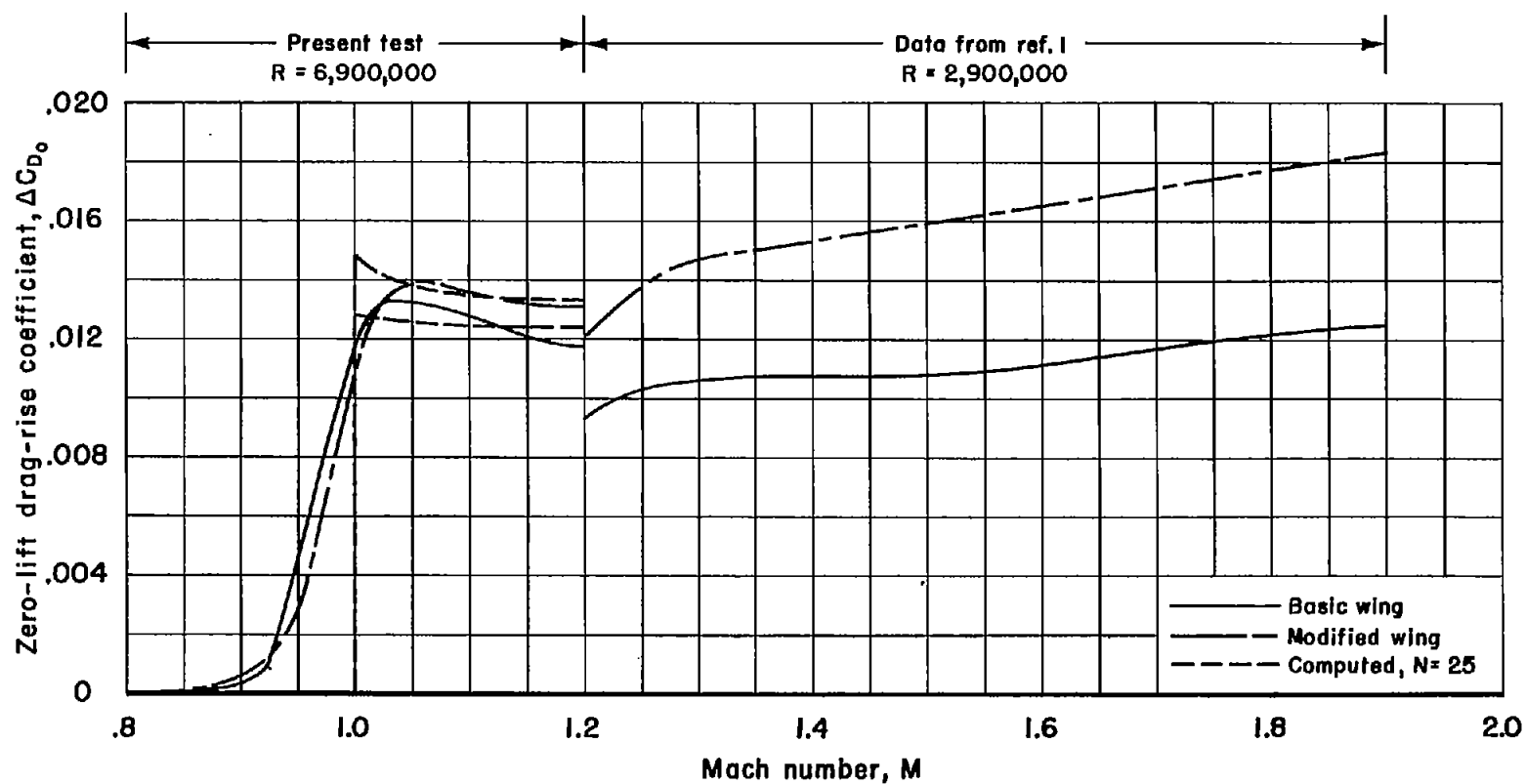
Figure 16.- Zero-lift drag-rise coefficients for the basic- and modified-wing models with the Sears-Haack body. (The modified wing of ref. 1 had slight forward camber.)
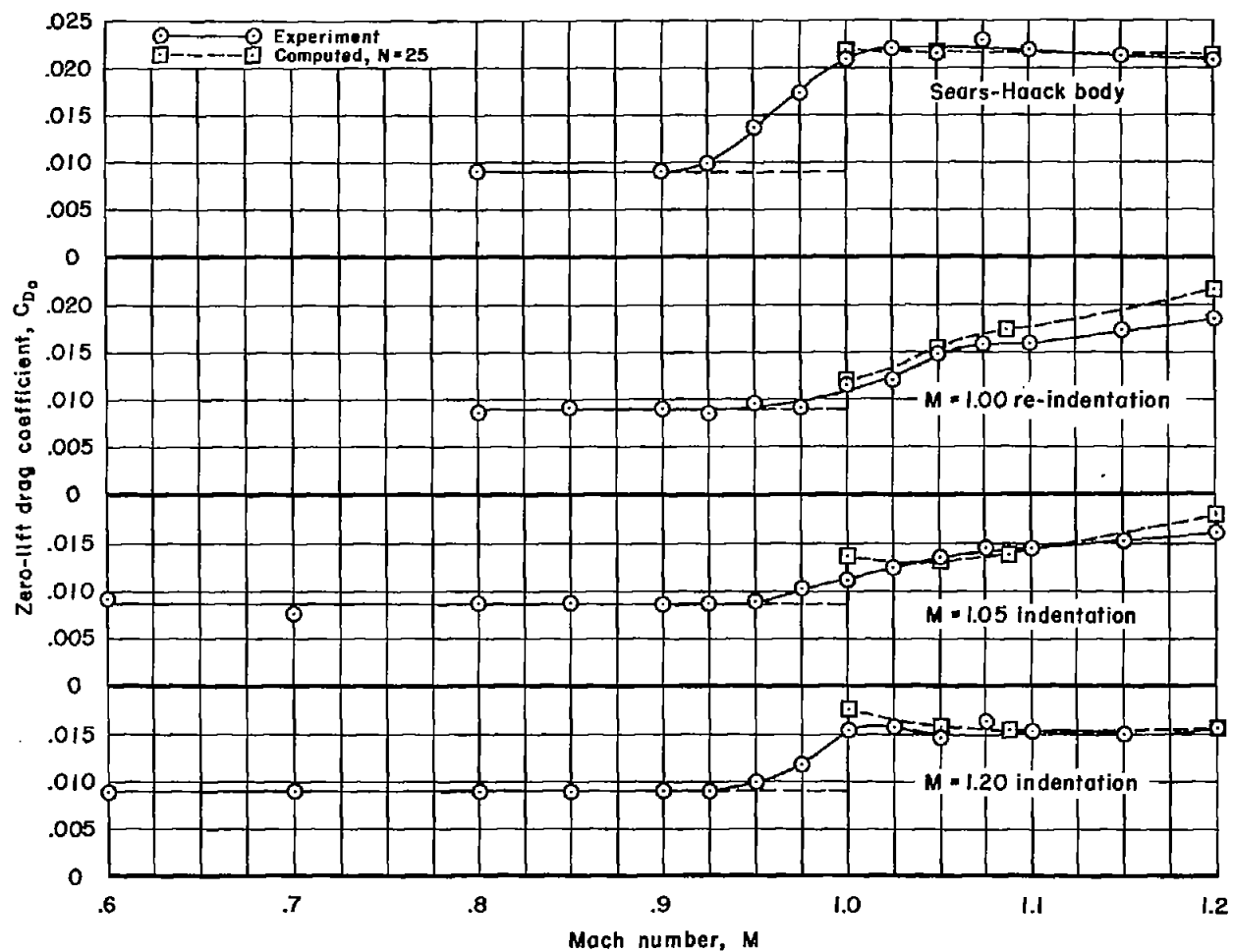
(a) Basic-wing models.

Figure 17.- Experimental and computed zero-lift drag coefficients for the two wing models with various bodies.
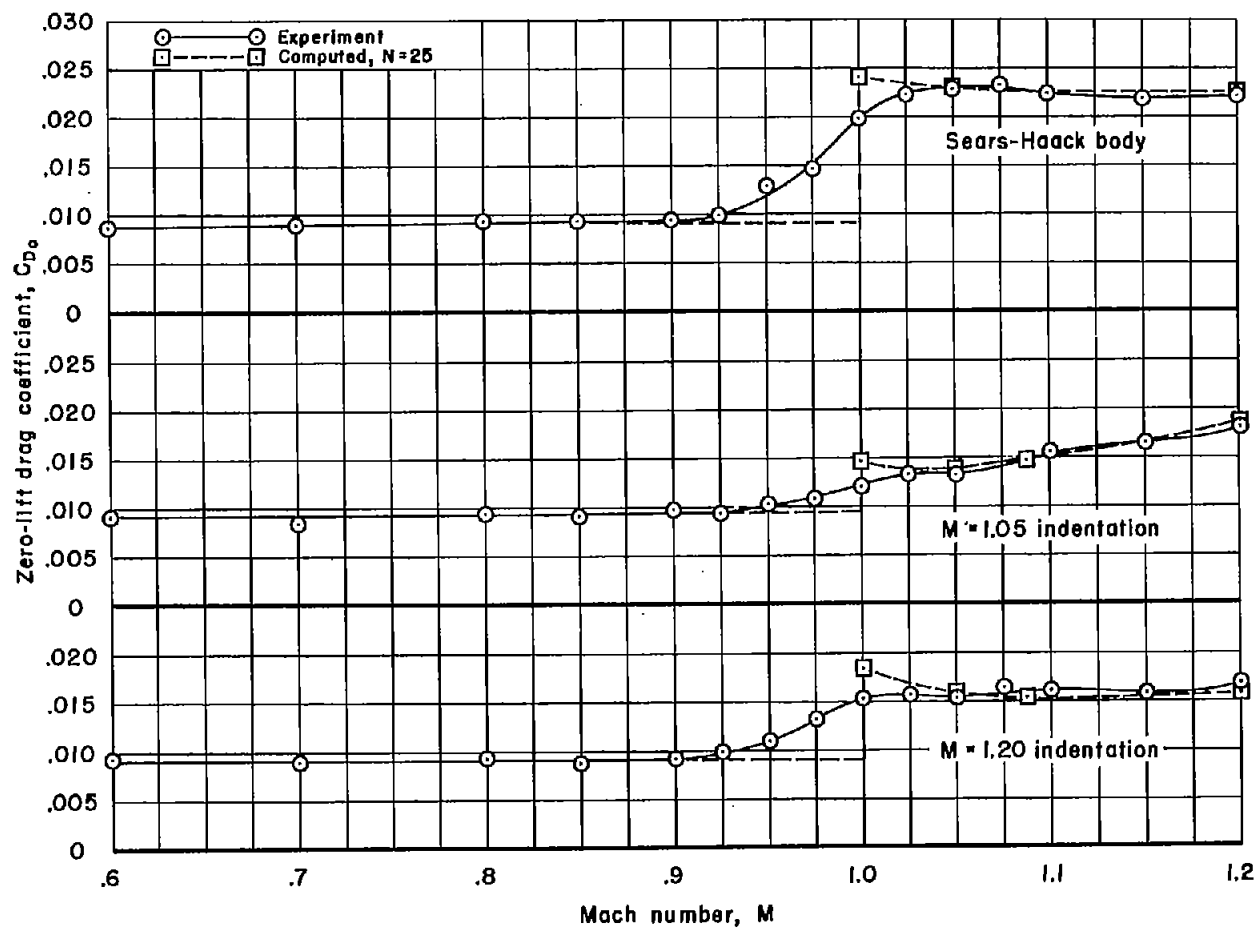
(b) Modified-wing models.

Figure 17.- Concluded.
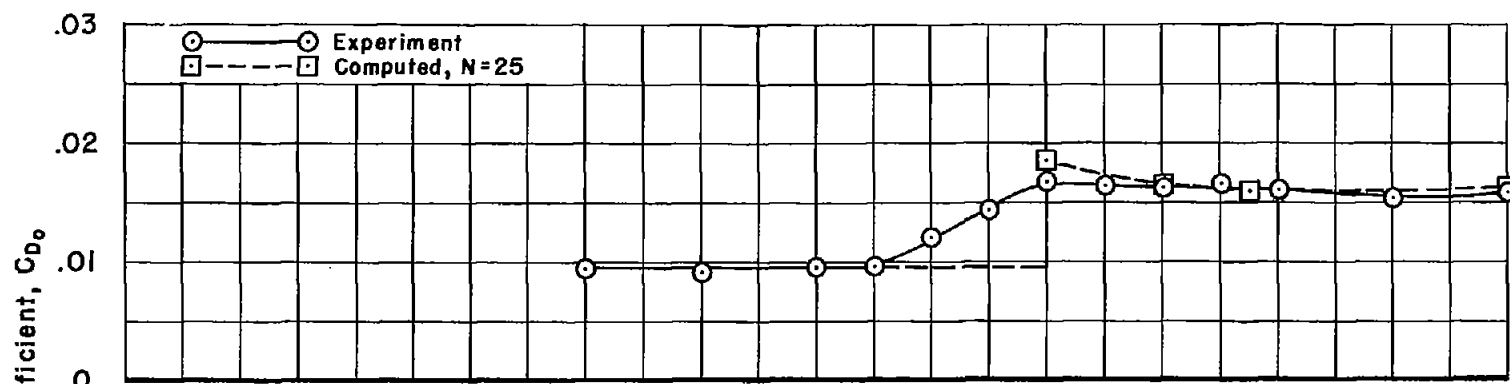
(a) Basic wing.
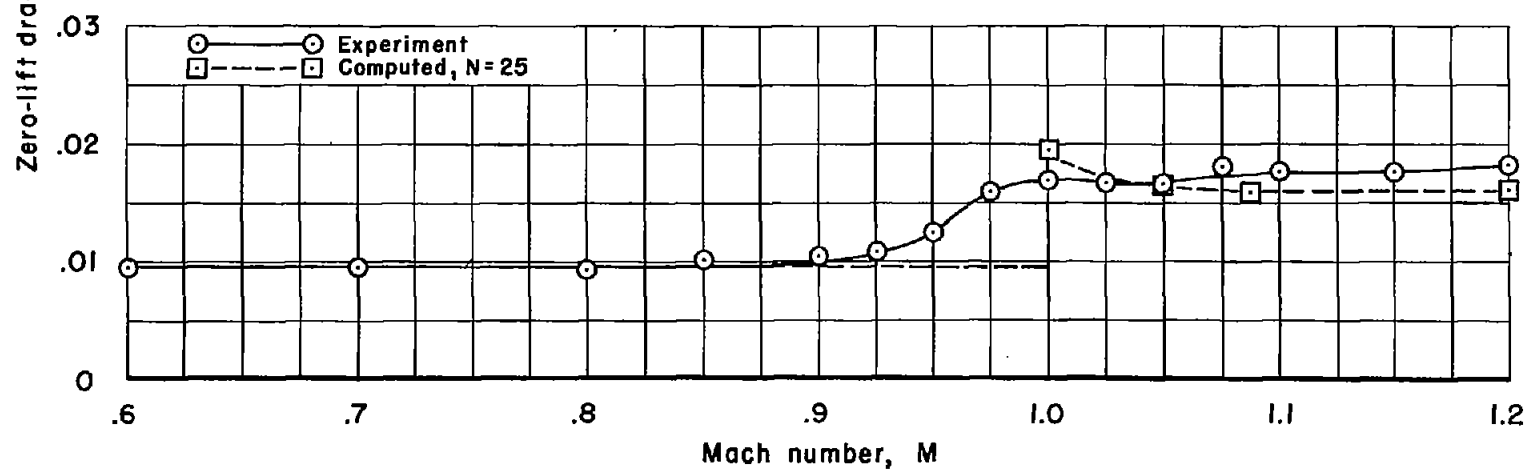
(b) Modified wing.

Figure 18.- Experimental and computed zero-lift drag coefficients for the basic- and modified-wing models with the $M = 1.20$ re-indented bodies.
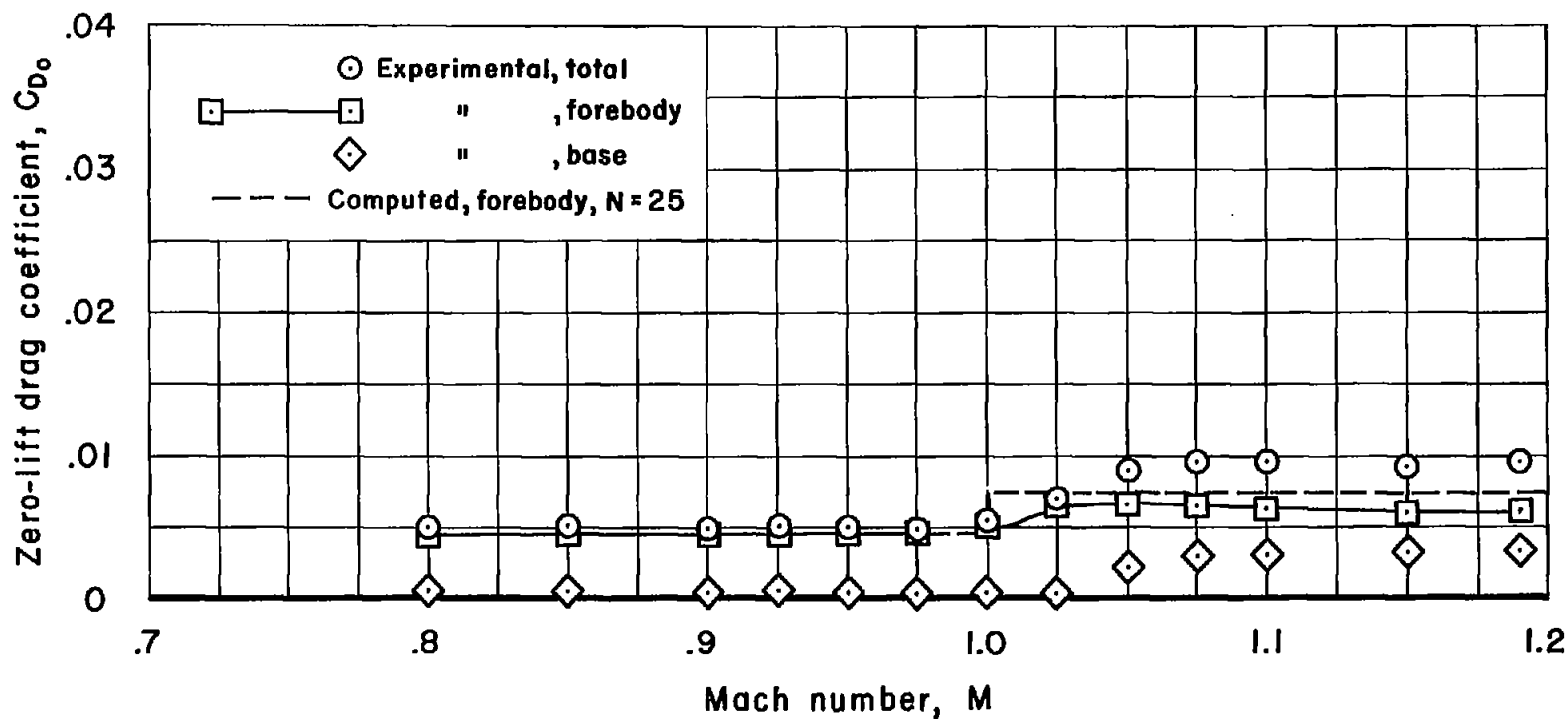
Figure 19.- Representative figure of base drag coefficients which were subtracted from the total values to obtain the forebody drag coefficients (Sears-Haack body alone).

S   Theory, cut-off Sears-Haack body
I (1.05) Theory, basic wing with M=1.05 indented body
I (1.20) Theory, basic wing with M=1.20 indented body
O   Theory, basic wing with original body
▨   Theory, effect of wing modification
⊙   Experiment, basic wing and body
⊡   Experiment, modified wing and body

Zero-lift drag-rise coefficient, ΔC_{D_0}

.024
.020
.016
.012
.008
.004
0

S   I (1.05)   I (1.20)   O

M = 1.00   M = 1.05   M = 1.20
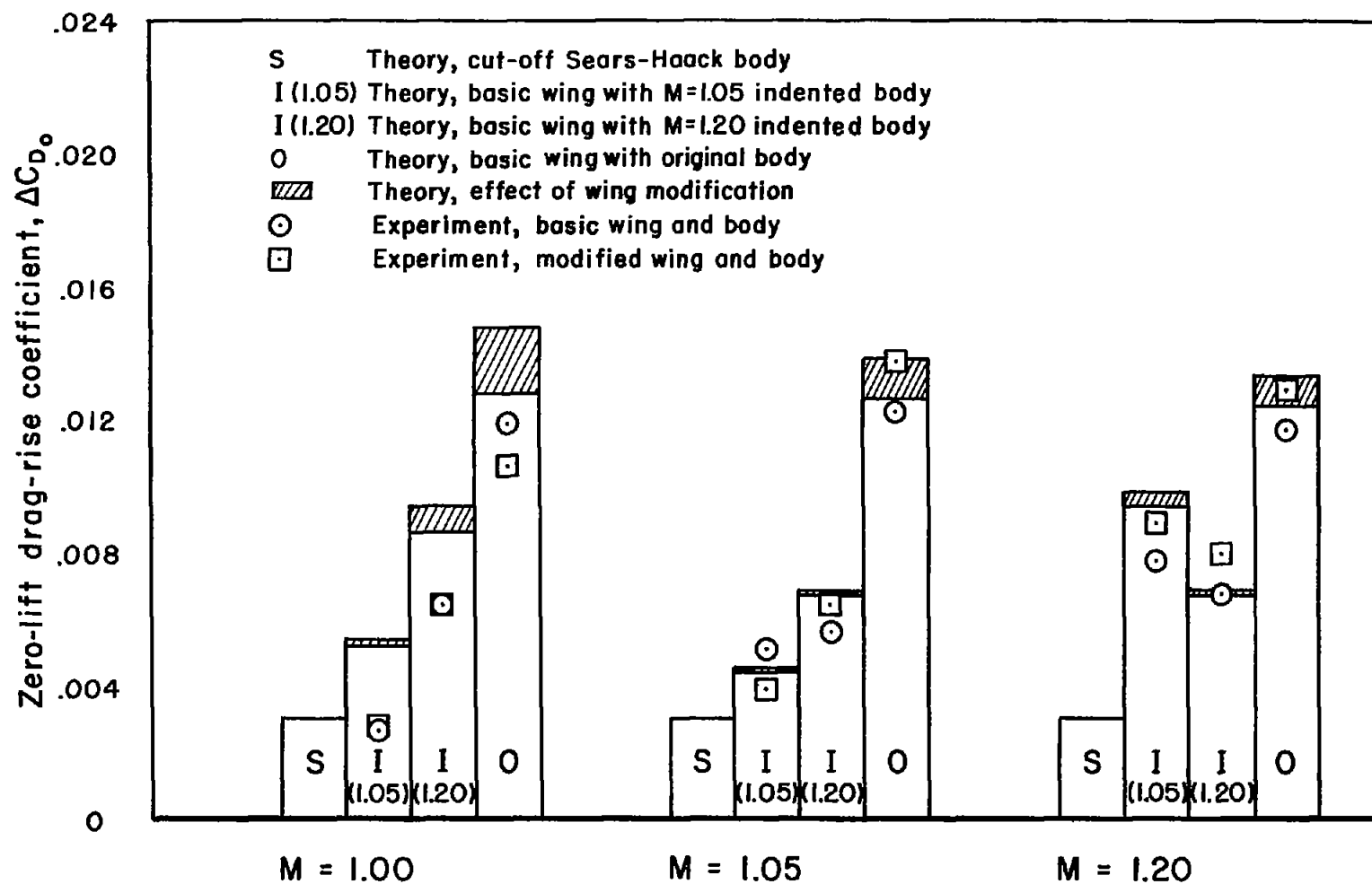
Figure 20.- Bar graph of computed zero-lift wave-drag coefficients for various models at three Mach numbers and the experimental drag-rise coefficient.
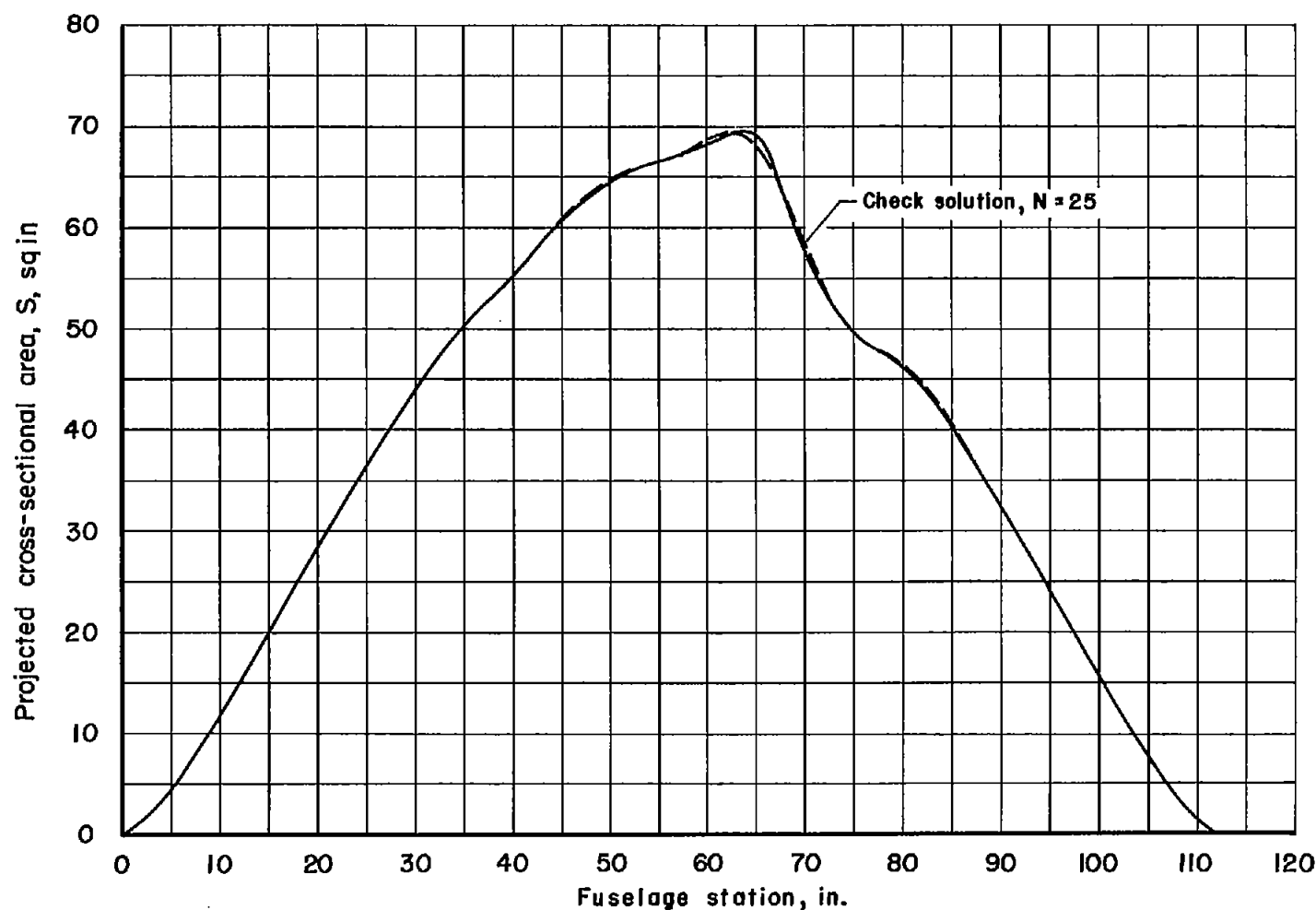
(a) M = 1.20, θ = 90°, ψ = 0°, and M = 1.00.

Figure 21.- Representative plots of the theoretical check solutions for N = 25 in comparison with the given area distributions (modified-wing model with M = 1.05 indented body).
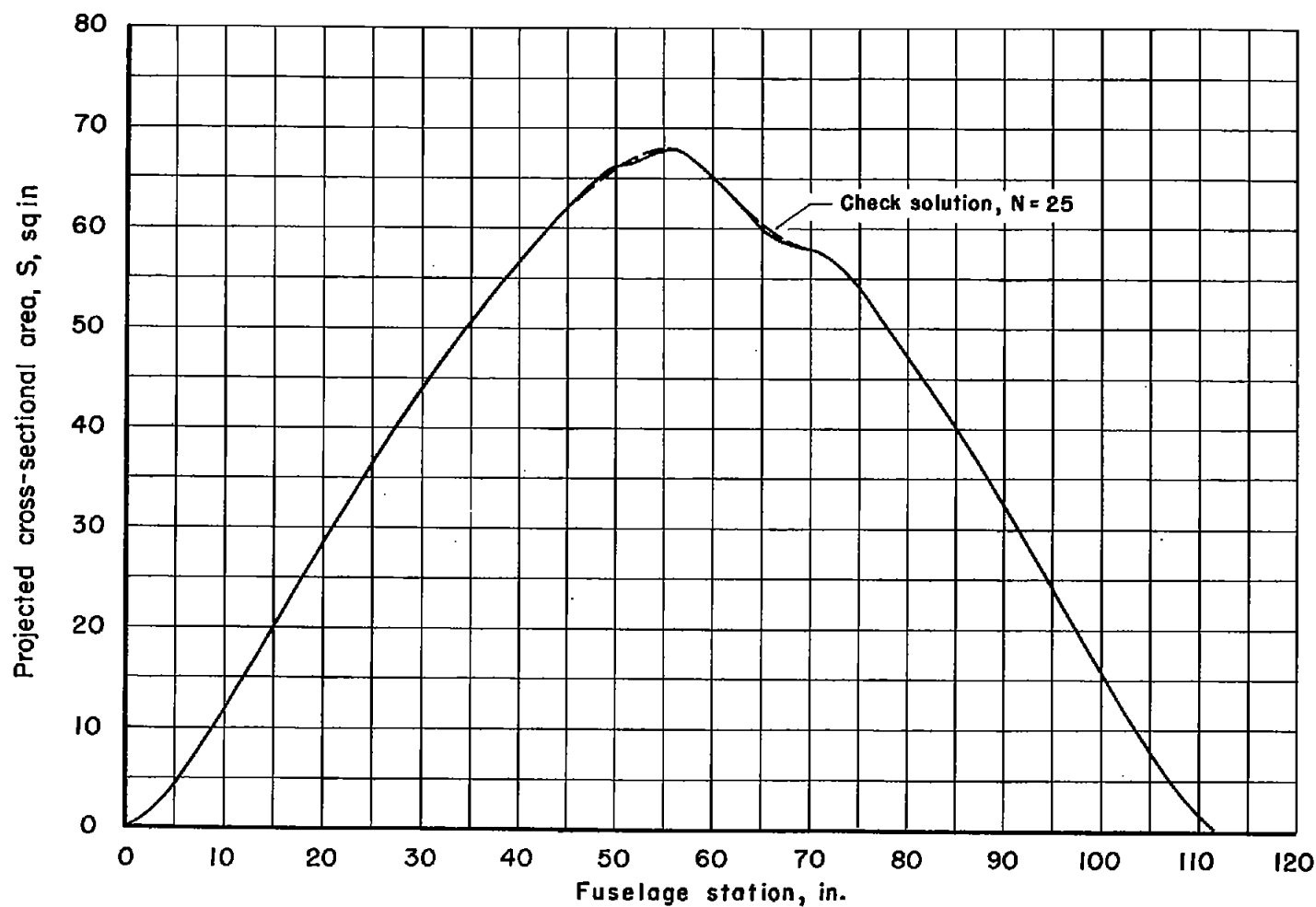
(b) $M = 1.20$, $\theta = 70^\circ$, $\psi = 12.75^\circ$

Figure 21.- Continued.
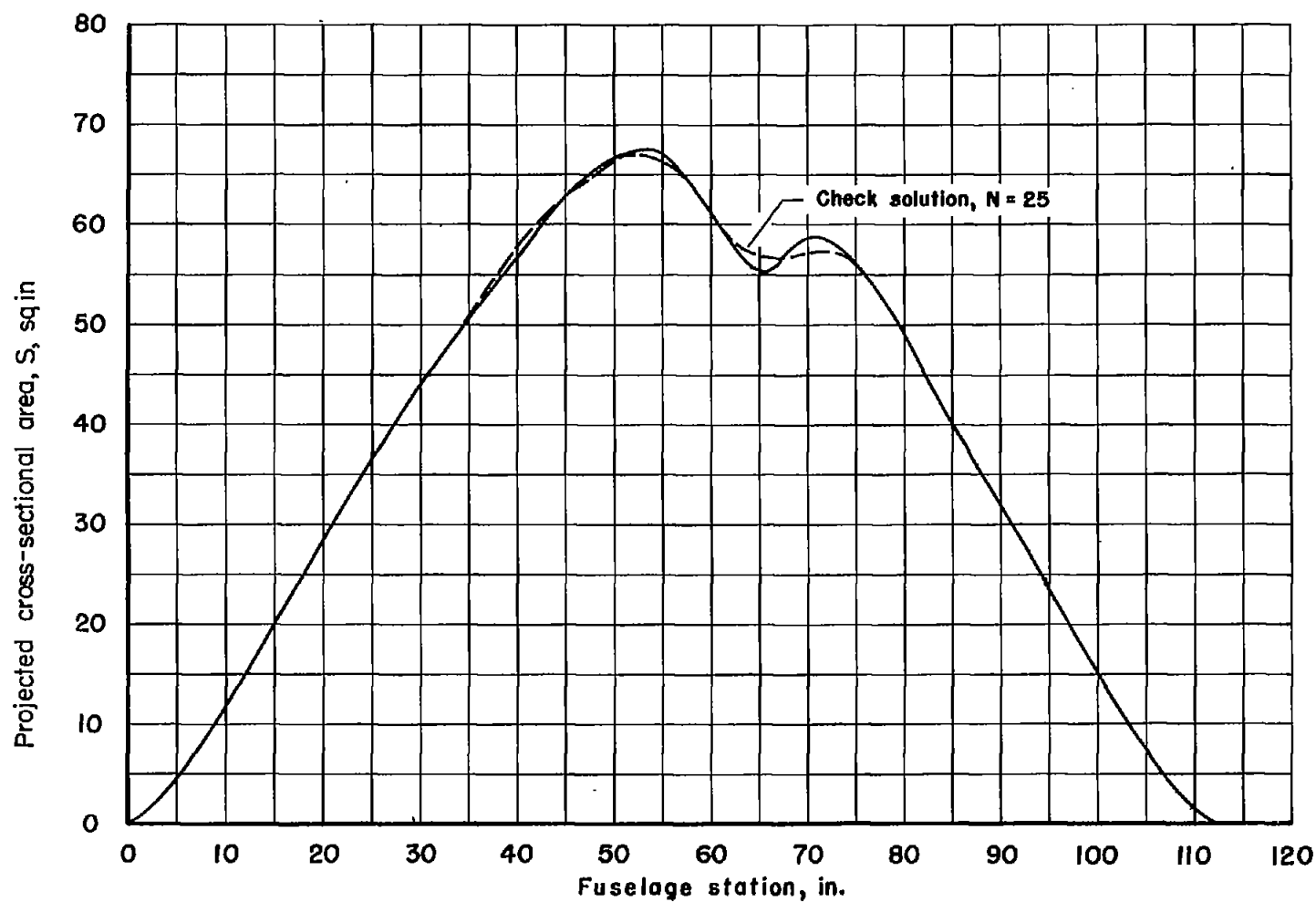
(c) M = 1.20, θ = 61.2°, ψ = 17.75°

Figure 21.- Continued.
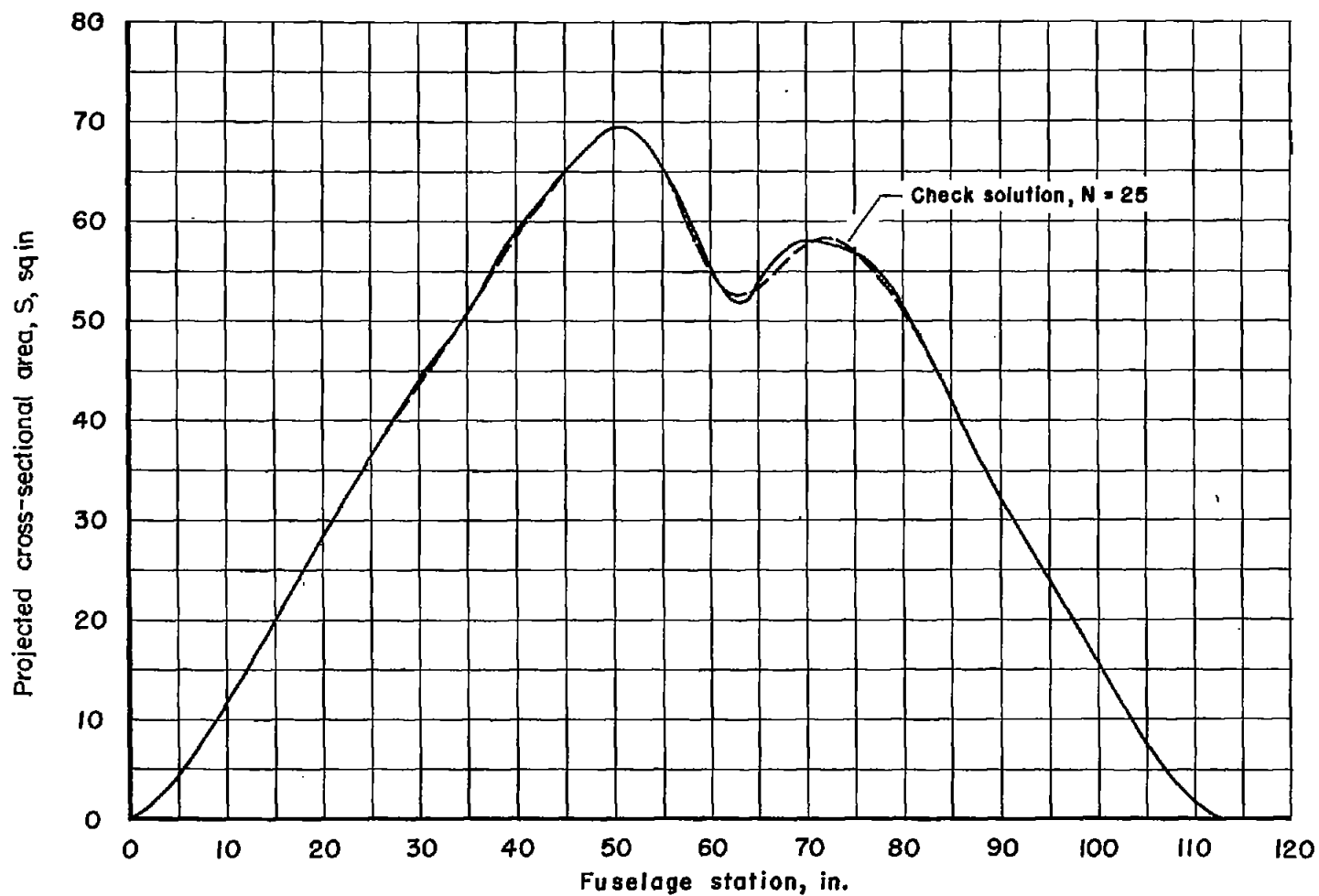
(d) $M = 1.20$, $\theta = 49.7^\circ$, $\psi = 23.2^\circ$

Figure 21.- Continued.
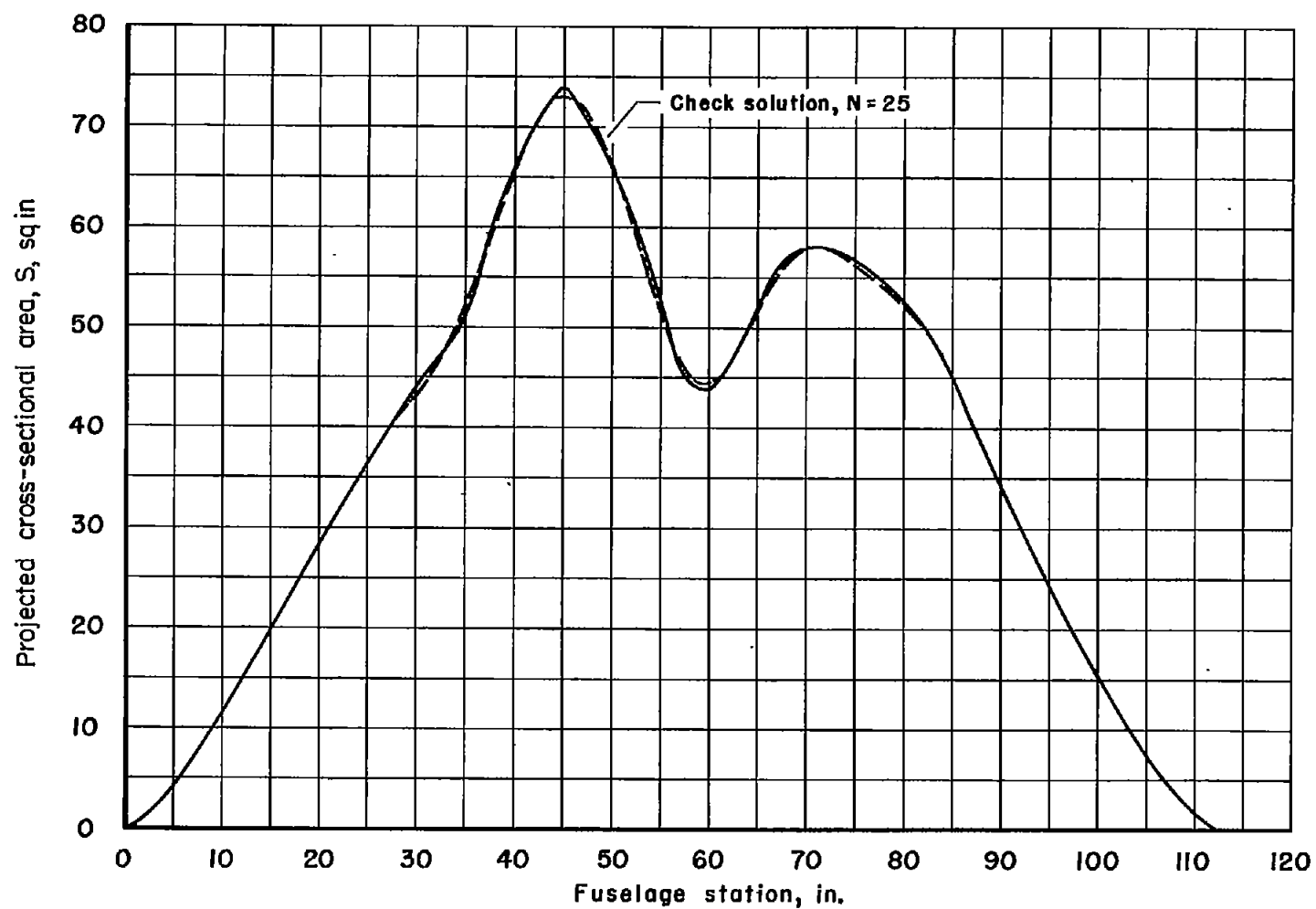
(e) $M = 1.20$, $\theta = 0^\circ$, $\psi = 33.6^\circ$

Figure 21.- Concluded
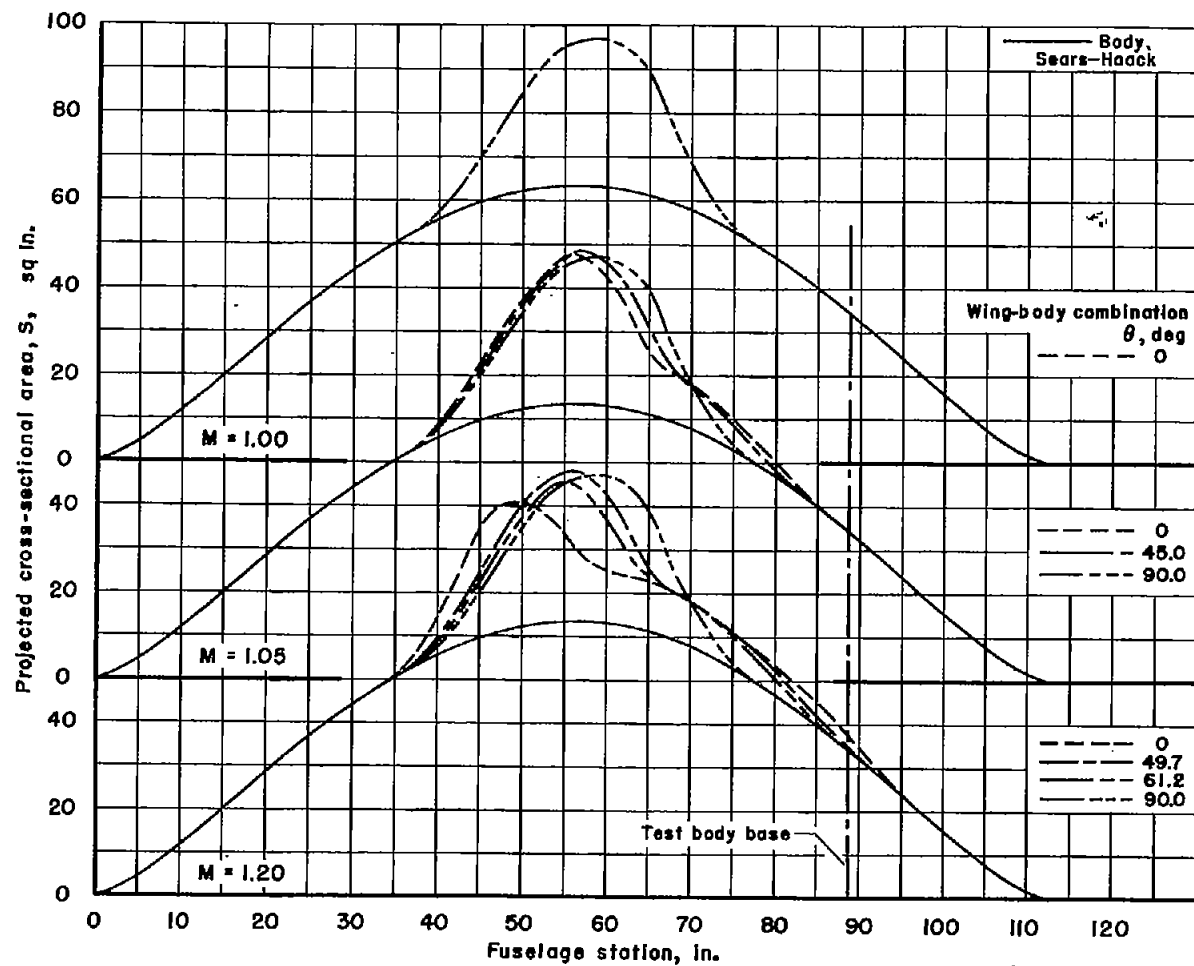
(a) Basic wing with Sears-Haack body.

Figure 22.- Variation of model area distributions with different cutting angles (θ) at Mach numbers of 1.00, 1.05, and 1.20.
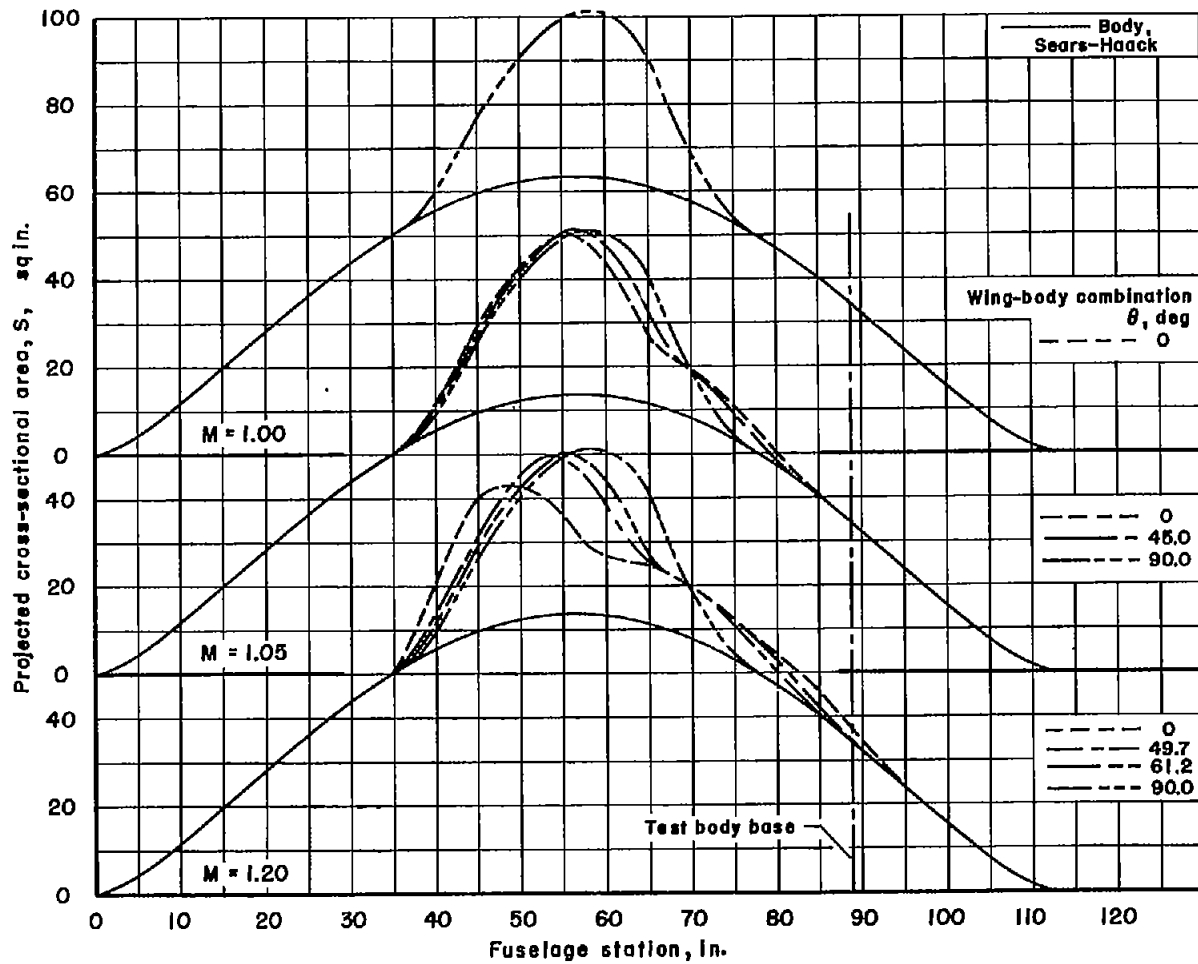
(b) Modified wing with Sears-Haack body.

Figure 22.- Continued.
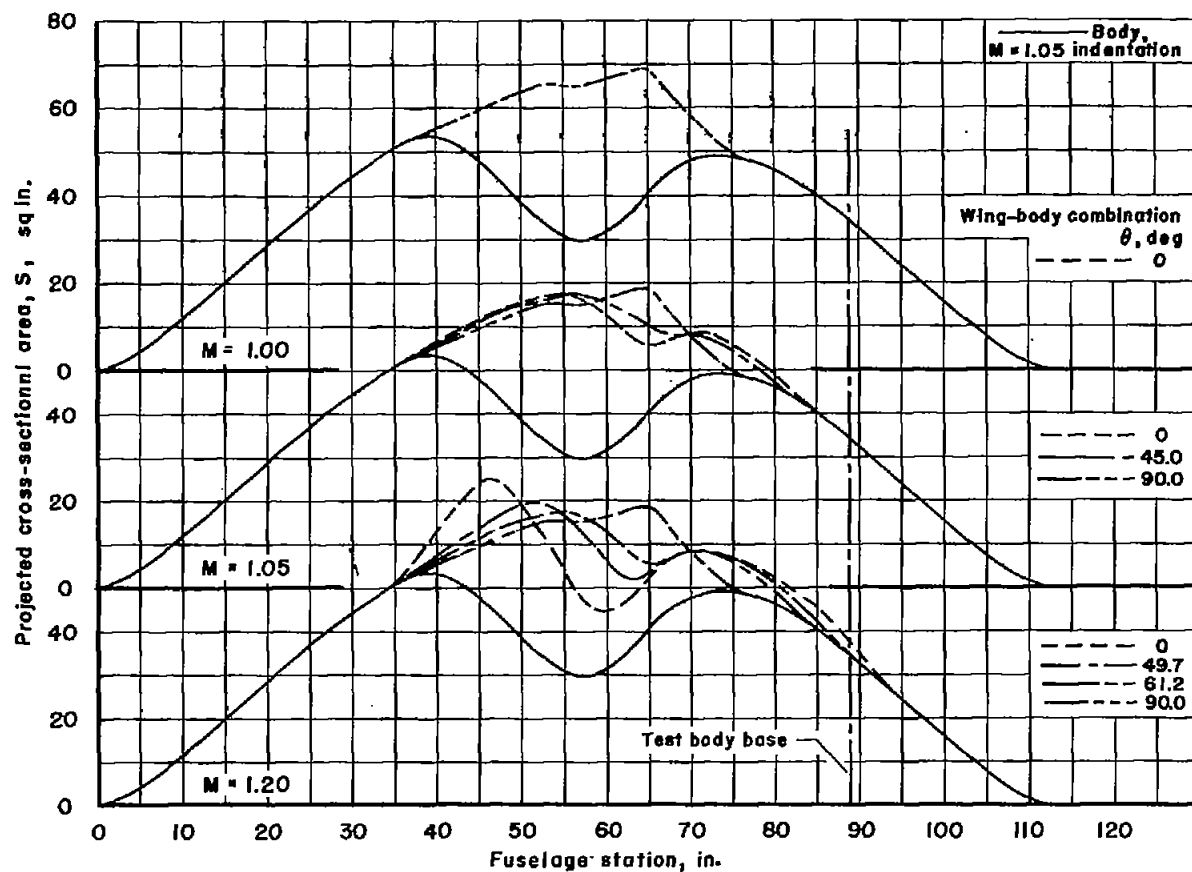
(c) Basic wing with M = 1.05 indented body.

Figure 22.- Continued.
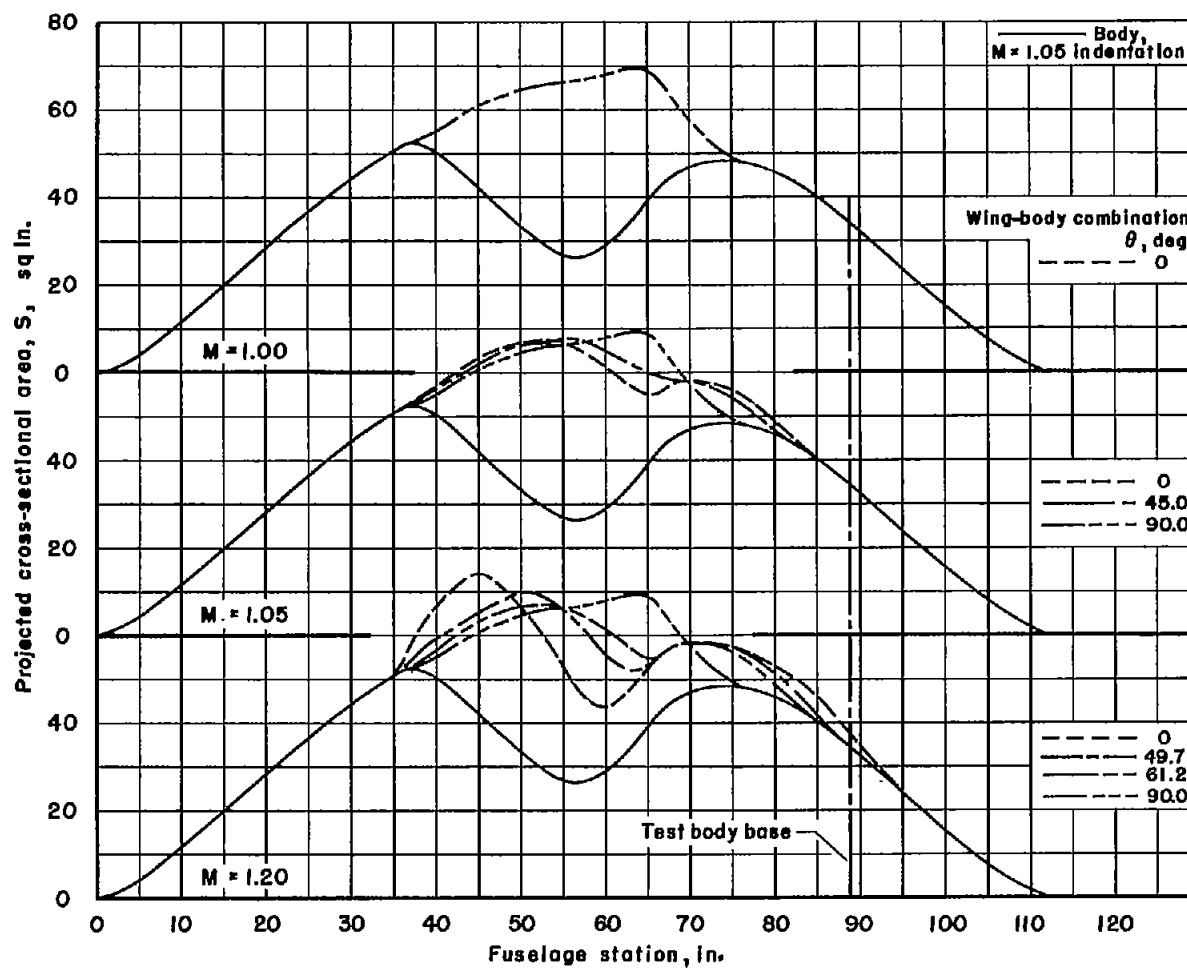
(d) Modified wing with M = 1.05 indented body.

Figure 22.- Continued.
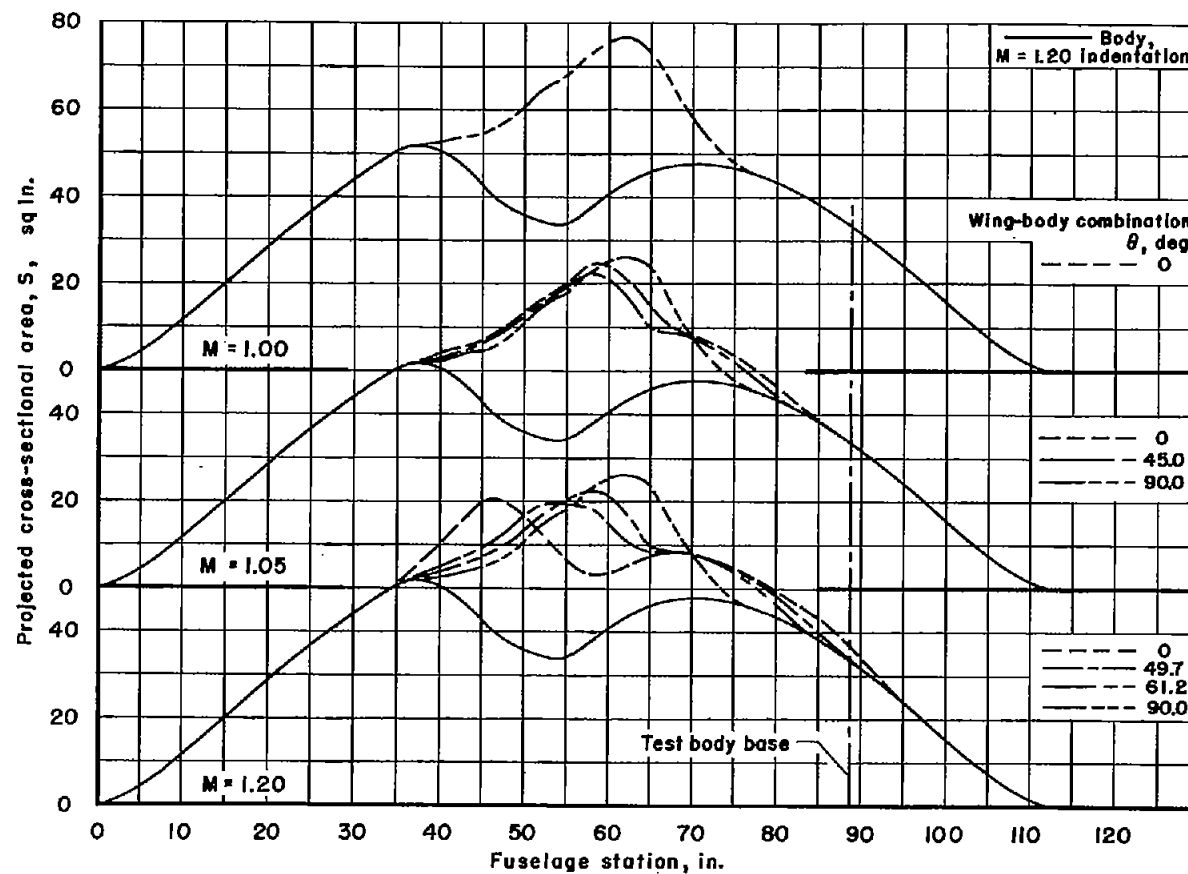
(e) Basic wing with M = 1.20 indented body.

Figure 22.- Continued.
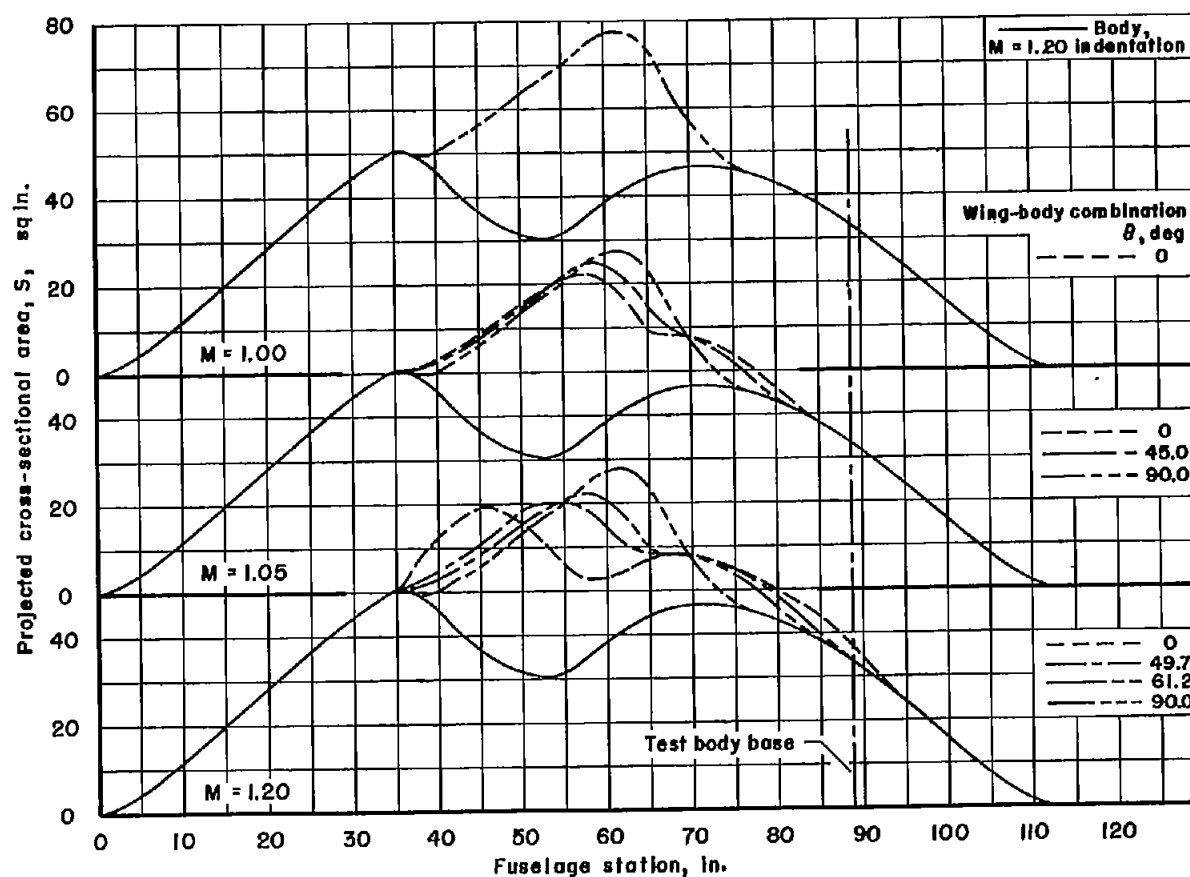
(f) Modified wing with M = 1.20 indented body.

Figure 22.- Continued.
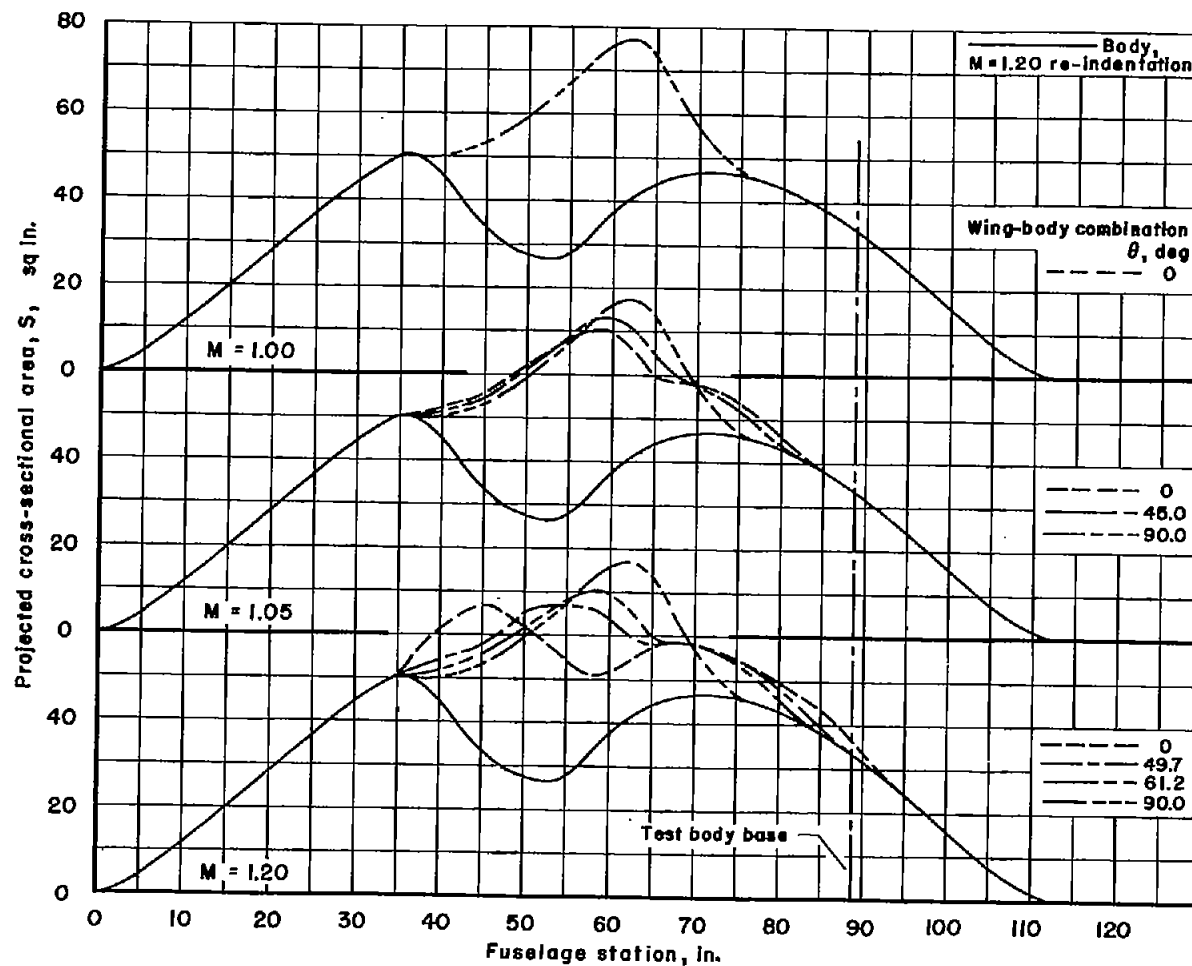
(g) Basic wing with M = 1.20 re-indented body.

Figure 22.- Continued.
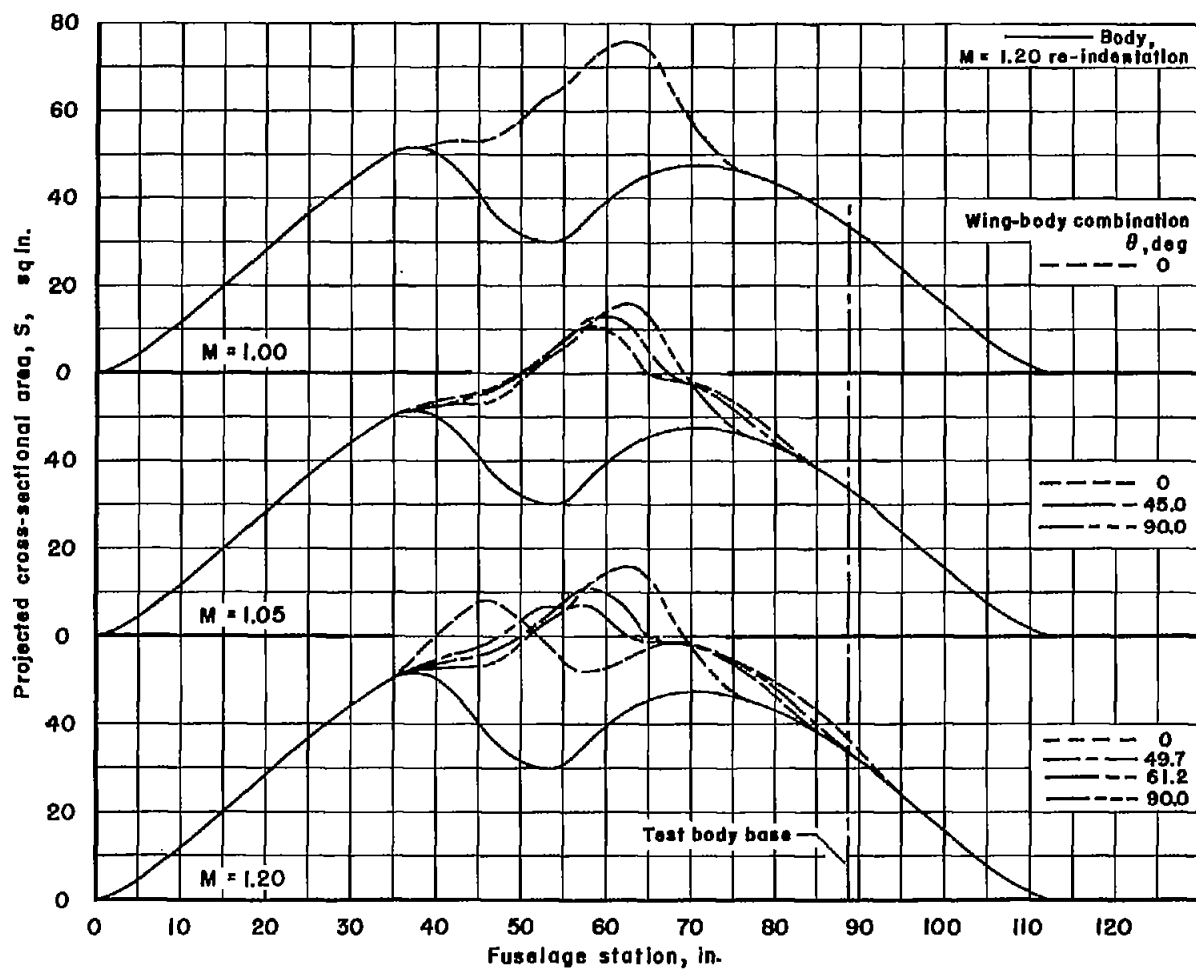
(h) Modified wing with M = 1.20 re-indented body.

Figure 22.- Concluded.
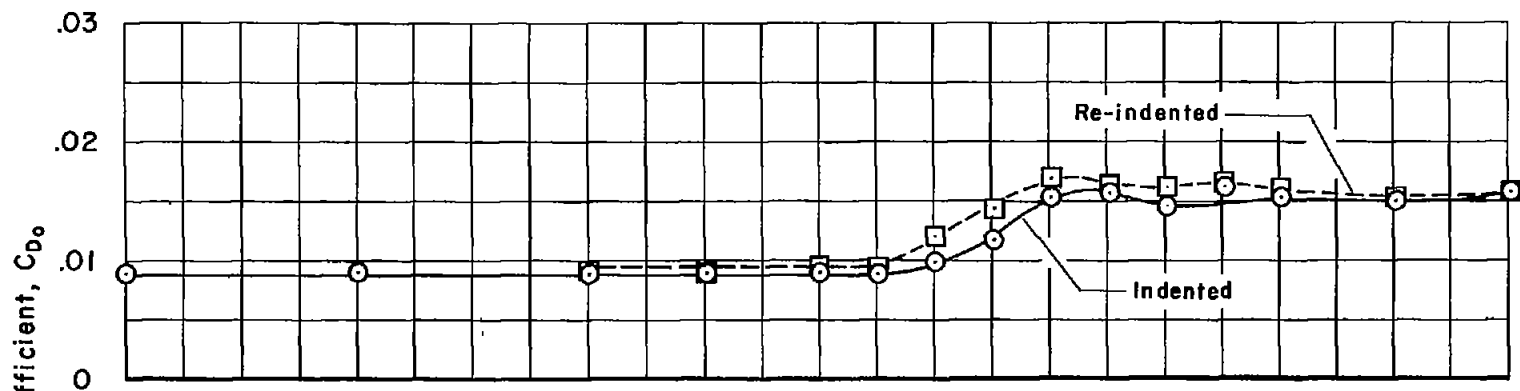
(a) Basic wing.
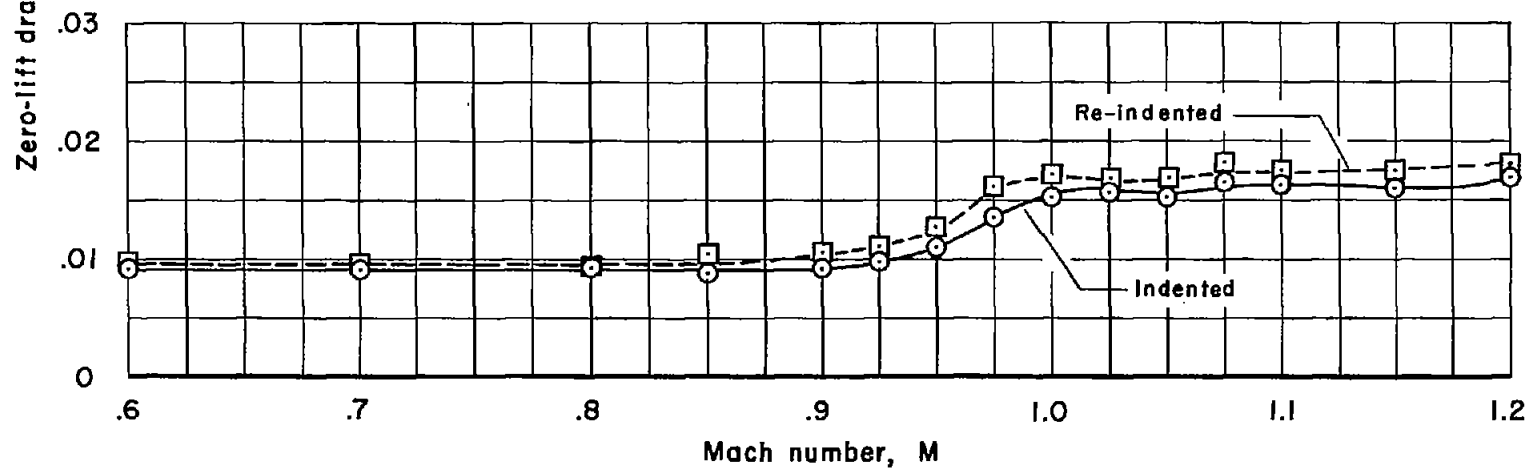
(b) Modified wing.

Figure 23.- Experimental zero-lift drag coefficients for the M = 1.20 indented and re-indented bodies with the basic and modified wings.

(a) Basic wing.
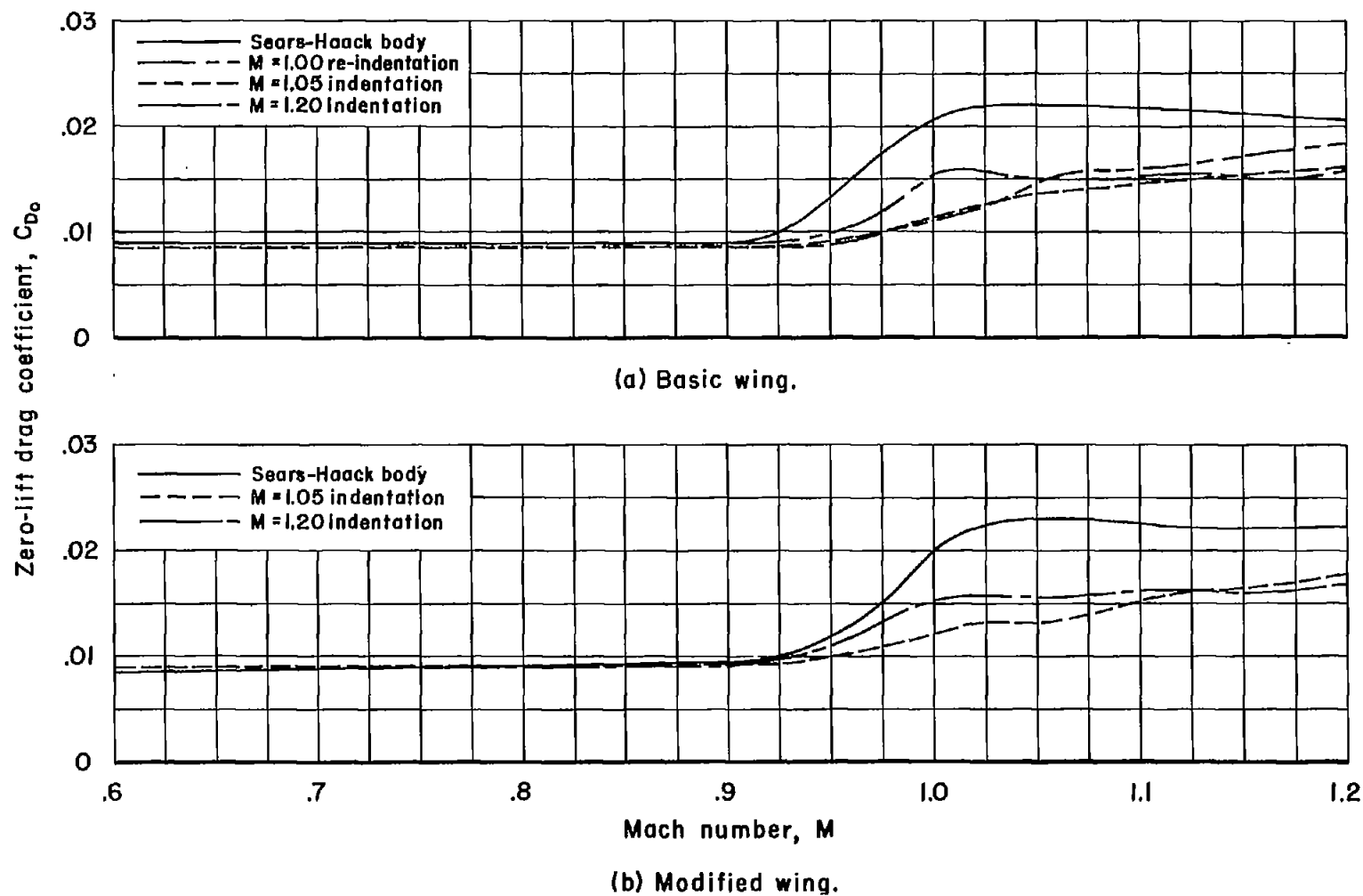
(b) Modified wing.

Figure 24.- Effect of various body indentations on the zero-lift drag coefficients for the basic- and modified-wing models.

(a) Basic wing.
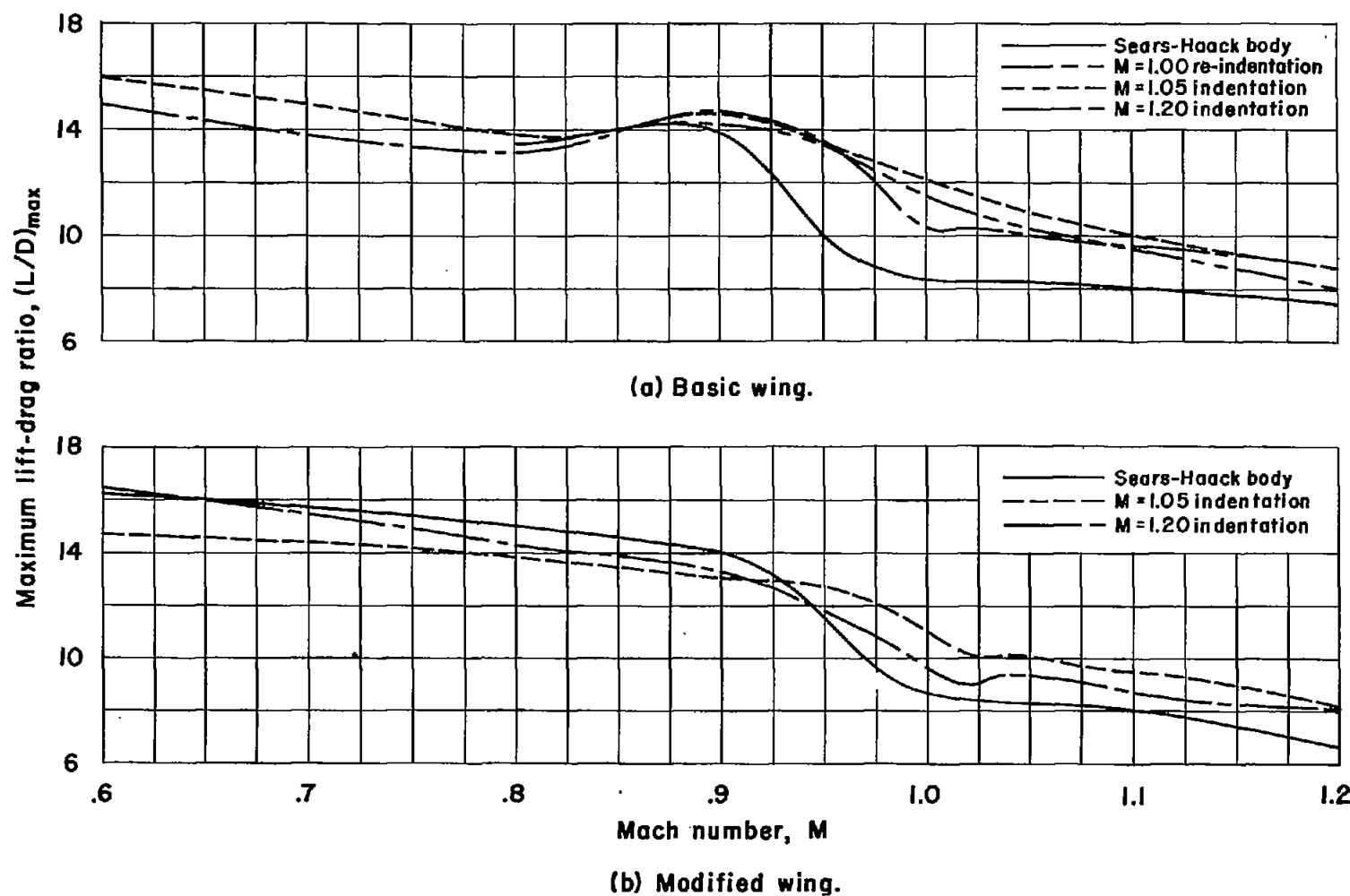
(b) Modified wing.

Figure 25.- Effect of various body indentations on the maximum lift-drag ratios for the basic- and modified-wing models.

(a) Basic wing.
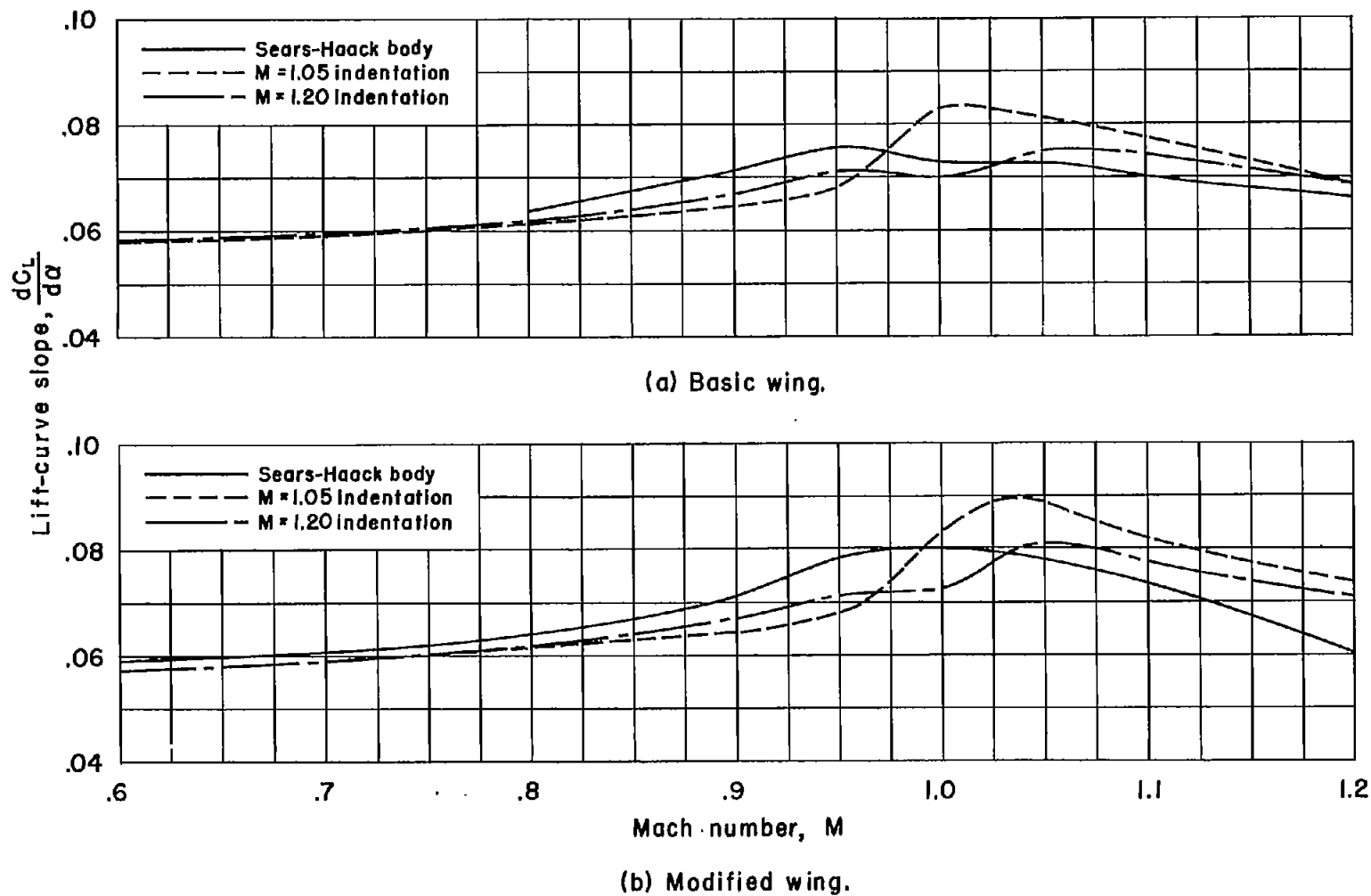
(b) Modified wing.

Figure 26.- Effect of various body indentations on the lift-curve slopes for the basic- and modified-wing models at low angles of attack.
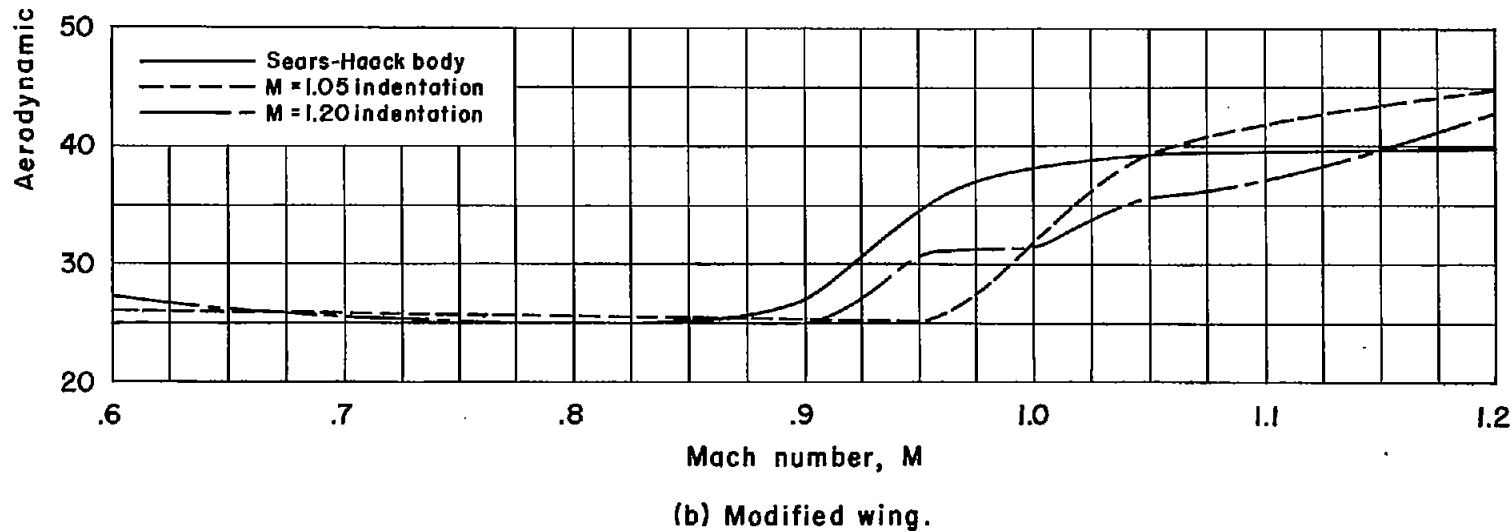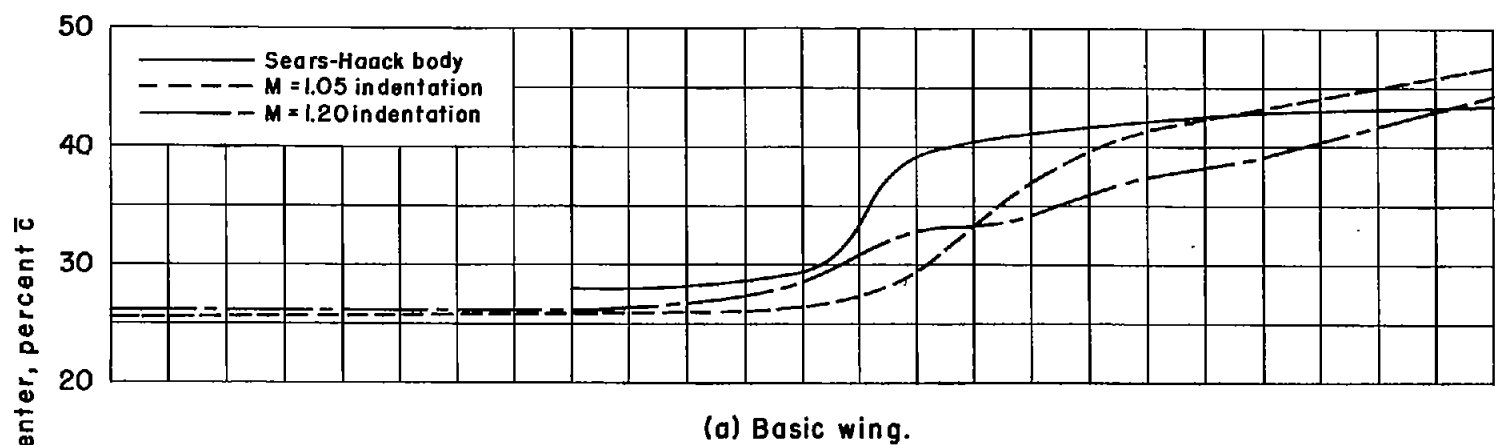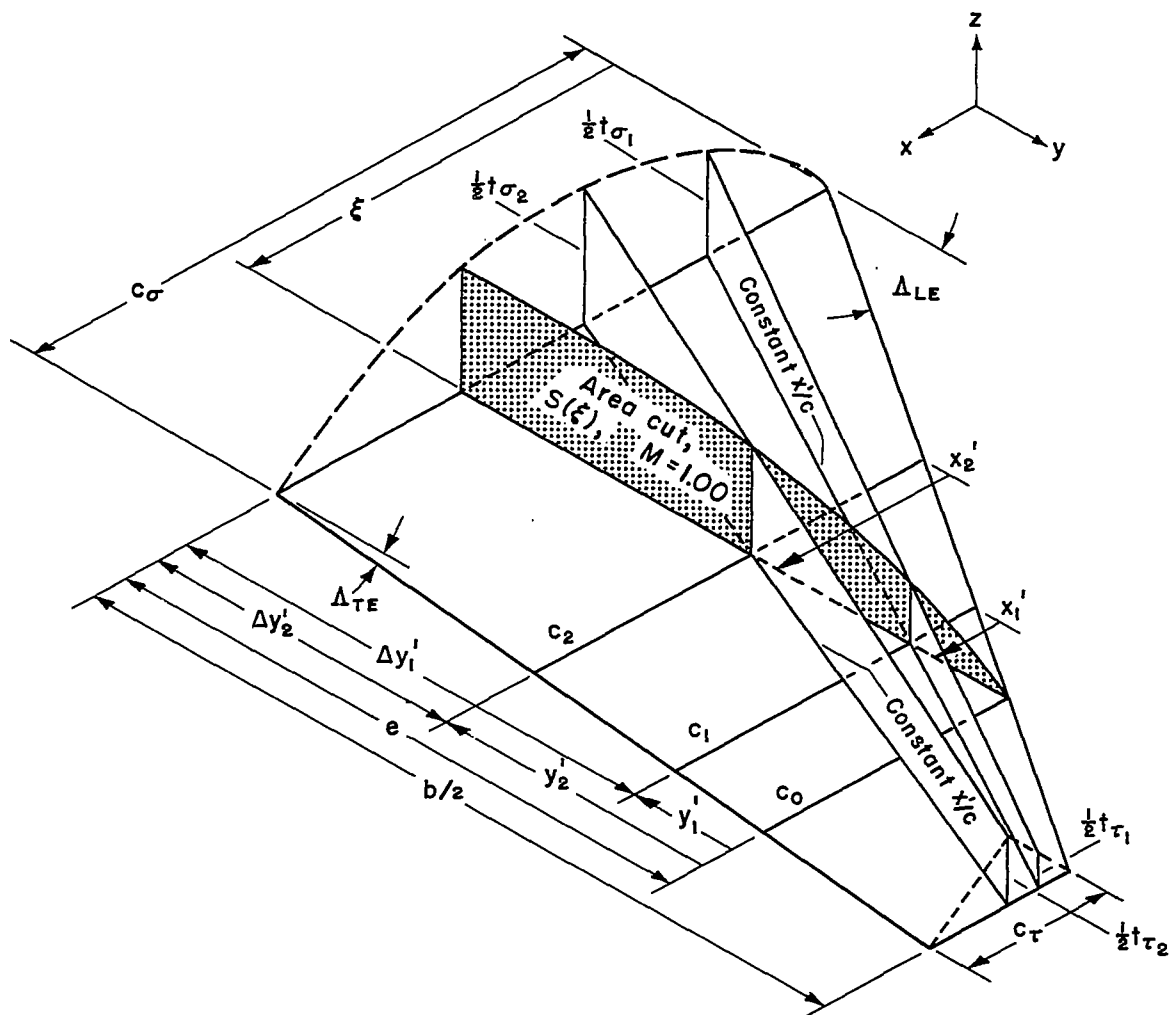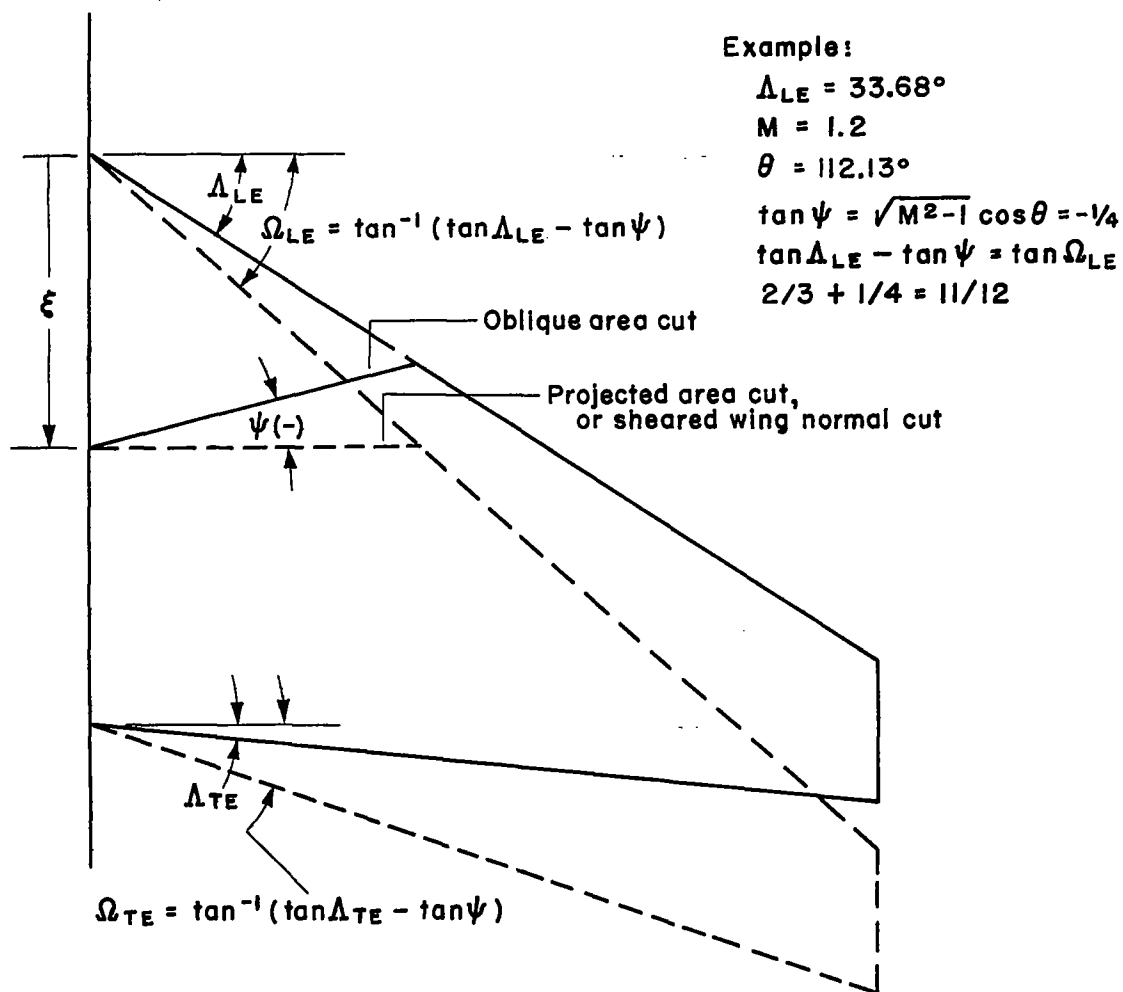
Figure 27.- Effect of various body indentations on the aerodynamic-center positions for the basic- and modified-wing models at low angles of attack.

(a) Typical M = 1.00 area cut; upper half of wing panel.

Figure 28.- Definition of primary dimension symbols used in Appendix B.

Example:

$\Lambda_{LE} = 33.68°$

$M = 1.2$

$\theta = 112.13°$

$\tan\psi = \sqrt{M^2-1}\,\cos\theta = -\tfrac{1}{4}$

$\tan\Lambda_{LE} - \tan\psi = \tan\Omega_{LE}$

$2/3 + 1/4 = 11/12$

(b) The sheared wing for supersonic Mach numbers.

Figure 28.- Continued.

$$\Omega_{LE} = tan^{-1}(tan\Lambda_{LE} - tan\psi)$$

$$\eta = \frac{y'}{c_0}(tan\Omega_{LE})$$

$$\eta_e = \frac{e}{c_0}(tan\Omega_{LE})$$

$$\eta_{b/2} = \frac{b/2}{c_0}(tan\Omega_{LE})$$

$$\Omega_{TE} = tan^{-1}(tan\Lambda_{TE} - tan\psi)$$

(a) $\eta_e < \eta_{b/2}$

(b) $\eta_e > \eta_{b/2}$

(c) Values of ξ, c_0, y'_{max} for two locations on a typical wing.

Figure 28.- Concluded.